Inaugural Dissertation

submitted to the

Combined Faculties of Natural Sciences and Mathematics

of the

Ruperto-Carola University of Heidelberg, Germany

for the degreee of

Doctor of Natural Sciences

Presented by

Dipl. Biol. Zeljko Durdevic

born in Petrovac na Mlavi, Serbia

Oral-examination:.....

Characterization of the Biological Function of Dnmt2

in *Drosophila melanogaster*

Referees:

Prof. Dr. Frank Lyko

Dr. Georg Stöcklin

Zusammenfassung

Dnmt2 Enzyme sind hoch konservierte und phylogenetisch weitverbreitete RNA Methyltransferasen, deren biologische Funktion nur teilweise charakterisiert ist. Vorherige Untersuchungen zeigten, dass Dnmt2-abhängige tRNA-Methylierung die Fragmentierung von tRNA während der zellulären Reaktion auf Hitze-Stress beeinflusst und es wurde damit eine Rolle von Dnmt2 in die zellulären Stressantwort vorausgesagt.

Um die biologische Funktion von Dnmt2 näher zu charakterisieren, wurden im Rahmen dieser Arbeit die Rolle von Dnmt2 während der zellulären Antwort auf biotischen (pathogen), abiotischen (Hitze) und endogenen RNA Stress (Transposons) untersucht. Mit Hilfe des Modellorganismus *Drosophila melanogaster* und molekularen als auch biochemischen Methoden konnten wichtige Funktionen von Dnmt2 bei der Kontrolle von exogenen und endogenen mobilen Elementen gezeigt werden.

Fliegen mit einer Deletion des Dnmt2 Gens (Dnmt2-Mutante) wiesen stress- und altersabhängige phänotypische Veränderungen auf. Molekularen Analysen zeigten erhöhte Mengen von spezifischen RNA Viren in alternden *Dnmt2*-Mutanten und Infektionsexperimente bestätigten, dass *Dnmt2*-Mutanten Infektionen mit *Drosophila* C Virus (DCV) nicht kontrollieren konnten. Besonders auffallend war dabei, dass die katalytische Aktivität des Enzyms wichtig für die wirksame Viruskontrolle ist. Desweiteren konnte die Bindung von Dnmt2 Komplexen an DCV RNA gezeigt und damit RNA-Methylierung in diesem Prozess impliziert werden. Diese Ergebnisse beschreiben eine neue biologische Funktion für Dnmt2, die RNA Methylierung zur Kontrolle von RNA Viren suggeriert.

Um die Untersuchung der Dnmt2-Funktionen in der Kontrolle von mobilen Elementen zu erweitern, wurden endogene mobile Elemente in *Dnmt2*-Mutatanten analysiert. *Dnmt2*-Mutanten zeigten eine ineffiziente Widerstilllegung von stressinduzierten Transposons. Es konnte gezeigt werden, dass auch für diesen Prozess die katalytische Aktivität des Enzyms benötigt wird. Darüber hinaus konnte erhöhte Transposonmobilität in *Dnmt2* Mutanten beobachtet werden. Hitze verursachte auch signifikant unterschiedliche tRNA-Fragmentierungsmuster in *Dnmt2* Mutanten und bestimmte tRNA Fragmente assoziierten vermehrt mit Argonaute-2. Weitere Untersuchungen zeigten, dass Dnmt2-Mutanten zunehmend Dicer-2-abhängige doppelsträngige RNAs akkumulierten, was auch zu einer verminderten Produktion von endo-siRNAs führte. Infolgedessen zeigten *Dnmt2*-Mutanten eine Fehlregulation von siRNA-abhängigen Prozessen, die sich in ineffizienter Transposonkontrolle widerspiegelten. Die Ergebnisse beschreiben eine biologische Funktion von Dnmt2 in der stressinduzierten Transposonkontrolle und weisen daraufhin, dass tRNA-Fragmentierung die RNAi-Signalwegen beeinträchtigen können.

Die in dieser Arbeit enthaltenen Ergebnisse erlauben die Schlussfolgerung, dass eine bisher unbekannte Funktion von Dnmt2 der Beitrag zur zellulären Antwort auf stress-induzierte mobile Elemente ist und dass sich die hohe Konservierung von Dnmt2 Enzymen durch diese wichtige Funktion begründen lässt.

Abstract

Dnmt2 genes encode highly conserved and widely distributed RNA methyltransferases with poorly understood biological functions. Recently, it has been shown that Dnmt2-mediated tRNA methylation interfered with stress-induced tRNA fragmentation, which suggested roles for Dnmt2 during cellular stress responses.

The aim of this work was to investigate the roles of Dnmt2 during the response to biotic (pathogens), abiotic (heat) and endogenous RNA (transposon) stress in an attempt to further characterize the biological function of Dnmt2. Using the model organism *Drosophila melanogaster* and molecular and biochemical approaches this investigation revealed important roles for Dnmt2 in the control of exogenous and endogenous mobile elements.

Dnmt2 mutants showed stress- and age-dependent morphological phenotypes. Molecular analysis identified increased levels of RNA viruses in *Dnmt2* mutants and virus infection experiments confirmed that *Dnmt2* mutants failed to control specific pathogens like *Drosophila* C virus (DCV). Expression analysis for immune response genes showed that *Dnmt2* mutant flies were not able to efficiently activate innate immune responses. Importantly, the RNA methyltransferase function of Dnmt2 contributed to virus control and binding of Dnmt2-containing protein complexes to DCV-derived RNA implicated RNA methylation in the process. These findings revealed a novel biological role for Dnmt2 enzymes and suggest that RNA methylation may regulate viral RNA metabolism.

To extend the investigation of Dnmt2 function in mobile element control to endogenous sequences, transposon control in *Dnmt2* mutants was investigated. *Dnmt2* mutants showed defects in the re-silencing of heat shock-induced transposons and this depended on the catalytic activity of Dnmt2. Furthermore, increased transposon-derived DNA and transposon mobility could be detected in *Dnmt2* mutants. Heat shock caused significantly different tRNA fragmentation patterns in *Dnmt2* mutants and Dnmt2 substrate tRNA fragments associated with Argonaute-2 after heat shock. Further analysis showed that *Dnmt2* mutants accumulated increasing levels of Dicer-2-dependent double-stranded RNA precursors leading to inefficient endo-siRNA production. Consequently, *Dnmt2* mutants displayed signs of mis-regulated siRNA pathways including reduced transposon silencing, which led to genomic instability. These findings uncovered a stress-related function for Dnmt2 in transposon regulation, which suggests that the increase in stress-induced tRNA fragments in *Dnmt2* mutants affects the efficiency of small RNAi pathways.

This thesis describes novel functions of *Dnmt2* in cellular stress responses to biotic and abiotic stresses and indicates that the high conservation of Dnmt2 enzymes is founded in its contribution to defense mechanisms against external and internal mobile elements.

Contents

List of Figures

List of Tables

List of Abbreviations

°C	Degree Celsius
1mA	1-methyadenosine
5mC	5-methylcytosine
5mcmU	5-methoxycarbonylmethyluridine
5mcm2sU	5-methoxycarbonylmethyl-2-thiouridine
6mA	N6-methyladenosine
6m6A	N6-methyl-2′-O-methyladenosine
7mG	N7-methylguanosine
AC	Anticodon
Ago-2	Argonaute-2
AMP	Antimicrobial Peptide
β-Tub	β-Tubulin
bp	Base Pair
cDNA	Complementary DNA
cis-NAT	cis-Natural Antisense Transcript
Dcr-2	Dicer-2
DCV	Drosophila C Virus
Dnmt	DNA Methyltransferase
ER	Endoplasmic Reticulum
HMW	High Molecular Weight
IR	Inverted Repeat
IRES	Internal Ribosome Entry Site
JAK/STAT	Janus Kinase/Signal Transducer and Activator of Transcription
kb	Kilobase
kDa	Kilo-Dalton
LTR	Long Terminal Repeat
µg	Microgram
µl	Microliter
METTL3	Methyltransferase like 3
mg	Milligram
ng	Nanogram
Nm	2′-O-methylated Nucleosides
Nsun2	NOP2/Sun domain protein 2
PB	Processing Body
PCR	Polymerase Chain Reaction
qPCR	Quantitative Polymerase Chain Reaction
RIG	Retinoic Acid Inducible Gene
RIP	RNA Immunoprecipitation
RNAi	RNA Interference
SG	Stress Granule
T	5-methyluridine
tiRNA	tRNA-derived Stress-induced RNA
tRF	tRNA-derived RNA Fragment
TRM4	tRNA-specific methyltransferase 4
UPR	Unfolded Protein Response
UTR	Untranslated Region

Chapter 1

Introduction

Covalent nucleotide modifications were first discovered in 1948 as 5-methylcytosine (5mC) in DNA {Hotchkiss:1948va} and are a common feature of nucleic acids, which play an important role in the regulation of their function. The methylation of carbon 5 of the nucleobase cytosine is a widespread and highly conserved nucleotide modification in both DNA and RNA found in all three domains of life. Additionally, DNA methylation on adenine residues (6mA) has also been detected, whereas RNA harbors a much wider spectrum of nucleotide methylation modifications.

1.1 RNA Methylation

Different types of modifications involving methyl groups have been discovered in eukaryotic RNAs. For instance, methylated nucleotides in mRNA are represented by N7-methylguanosine (7mG) at the 5′ cap structure (Rottman et al., 1974), N6-methyl-2′-O-methyladenosine (6mAm) at the first position of the 5′ terminus and various internal positions (Wei et al., 1976), 2′-O-methylated nucleosides (Nm = Am, Cm, Um, Gm) on the first two starting positions at the 5′ terminus and in internal sequences (Wei et al., 1976), internal N6-methyladenosine (6mA) (Perry et al., 1975) and the recently discovered internal 5-methylcytosine (5mC) (Khoddami and Cairns, 2013; Squires et al., 2012). With the exception of the mRNA cap structure, the biological functions of many of these modifications are largely unknown, although almost all of them were discovered in 1970s.

The prevailing nucleoside methylation in eukaryotic RNA is 6mA, which represents more than 80% of all RNA base methylations (Niu et al., 2013). Adenine methylation is catalyzed by a methyltransferase complex comprised of mostly unidentified multi-component factors including one known and conserved subunit, the methyltransferase like 3 (METTL3) (Bokar et al., 1997; Bujnicki et al., 2002). The recent discovery of RNA demethylases indicated that adenine methylation can change dynamically and suggested broader regulatory roles for this modification (Jia et al., 2011; Zheng et al., 2013a). Even though, this RNA modification is expected to function in every aspect of mRNA metabolism, the mechanism of 6mA-mediated regulation of mRNA metabolic processes is poorly understood. (Niu et al., 2013). The identification of 6mA-binding proteins (Dominissini et al., 2012) and the reversibility of 6mA modification in RNA have been discussed in terms of

RNA epigenetics (Zheng et al., 2013b), suggesting that 6mA might represent a novel RNA epigenetic marker with broader roles in fundamental cellular processes.

The methylation of cytosine in DNA is well-established epigenetic mark. While the functions of 5mC in DNA in epigenetic regulation of gene expression, inheritance and diseases have been intensively studied the functions of the 5mC in RNA are not well characterized. The recent development of various techniques to analyze 5mC in RNA, including mass spectrometry (Chan et al., 2011), high throughput RNA bisulfite sequencing (Schaefer et al., 2009) and 5-azacytidine-mediated RNA immunoprecipitation (Khoddami and Cairns, 2013) formed the basis for the characterization of the biological functions of 5mC RNA methyltransferases. In eukaryotes, numerous putative RNA 5mC-methyltransferases have been identified but only two have been shown to catalyze the formation of 5mC at specific positions. First RNA 5mC-methyltransferase shown to have a specific target was discovered in budding yeast (Motorin and Grosjean, 1999). The enzyme named tRNA-specific methyltransferase 4 (TRM4) methylates cytosines in positions 34, 40, 48 and 49 in various transfer RNAs (tRNAs) (Motorin and Grosjean, 1999). Later studies revealed that mammalian orthologue known as NOP2/Sun domain protein 2 (Nsun2) has the same function in human cells (Brzezicha et al., 2006; Squires et al., 2012; Tuorto et al., 2012). Additionally, Nsun2 was shown to methylate messenger RNAs (mRNAs) as well (Khoddami and Cairns, 2013; Squires et al., 2012). Another RNA 5mC-methyltransferase with high target specificity found to methylate several tRNA species in protist, plants, fungi and animals is DNA methyltransferase 2 (Dnmt2) (Goll et al., 2006; Schaefer et al., 2010).

1.2 Cytosine-5-Methyltransferase Dnmt2

During the evolution of eukaryotes Dnmt2 became the most conserved and most widely distributed DNA methyltransferase (Dnmt) family member. Interestingly, numerous organisms contain Dnmt2 as their only Dnmt homologue (Figure 1.1). Dnmt2 contains all catalytic Dnmt motifs in canonical order but lacks N-terminal regulatory domains that are common in other eukaryotic Dnmts (Figure 1.2). Despite the strong conservation and wide phylogenetic distribution (Figure 1.1) genetic studies showed that *Dnmt2*-mutant organisms are fertile and do not display any obvious developmental abnormalities under standard laboratory conditions (Goll et al., 2006; Kunert et al., 2003; Wilkinson et al., 1995).

According to the protein structure Dnmt2 was predicted to be a *bona fide* DNA methyltransferase (Okano et al., 1998; Yoder and Bestor, 1998). Even though Dnmt2 can form denaturant-resistant complexes with DNA (Dong et al., 2001), the enzyme shows only week and distributive DNA methylation activity (Fisher et al., 2004; Hermann et al., 2003). In contrast, recent experiments uncovered a robust tRNA methylation activity for Dnmt2 with

high specificity towards cytosine at position 38 within the anticodon loop of several tRNAs (Goll et al., 2006; Schaefer et al., 2010). Of note, unlike classical RNA methyltransferases, which methylate RNAs by using a specific RNA methyltransferase catalytic mechanism (Liu and Santi, 2000), Dnmt2 enzymes use a DNA methyltransferase mechanism to methylate tRNAs (Jurkowski et al., 2008).

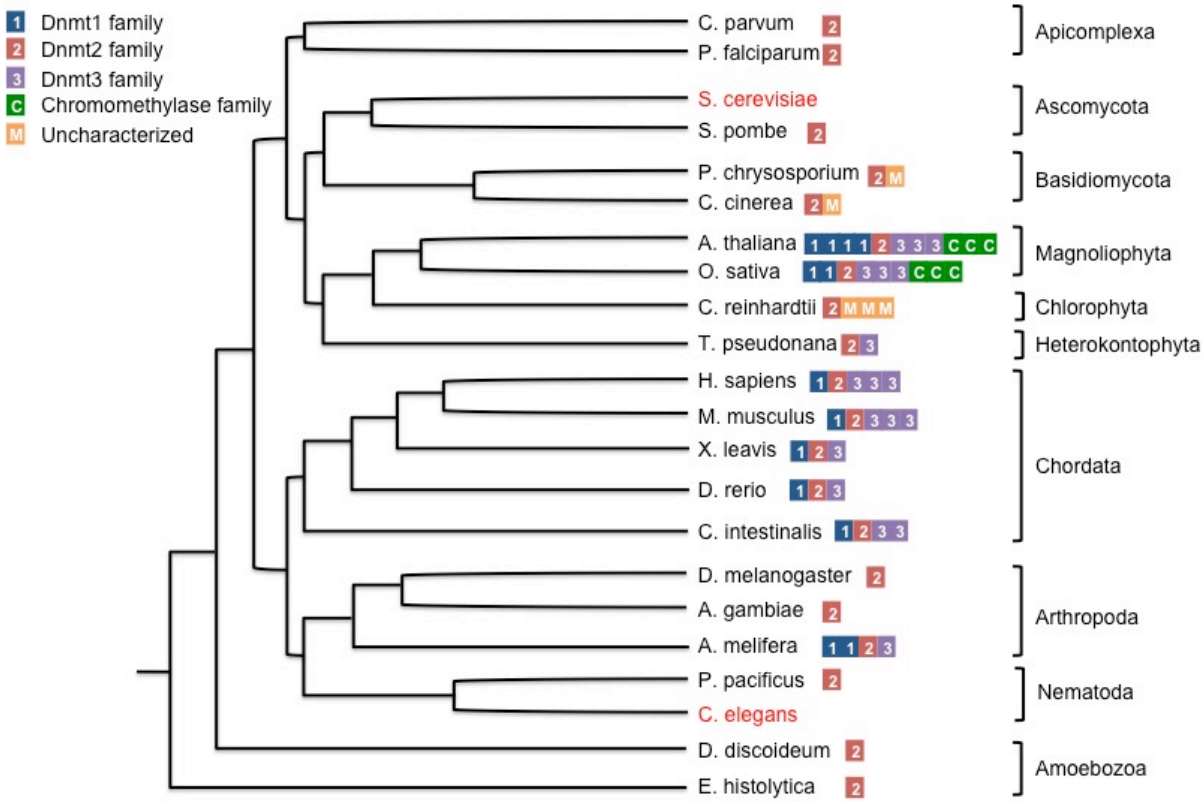

Figure 1.1: Distribution of the DNA methyltransferase families in eukaryotes.
In the organisms that contain Dnmt1 and Dnmt3 families Dnmt2 is always present, but many organisms contain only Dnmt2 homologues. The organisms marked in red do not contain any Dnmt. The colored scheme represents different Dnmt families. (Adapted from Goll et al., 2005)

The strong conservation of Dnmt2 enzymes suggested that the eukaryotic Dnmt1 and Dnmt3 families evolved from Dnmt2-like RNA methyltransferase, which changed their substrate specificities from RNA to DNA (Goll et al., 2006). Modeling the evolutionary origin of eukaryotic Dnmts indicated their presence in the last eukaryotic common ancestor (LECA), which most likely were acquired from independent prokaryotic DNA methyltransferases, which are still present in form of bacterial restriction-modification system (Jurkowski and Jeltsch, 2011). Therefore, a scenario in which Dnmt2 enzymes evolved from prokaryotic DNA methyltransferase and changed their substrate specificities to tRNAs (Jurkowski and Jeltsch, 2011) is more likely then an expansion from Dnmt2-based RNA methyltransferases that gave rise to other Dnmts by shifting their substrate specificity towards DNA (Goll et al., 2006).

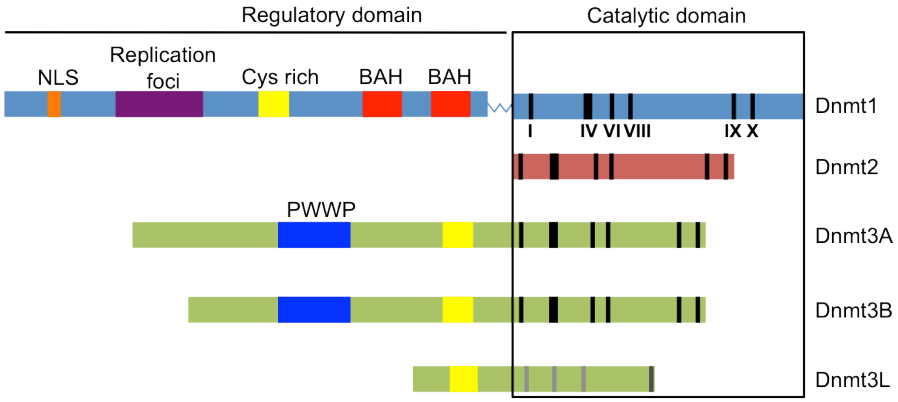

Figure 1.2: Organization and sequence relationships of mammalian DNA methyltransferases.
All Dnmt families have typical organization of catalytic domain but differ in N-terminal regulatory domain. Dnmt2 family contains only catalytic domain with 10 motifs in canonical order. Dnmt3L are catalytically inactive member of Dnmt3 family and gray bars represent degenerated catalytic motifs.

Although *Dnmt2* mutant organisms are viable and fertile under standard laboratory conditions, recent work suggested that Dnmt2 becomes important under non-standard laboratory conditions. First, genetic experiments indicated that Dnmt2 is involved in the control of transposable elements in *Dictyostelium* and *Drosophila* (Kuhlmann et al., 2005; Phalke et al., 2009) suggesting that Dnmt2 function contributes to the regulation of genomic stability. However, the exact molecular function of Dnmt2 in transposon control has been controversially discussed (Schaefer and Lyko, 2010). Secondly, Dnmt2 has been implicated in cellular stress responses (Becker et al., 2012; Schaefer et al., 2010; Thiagarajan et al., 2011). In light of the absence of Dnmt2-mediated DNA methylation in Dnmt2-only organisms (Radatz et al., 2013), these findings suggested a link between tRNA methylation, mobile element control and stress responses. Indeed, the tRNA methyltransferase activity of Dnmt2 interferes directly with the stress-induced fragmentation of various tRNAs (Schaefer et al., 2010), indicating a connection between tRNA methylation and tRNA metabolism during the cellular stress responses.

1.3 tRNA Modification and Fragmentation

Transfer RNAs are ancient molecules that play a central role in the decoding of messenger RNAs (mRNAs) into protein in all living organisms. The biogenesis of functional tRNAs includes different processing steps. One of the important processes is the modification of ribonucleotides, which involves various enzymes and complex enzymatic reactions.

1.3.1 tRNA Modification

Post-transcriptional modifications are a conspicuous feature of all tRNAs in prokaryotes, eukaryotes and organelles (mitochondria and chloroplasts). There are approximately 100 different modifications identified in tRNA molecules (Phizicky and Hopper, 2010). Different ribonucleotide modifications (Figure 1.3) have different functions but mostly conform to three functional categories (Phizicky and Hopper, 2010): First, modifications in or around the anticodon loop are responsible for correct codon usage and affect translation. The role of tRNA modification in codon usage is best demonstrated for modified uridine at position 34. Modification of uridine into 5-methoxycarbonylmethyl-2-thiouridine (5mcm2sU) is important for reading G and A in wobble position of corresponding tRNAs (Johansson et al., 2008), whereas the modification of uridine into 5-methoxycarbonylmethyl-uridine (5mcmU) is responsible for reading G in wobble position of corresponding tRNAs (Johansson et al., 2008) and for the efficient translation of DNA damage response genes (Begley et al., 2007).

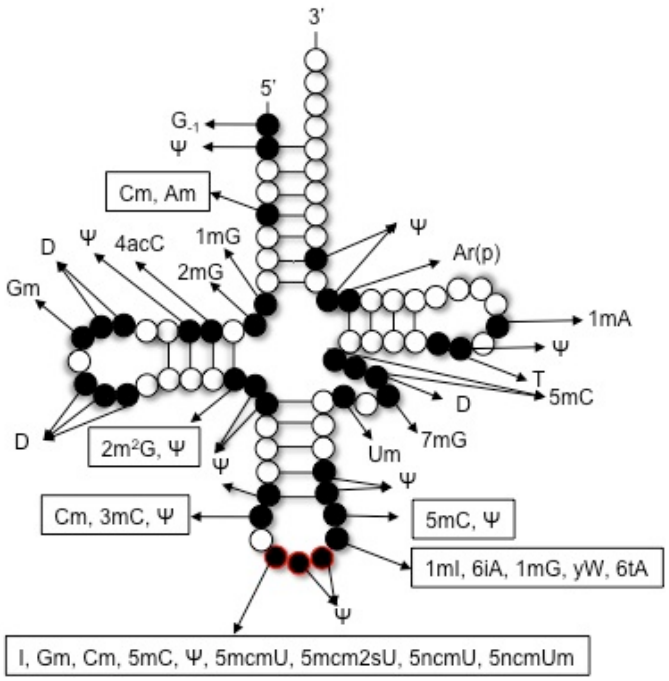

Figure 1.3: Schematic presentation of identified modifications in eukaryotic cytoplasmic tRNAs.
White circles: unmodified nucleotide; black circles: nucleotides that are modified in some or all tRNA species; red circles: anticodon nucleotides; red-framed black circles: anticodon nucleotides that are modified in some tRNAs. (Adapted from Phizicky and Hopper, 2010).

Second, several modifications (in different positions) specifically affect tRNA identity and ensure proper acylation by aminoacyltransferases. For example, in eukaryotes 2'-O-ribosyl phosphate modification of adenine (Ar(p)) at position 64 discriminates the initiator $tRNAi^{Met}$ from the elongator $tRNA^{Met}$ during protein synthesis (Aström and Byström, 1994), whereas G_{-1} of $tRNA^{His}$ is a positive determinant for histidyl-tRNA synthetase (Nameki et al., 1995).

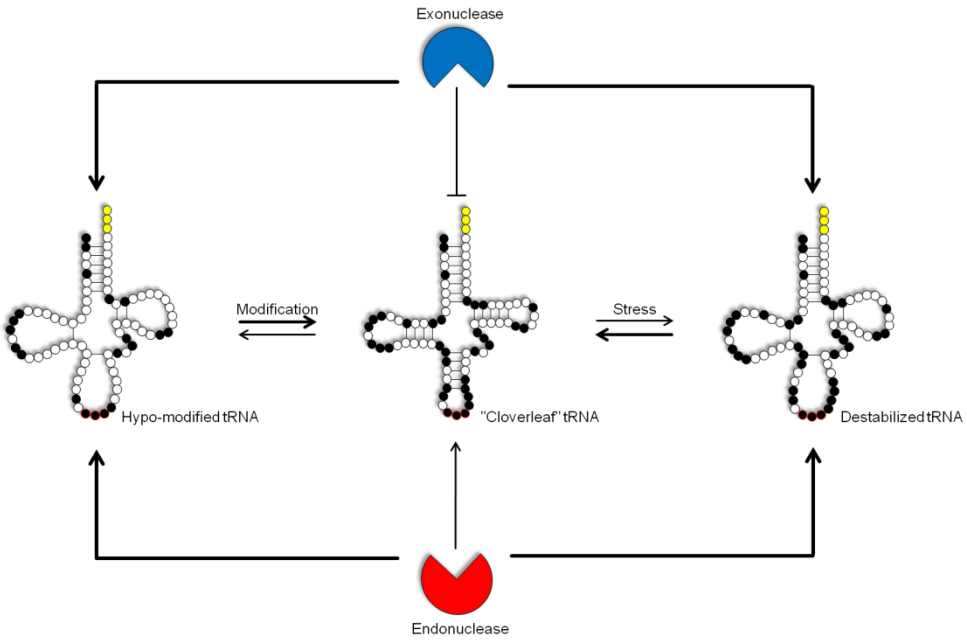

Figure 1.4 Potential impact of nucleoside modification and stress dependent structural destabilization on the fragmentation and degradation of tRNAs.
Ribonucleotide modifications stabilize three-dimensional structure and protect tRNA from exonucleolytic degradation and to high extent from endonucleolytic cleavage. The hypo-modified tRNAs are degraded by exonucleases but they are also a perfect substrate for endonucleolytic cleavage. Various stresses can disturb three-dimensional structure making tRNAs more accessible to exo- and endonucleases. White circles: unmodified nucleotide; black circles: nucleotides that are modified in some or all tRNA species; red-framed black circles: anticodon nucleotides that are modified in some tRNAs; yelow circles: the CCA 3' terminus.

Third, tRNA modifications play an important role in the stability of tRNAs. tRNA molecules are known to be extremely stable with half-lives measured in days. Their stability is associated with nucleotide modifications and proper tertiary structure. tRNAs spontaneously form cloverleaf structures due to base-pairing of highly conserved regions and it was argued that modifications do not significantly alter this structure but rather contribute to the stabilization of already formed cloverleaf or three-dimensional L structures (Motorin and Helm, 2010). Indeed, some modifications can increase the thermal stability of tRNAs as 5-methyiluridine (T) at position 54 (Davanloo et al., 1979), stabilize the 3'-end of tRNAs through 2'-O-methylated nucleotides (Kawai et al., 1992) or stabilize the cloverleaf structure through 1-methyladenine (1mA) at position 9 (Helm et al., 1999). Although the loss of tRNA modifications are mostly inconsequential, it has been shown that hypo-modified tRNAs can elicit tRNA degradation by different tRNA turnover pathways such as the TRAMP and the nuclear exosome complex or the "rapid tRNA decay" (Phizicky and Hopper, 2010). Hypo-modified tRNAs can also be cleaved by endonucleases, which leads to increased tRNA fragmentation as shown for tRNAs lacking Dnmt2-dependent 5mC (Schaefer et al., 2010). Therefore ribonucleotide modifications also stabilize tRNA structures and impact on tRNA degradation and fragmentation (Figure 1.4).

1.3.2 tRNA Fragmentation

In addition to the canonical function of tRNAs in protein synthesis, recent observations have drawn considerable attention to the generation and cellular function of tRNA-derived fragments. It has been shown that tRNA fragmentation represents an evolutionary conserved, tissue- and cell type-specific phenomenon. Depending on the organism, tissue or cell type tRNA-derived fragments have been observed that differ in tRNA origin and sequence length. In contrast to other small non-coding RNAs, the 5' and 3' termini of tRNA fragments are heterogeneous. On the other hand, a common denominator for all observed tRNA fragments is the clustering of their ends within the open loop structures of tRNAs (D-, anticodon-, variable and T-loop) (Figure 1.5).

Importantly, tRNA fragments are already produced under steady-state conditions. These fragments have been called tRNA-derived RNA fragments (tRFs, (Lee et al., 2009a)) or tRNA-derived small RNAs (tsRNAs, (Haussecker et al., 2010)). tRFs have been deliberately classified as tRF-1, tRF-3 and tRF-5 according to the tRNA region from which they originate (Lee et al., 2009a). tRF-1 fragments correspond to the 3' trailers of pre-tRNAs (Figure 1.5) that are generated by the endonucleolytic activity of RNaseZ/ELAC2 (Lee et al., 2009a), an enzyme that is normally involved in the maturation of tRNAs (Phizicky and Hopper, 2010). tRF-3 and tRF-5 fragments derive from the 3'- and 5'- ends of mature tRNAs (Figure 1.5) that have been cleaved within the T- or D-loop, respectively (Heyer et al., 2012; Lee et al., 2009a; Li et al., 2012). The function of tRNA-derived fragments is not well understood. tRFs are found to associate with Argonaute complexes (Burroughs et al., 2011; Cole et al., 2009; Haussecker et al., 2010) and it was proposed that they can act as *bona fide* small silencing RNAs (Burroughs et al., 2011; Cole et al., 2009; Haussecker et al., 2010) or compete with Ago binding for other small RNAs (Haussecker et al., 2010).

tRNA fragments can be produced by various prokaryotic and eukaryotic toxin anticodon nucleases (Ardelt et al., 1991; Butler et al., 1991; Jiang et al., 2001; Klassen et al., 2008; Lu et al., 2008; Ogawa et al., 1999; Saxena et al., 2002; Tomita et al., 2000), are developmentally controlled (Haiser et al., 2008; Lee and Collins, 2005; Li et al., 2008) or are caused by stress-released endonucleases during many conditions (starvation, oxidative stress, heat or cold, UV, hypoxia) (Fu et al., 2009; Hsieh et al., 2009; Lee and Collins, 2005; Schaefer et al., 2010; Thompson et al., 2008; Yamasaki et al., 2009; Zhang et al., 2009).

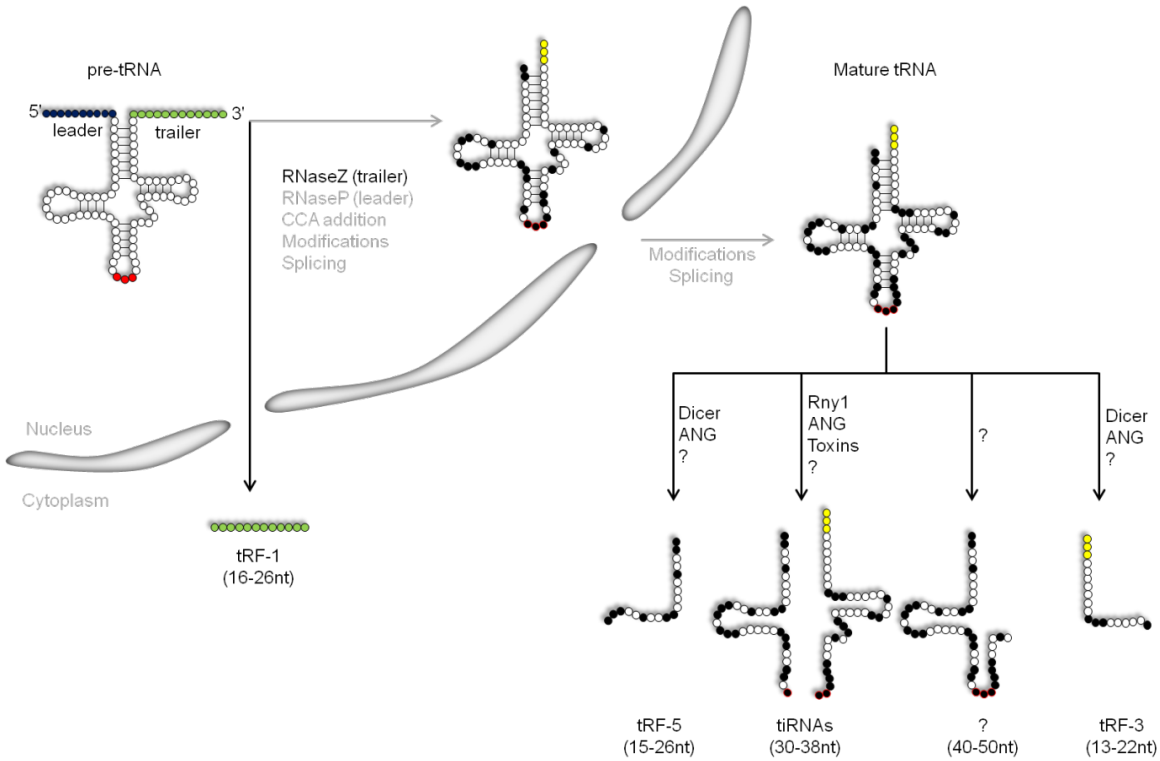

Figure 1.5: A schematic representation of tRNA fragments.

tRNA fragments form a heterogeneous group of molecules generated by endonucleolytic cleavage of intact tRNAs. During the nuclear pre-tRNAs processing endonuclease RNaseZ cleaves tRF-1 (trailer) from 3' terminus of pre-tRNAs. tRF-3 and tRF-5 are generated by the endonucleolytic cleavage in T- and D-loop of mature tRNAs, respectively. Stress induces cleavage of mature tRNAs in the anticodon loop. The tRNA fragments are also produced by endonucleolytic cleavage in the variable loop of mature tRNAs. White circles: unmodified nucleotide; black circles: nucleotides that are modified in some or all tRNA species; red circles: anticodon nucleotides; red-framed black circles: anticodon nucleotides that are modified in some tRNAs; yellow circles: the CCA 3' terminus; blue circles: leader sequence; green circles: trailer sequence.

Two stress-induced endonucleases have been described that specifically cleave mature tRNAs in the anticodon loop in yeast (Rny1, an RNase T2 family protein, (Thompson and Parker, 2009)) and angiogenin in mammalian cells (Saikia et al., 2012; Yamasaki et al., 2009). Their endonucleolytic activities produce tRNA fragments that have been named stress-induced tRNA-derived RNAs (sitRNAs, (Li et al., 2008)) or tRNA-derived stress-induced RNAs (tiRNAs, (Yamasaki et al., 2009)) (Figure 1.5). Stress-induced tRNA fragments appear to be important for stress survival (Thompson et al., 2008) but their exact function is still elusive. One mode of action is the direct interference of tRNA halves with the translation machinery (Saikia et al., 2012; Yamasaki et al., 2009). Studies in plants and human cells showed that 5'-fragments cause translational arrest (Ivanov et al., 2011; Zhang et al., 2009). In addition, only 5'- but not 3'-derived tRNA fragments promoted the assembly of stress granules (Emara et al., 2010). Stress-induced tRNA fragments could also serve as long-distance signals as indicated by work in starving plants (Zhang et al., 2009) implicating tRNA fragments in the adaption to certain stresses.

1.4 Cellular Stress Responses

All living organisms are exposed to biotic stressors such are various pathogen infections as well as to abiotic stresses like extreme temperature change, UV, dehydration, starvation, oxidative and osmotic insult and various toxins. Throughout evolution organisms have developed highly efficient mechanisms in response to these environmental influences, which allowed continuous adaptation and was crucial for the survival of present day species.

1.4.1 Stress Responses to Abiotic Stresses

During stress responses, a wide range of mechanisms is activated to neutralize stress stimuli. One important component of these mechanisms is the regulation of RNA metabolism. The transcriptional stress response is based on nucleosome remodeling and recruitment of stress-induced transcription factors. Changes in nucleosome organization facilitated by chromatin-remodeling complexes is essential for the correct activation of stress response genes (Mas et al., 2009; Petesch and Lis, 2008). In addition, recruitment of specific transcription factors is important for efficient transcriptional stress responses (Miller et al., 2011; Zanton and Pugh, 2006).

The control of translation is particularly important for the cellular stress response as it allows for rapid changes in gene expression. All stresses impinge on the activation of signaling cascades that lead to reversible phosphorylation changes of proteins, which are involved in translation initiation thereby causing the global inhibition of protein synthesis (Holcik and Sonenberg, 2005; Spriggs et al., 2010). Also, RNA interfering (RNAi) plays an important role in post-transcriptional modulation of gene expression following stress responses (Leung and Sharp, 2010). In contrast to global translational inhibition multiple mechanisms are evolved to enable the expression of stress response genes. Cap-independent recruitment of stress-response mRNAs via internal ribosome entry sites (IRESs) or the presence of upstream open reading frames (within 5'UTR) allows protein synthesis when cap-dependent translation is compromised (Spriggs et al., 2008).

Various stresses can induce the accumulation of misfolded or unfolded proteins causing endoplasmic reticulum (ER) stress. The mechanism referred to as unfolded protein response (UPR) in ER activates specific signaling cascades that lead to the expression of ER homeostasis genes (Lee et al., 2003; Yoshida et al., 2001) and in extreme cases to growth arrest and the induction of apoptosis (Kojima et al., 2003; Marciniak et al., 2004; Zinszner et al., 1998). Recent studies revealed that not only abiotic stresses which cause ER stress are able to activate UPR but also infections by different pathogens (Clavarino et al., 2012; Zhang and Kaufman, 2008) suggesting an interplay between stress signaling and immunity.

1.4.2 Stress Responses to Biotic Stresses/Innate Immune Responses

Eukaryotes evolved complex and systemic responses to various biotic stressors (e.g. viruses, bacteria and fungi). Although vertebrates developed also adaptive immune systems, innate immunity is an ancient and conserved survival mechanism in eukaryotes. An intricate system of cell-surface based receptors is the hallmark of eukaryotic innate immunity. These receptors detect RNA, DNA or specific surface molecules of invading pathogens and induce immune system responses. These responses are complex and engage a variety of cells and signaling cascades, which are involved in different processes (e.g. phagocytosis, encapsulation, coagulation, melanization) to suppress the pathogen infection (Figure 1.6 represents host defense system in *Drosophila*).

Innate immunity pathways are not well conserved at the molecular level since different organisms vary greatly in the complexity of their innate immune responses. However, the Toll pathway is a strongly conserved signaling cascade that activates antimicrobial peptides (AMPs) in response to infections with different pathogens (Flajnik and Pasquier, 2004). Although also existent in invertebrates, Toll proteins do not function as pattern recognition receptors but are activated by cytokines (Figure 1.6) (Lemaitre and Hoffmann, 2007). In contrast to the Toll pathway, various Toll-independent pathways exist in different species and their mode of action is still poorly understood.

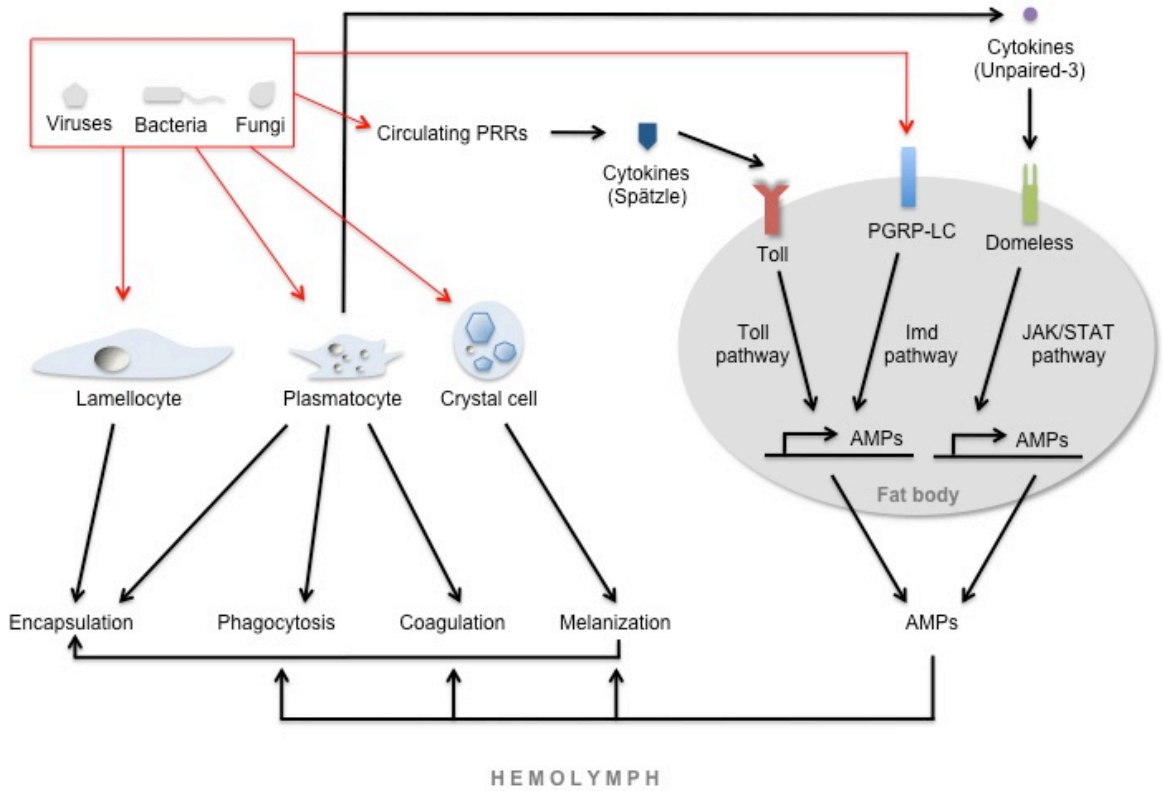

Figure 1.6: Schematic representation of *Drosophila* host defense.

Pathogen infections elicit a broad range of interconnected and synergistic defense elements that include different cells and signaling pathways. PRR= pattern recognition receptors. (Adapted from (Lemaitre and Hoffmann, 2007))

For instance, *Drosophila* uses the Imd (Immune deficiency) and JAK/STAT pathways in a Toll-independent manner to react to infections (Figure 1.6). The Imd pathway employs peptidoglycan recognition protein LC (PGRP-LC) as pattern recognition receptor, which triggers the expression of AMPs (Gottar et al., 2002; Lemaitre and Hoffmann, 2007). Although the Imd pathway shares some similarities with the vertebrate TNF-receptor pathway the level of conservation between these signaling cascades is still disputed (Lemaitre and Hoffmann, 2007). The JAK/STAT pathway is required but not sufficient for the control of viral infections and is dispensable for the response to infections with other pathogens (Dostert et al., 2005). Although the JAK/STAT signaling cascade is well described (Agaisse et al., 2003), the exact role in host defense mechanisms is still elusive.

In addition to these signaling cascades, plants and invertebrates use also RNA interference (RNAi)-based mechanisms to suppress infections with abundant biotic stressors such as viruses. Recent work in *Drosophila* has revealed the importance of small interfering RNA (siRNA) in the response to the virus infection (van Rij et al., 2006; Wang et al., 2006)

1.5 Small Interfering RNA Pathway

Small RNAs with silencing capability were first discovered in C. elegans (Lee et al., 1993). Since the basic mechanism of RNAi was established (Fire et al., 1998) many classes of small RNAs have emerged. Common features of all small RNAs are that their length is between 20-30 nucleotides and that all associate with members of the Argonaute family of proteins. Based on their biogenesis and modes of target regulation small RNAs are divided in three main classes: microRNAs (miRNAs), small interfering RNAs (siRNAs) and Piwi-interacting RNAs (piRNAs).

miRNAs and siRNAs are produced by activity of Dicer proteins, which cleaves double-stranded RNA (dsRNA) precursors into small RNA duplexes. Both, miRNAs and siRNAs, are loaded into members of the Ago clade of Argonaute proteins and together with additional factors they constitute the effector complex known as RNA-induced silencing complex (RISC) (Carthew and Sontheimer, 2009; Kim, 2005). The biogenesis of piRNAs does not involve Dicer proteins nor dsRNA precursors but the activity of various members of the Piwi clade of Argonaute proteins (Ishizu et al., 2012). While the biological function of miRNA is the inhibition of protein translation or mRNA degradation, siRNAs and piRNAs play many different roles including mobile element control (Ghildiyal and Zamore, 2009; Malone and Hannon, 2009), post transcriptional gene silencing (PTGS) (Smalheiser et al., 2011; Watanabe et al., 2008) and maternal mRNA decay and translational inhibition in early embryogenesis (Rouget et al., 2010). After their initial classification, it has become clear that the distinction between various small RNA classes and their biological functions cannot be

made solely on the basis of small RNA identity and Argonaute interaction. It appears now that small RNA pathways are more interconnected than previously thought (Malone and Hannon, 2009) and that all of them impact on gene regulation and protect the cell from exogenous and endogenous biotic stressors.

Maintenance of the genome stability is equally important in germ line and in somatic tissues. According to the origin of double stranded precursors RNAs, siRNAs are divided in exogenous and endogenous siRNAs (Figure 1.7, exo-siRNA and endo-siRNA, respectively). Exo-siRNAs arise from ectopically introduced double stranded RNA precursors and occur in response to virus infection in different organisms (Myles et al., 2008; Qu et al., 2005; van Rij et al., 2006; Voinnet, 2008; Wang et al., 2006). While vertebrates evolved protein-based immune systems (Vilcek, 2006), plants and invertebrates exhibit antiviral defense through the process of RNA silencing (Katiyar-Agarwal et al., 2006; Li et al., 2002; Lu et al., 2005; Myles et al., 2008; Qu et al., 2005; van Rij et al., 2006; Voinnet, 2008; Wang et al., 2006; Wilkins et al., 2005). The exo-siRNA-dependent antiviral immunity involves production of virus-derived exo-siRNAs and results in specific silencing of viruses by Ago-mediated cleavage of viral RNA (Figure 1.7).

Recent work also revealed existence of endo-siRNAs in many species (Ambros et al., 2003; Chen et al., 2005; Czech et al., 2008; Kawamura et al., 2008; Okamura et al., 2008b; Tam et al., 2008; Watanabe et al., 2008; Zilberman et al., 2003). The dsRNA precursors for endo-siRNA production originate form transposons and other mobile and repetitive elements, from convergent transcription of protein-coding genes (cis-natural antisense transcripts; cis-NATs) and from structured genomic loci (Figure 1.7) (Chung et al., 2008; Czech et al., 2008; Ghildiyal et al., 2008; Iida et al., 2008; Kawamura et al., 2008; Okamura et al., 2008b; 2008a; Tam et al., 2008; Vazquez et al., 2004; Watanabe et al., 2008). Endo-siRNAs guide Argonautes to mediate RNA cleavage, which plays an important role in the regulation of endogenous transposable elements (Chung et al., 2008; Ghildiyal et al., 2008; Iida et al., 2008), in the post-transcriptional gene regulation (Rehwinkel et al., 2006; Tam et al., 2008; Vazquez et al., 2004; Watanabe et al., 2008) as well as in the regulation of gene expression in response to developmental and environmental stimuli (Borsani et al., 2005; He et al., 2008; Lucchetta et al., 2009; Ron et al., 2010; Smalheiser et al., 2011; Watanabe et al., 2008).

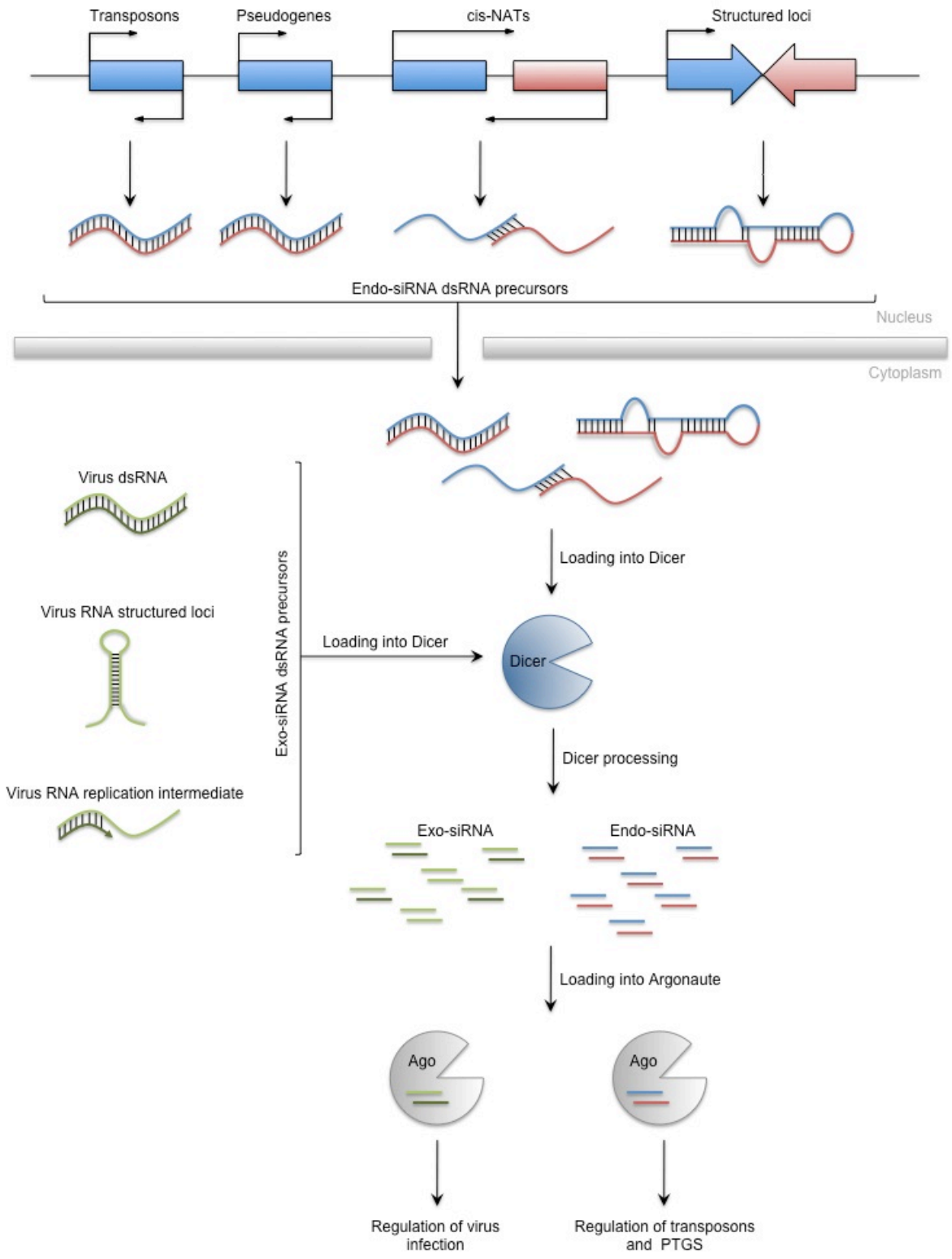

Figure 1.7: Exo- and endo-siRNA biogenesis pathways.

Exo-siRNAs are derived from viral dsRNA, viral RNA structured loci or from viral RNA replication intermediate that are processed by Dicer and loaded into Argonaute to target and cleave viral RNA. Endo-siRNAs can arise from bi-directionally transcribed transposons, from protein-coding genes that can pair with their cognate pseudogenes, from complementary overlapping transcripts (cis-NATs) or structured loci that can pair intra-molecularly to produce long dsRNA. These dsRNA precursors are processed by Dicer and loaded into Argonaute to silence transposon and protein coding mRNAs.

1.6 Aims of the PhD Thesis

Dnmt2 genes have been strongly conserved during evolution, suggesting a biological function that would justify long-term evolutionary selection. While the molecular function of Dnmt2 enzymes is tRNA methylation still very little is known about the biological function of Dnmt2 proteins and their methylated substrates.

The main aim of this doctoral thesis was to characterize the biological function of the RNA methyltransferase activity of Dnmt2 on tRNAs in *Drosophila melanogaster* in the context of mobile element control during biotic and abiotic stress conditions.

1. Increased expression of immune response genes indicated increased and thereby inefficient responses of *Dnmt2* mutant flies to pathogen infections. The aim of this work was to identify the stressor causing upregulated immune pathways in *Dnmt2* mutants and to explore the role of Dnmt2 in the suppression of pathogen infections.

2. The up-regulation of mobile elements in *Dnmt2* mutant flies and association of Dnmt2 with cellular stress responses indicated connections between these phenotypes. The aim of this work was to investigate Dnmt2 functions in mobile element control under abiotic stress conditions.

Chapter 2

Materials and Methods

2.1 Materials

Table 2.1: Technical devices and consumptive materials

Name	Manufacturer
96-well Plates	ThermoScientific
384-well Plates	Steinbrenner Laborsysteme
454 Genome Sequencer FLX Titanium	Roche
Agarose Gel Electrophoresis Chamber	BioRad
Bio-Dot® Microfiltration Apparatus, 96-well	BioRad
Centrifugal Tubes (15, 50 ml)	Greiner Bio One
Centrifuge 5415D	Eppendorf
Centrifuge 5415R	Eppendorf
Developing Cassette	Dr. Goos Suprema
Eppendorf Pipettes	Gilson
Filter tips 10, 20, 200, 1000 µl	Nerbe
Hybridization Oven	PeqLab
Illumina HiSeq 2000 System	Illumina
Microvolume Spectrometer, NanoDrop 2000	ThermoScientific, PeqLab
PAGE Chamber	Amersham Bioscience
Pasteur Pipettes	WU Mainz
PCR tubes	ThermoScientific
pH Meter	NeoLab
Pipette Tips 10, 200, 1000 µl	Sarstedt
Photometer	Eppendorf
Power Supply	Consort
Reaction Tubes	Eppendorf
Real Time PCR System, LightCycler 480	Roche
Serological Pipettes 5, 10, 20, 50 ml	Falcon
Thermocycler, DNA Engine	BioRad
Thermo Mixer	Eppendorf
Transfer Chamber, Semi-Dry Blotting	PeqLab
Transfer Chamber, Wet Blotting	BioRad
UV Crosslinker, Stratalinker	Stratagene
UV Cuvettes	Greiner Bio One
UV Gel Documentation, E.A.S.Y® Doc plus	Herolab
Water Bath, TW12	Julabo
X-ray Film	Fujifilm

Table 2.2: Chemicals, reagents and kits

Name	Manufacturer
^{32}P-αdCTP	Perkin Elmer
^{32}P-γATP	Hermann Analytics
β-Mercaptoethanol	Sigma-Aldrich
Acetic Acid	Merck
Acrylamide (37,5:1) Rotiphorese® 30	Roth
Agar	Gerbu
Agarose	Roth
Ammonium Acetate	Fluka
Ammoniumpersulfat	Sigma-Aldrich
Bio Spin 6 Chromatography Columns	BioRad
Bisulfite Kit, EpiTect	Qiagen
Bradford Solution (Protein Assay)	BioRad
Boric Acid	Sigma-Aldrich
Chloroform	VWR
Denhardt's Reagent, 50x	Invitrogen
Deoxynucleotides Mix (dNTPs)	Agilent
Deoxynucleotides (dATP, dGTP, dCTP, dTTP)	New England BioLabs
Dextrose	Fluka
Diethylpyrocarbonate (DEPC)	Sigma-Aldrich
Digoxygenin-11-dUTP	Jena Bioscience
Dithiothreitol (0.1 M) (DTT)	Invitrogen
Dithiothreitol (DTT)	Gerbu
DNeasy Blood and Tissue Kit	Qiagen
DNA Ladder, O'RangeRuler 10bp	Fermentas
DNA Ladder, O'RangeRuler 100bp+500bp	Fermentas
DNase, Turbo™	Ambion
Empigen®BB Detergent	Sigma-Aldrich
Ethanol	Sigma-Aldrich
Ethidium bromide	Roth
Ethylenediaminetetraacetic acid (EDTA)	Merck
Ethyleneglycol-bis(2-aminoethylether)- N, N, N', N'-tetraacetic acid (EGTA)	Roth
Formaldehyde	Sigma-Aldrich
Formamide	Merck
Gel Extraction Kit, QIAquick	Qiagen
GFP-Trap®-M	Chromotek
Glycerol	Sigma-Aldrich
Glycine	Sigma-Aldrich
Glyco Blue	Ambion
HEPES	Roth, Karlsruhe
Hydrogen Chloride (37%) (HCl)	Sigma-Aldrich
Immobilon™ Western Kit	Merck Millipore
Isopropanol	Sigma-Aldrich
Magnesium Acetat (MgOAc)	Roth
Methanol	Sigma-Aldrich,

Methylen Blue	Roth
MiniPrep Kit, QIAprep®	Qiagen
MOPS	Roth
N, N, N', N'- Tetramethylethylenediamine (TEMED)	Roth
Nick Translation Kit	Roche
Nipagin M	Nipa Laboratories
Nitrocellulose Transfer Membrane	Whatman
NP40	Sigma-Aldrich
Nylon Membrane, positively charged	Roche
PBS, Rnase/Dnase free	Gibco
Phenol	Roth
Phenylmethylsulfonylfluoride (PMSF)	VWR
Ponceau Solution	Sigma-Aldrich
Potassium Chloride (KCl)	Roth
Potassium Hydrogen Phosphate (K_2HPO_4)	Roth
Powdered Milk	Roth
Protease Inhibitors, Complete tablets	Roche
Protein Ladder, PageRuler #SM26616	ThermoScientific
Proteinase K	Ambion
Restriction Enzymes	New England Biolab
RNA ladder, RiboRuler HR #SM1821	ThermoScientific
RNA ladder, RiboRuler LR #SM1831	ThermoScientific
RNA Loading Buffer, 2x	ThermoScientific
Rnase Inhibitor, RiboLock	ThermoScientific
RnaseOne™	Promega
Sequencing Gel System Rotiphorese®	Roth
Small RNA Sample Preparation Kit, TrueSeq	Illumina
Sodium Acetate (NaOAc)	Roth
Sodium Chloride (NaCl)	Sigma-Aldrich
Sodium Citrate	Sigma-Aldrich
Sodium Dodecyl Sulfate (SDS)	Roth
Sodium Hydrogen Phosphate (Na_2HPO_4)	NeoLab
Sodium Hydroxide (NaOH)	Sigma-Aldrich
Streptavidin Magnetic Beads	Promega
Sucrose	Fluka
SuperScript® III First-Strand Synthesis System for RT-PCR	Invitrogen
SYBR Gold Dye	Invitrogen
SYBR Green Mix	ThermoScientific
T4 Ligase	New England Biolab
T4 Polynucleotide Kinase	Takara
Taq Polymerase	ThermoScientific
Terminal Deoxynucleotidyl Transferase (TdT)	Fermentas
Tris-Base (99.9 %)	Sigma-Aldrich
Triton X-100	Gerbu
Trizol	Ambion
Tween 20	Sigma-Aldrich
QuantiTect Reverse Transcription Kit	Qiagen

Table 2.3: Buffers and media

Name	Composition	
Borate Buffer, 10x, pH 8,8	15,46 g Boric Acid to 1 l H_2O	
Empigen Buffer	30 mM HEPES-KOH pH 7.4 150 mM NaCl 2 mM MgOAc 0.5% Empigen Add before use: 0,01 U/µl RNAsIn 5 mM DTT 1mM PMSF 1x Protease Inhibitors	
Formaldehyde Gel, 2%	3,6 g Agarose 282 ml 1x MOPS 16,2 ml Formaldehyde (37%)	
MOPS Electrophoresis Buffer	0,2 M MOPS 20 mM NaOAc 10 mM EDTA pH 8,0	
Northern-Hybridization Solution	5x SSC 20 mM Na_2HPO_4 pH 7.4 7% SDS 1x Denhardt's Reagent	
Northern-Wash 1	3x SSC 5% SDS	
Northern-Wash 2	1x SSC 1% SDS	
Phosphate Buffered Saline (PBS), 10x	1,37 M NaCl, 27 mM KCl, 100 mM Na_2HPO_4 x $2H_2O$ 18 mM KH_2PO_4	
PBS-Tween 20 (PBST)	1x PBS 0,1% Tween20	
Protein Extraction Buffer	25 mM Tris pH 8.0 27,5 mM NaCl 20 mM KCl 25 mM Sucrose 10 mM EDTA 10 mM EGTA 10% (v/v) Glycerol 0.5% NP40 1% Triton X-100 Add before use: 1 mM DTT 0.4 mM PMSF 1x Protease Inhibitors	
SDS-Polyacrylamide Gel (SDS-PAGE)	4 % Collecting Gel	1 ml Buffer B 1,7 ml Acrylamide 7,3 ml H_2O 50 µl 10%APS 18 µl TEMED

	10 % Separating Gel	6,8 ml Buffer A 6,8 ml Acrylamide 6,3 ml H2O 120 µl 10% APS 20 µl TEMED
	15 % Separating Gel	6,8 ml Buffer A 10,0 ml Acrylamide 3,2 ml H2O 120 µl 10% APS 20 µl TEMED
SDS-PAGE Buffer A, pH 8,8	34,1 g Tris 7,5 ml 10% SDS 6 ml 37% HCl to 250 ml H_2O	
SDS-PAGE Buffer B, pH 6,8	7,6 g Tris 5 ml 10% SDS 5 ml 37% HCl to 50 ml H_2O	
SDS-PAGE Loading Buffer, 2x	4 ml Buffer B 8 ml Glycerol 2 ml β-Mercaptoethanol 16 ml 10% SDS 2 ml Brom-Phenol Blue 8 ml H_2O	
SDS-PAGE Running Buffer, 10x	144 g Glycine 30,3 g Tris Add to 1x buffer: 0,1 % SDS	
Southern-Hybridization Solution	50 % De-ionized Formamide 6x SSPE 5x Denhardt's Reagent 0.5 % SDS 100 µg/ml Herring Sperm DNA	
Southern-Wash 1	7x SSPE 0.1% SDS	
Southern-Wash 2	1x SSPE 0.5% SDS	
Southern-Wash 3	0.1x SSPE 1 % SDS	
SSC, 20x	3 M NaCl 300 mM Sodium Citrate	
SSPE, 20x	3 M NaCl 200 mM Na_2HPO_4 x $2H_2O$ 200 mM EDTA	
Standard Drosophila Medium	18 g Agar 150 g Dextrose 170 g Maize Meal 30 g Dry Yeast 50 ml 10% Nipagin M 1700 ml H_2O	
TRIS-Borat-EDTA Buffer (TBE), 10x	890 mM Tris Base 890 mM Boric Acid 20 mM EDTA	

TBE-Agarose Gel	1% (w/v)Agarose 1x TBE			
UREA-PAGel (Sequencing Gel System Rotiphorese®)		Gel Solution	Diluent	Buffer
	15%	30 ml	15 ml	5 ml
	20%	40 ml	5 ml	5 ml
Western Blocking Solution	5% (w/v) Powdered Milk 1x PBS			
Western-Blotting Buffer	1x Borate Buffer 20% Methanol 1mM DTT 0,5mM EDTA			

Table 2.4: Primary antibodies

Name	Imunogen	Host	Manufacturer
Anti-Dnmt2	Dnmt2	Rabbit	Schaefer *et al.,* 2008
Anti-DCV	DCV capsid	Chicken	Cherry and Perrimon, 2004
Anti-Hsp70	Hsp70	Mouse	Abcam (AB5439)
Anti-Tub	Tubulin	Mouse	Sigma (T9026)
Anti-Dcr-2	Dicer-2	Mouse	Abcam (Ab4732)
Anti-dsRNA	dsRNA	Mouse	Schönborn *et al.,* 1991

Table 2.5: Secondary antibodies

Name	Imunogen	Host	Manufacturer
Anti-mouse	Mouse IgG	Goat	Jackson ImmunoResearch (115-035-003)
Anti-rabbit	Rabbit IgG	Goat	Jackson ImmunoResearch (111-035-003)
Anti-chicken	Chicken IgY	Rabbit	Abcam (AB6753)

Table 2.6: Primers and oligonucleotides

Name	Amplicon	Sequence (5'-3')
qPCR primers		
HD174	Rp49_fwd	CGGATCGATATGCTAAGCTGT
HD175	Rp49_rev	GCGCTTGTTCGATCCGTA
HD202	Hsp70A_fwd	CCTGGAGAGCTACGTCTTCAAT
HD203	Hsp70A_rev	GTCGTTGCACTTGTCCAA
ZD23	TART_fwd	CCGCCCACCCCCTTTAGCAC

ZD24	TART_rev	GACTTTGGACAGTCTTTTCC
ZD25	Thare_fwd	CCTCTCGATCGACAATACAG
ZD26	Thare_rev	GTTAGTGTGGGTCGTTGCTG
ZD32	Het-A_fwd	GCTTCAGGCATGCCAAAAACTC
ZD33	Het-A_rev	GTACGCGCTAATATGCTGCC
ZD43	Doc_fwd	CAACTAACAATTATTGACTATAGTAAT
ZD44	Doc_rev	AGAGCCGGCGCTCGTCTTGTT
ZD50	Inv4_fwd	GTGTTCAAGGGCGCCCATAGCGACTCAG
ZD51	Inv4_rev	CTTGTTGCTGACAAAGCTTCTGCCTTG
HD157	Gypsy_fwd	CTTCACGTTCTGCGAGCGGTCT
HD158	Gypsy_rev	CGCTCGAAGGTTACCAGGTAGGTTC
ZD_86	297_fwd	AAAGGGCGCTCATACAAATG
ZD_87	297_rev	TGTGCACATAAAATGGTTCG
HD970	Rover_fwd	CACAACAAGAACAGACAGCAC
HD971	Rover_rev	GATCCAGTGTCAATTAGGCAC
ZD109	GFP_fwd	ACCCTCGTGACCACCCTGACCTAC
ZD110	GFP_rev	GCTCCTGGACGTAGCCTTCGG
HD672	Drosocin _fwd	GTCCACCACTCCAAGCAC
HD673	Drosocin _rev	CTTTAGGCGGGCAGAATGGG
HD674	Metchnikowin _fwd	CGCCACCGAGCTAAGATGC
HD675	Metchnikowin _rev	GGTTAGGATTGAAGGGCGAC
HD611N	Vago_fwd	TGCAACTCTGGGAGGATAGC
HD821N	Vago _rev	AATTGCCCTGCGTCAGTTT
HD822N	Vir-1 _fwd	GATCCCAATTTTCCCATCAA
HD823N	Vir-1 _rev	GATTACAGCTGGGTGCACAA
HD824N	IM1 _fwd	TCCACTGTCGCCCGATCC
HD825N	IM1 _rev	CTTGGGTTGAAACTTCCTACTTGC
HD826N	Cecropin A1 _fwd	GCGTTGGTCAGCACACTC
HD827N	Cecropin A1 _rev	CAGTTGCGGCGACATTGG
HDT047	DCV _fwd	TCATCGGTATGCACATTGCT
HDT048	DCV _rev	CGCATAACCATGCTCTTCTG
HDT053	Turandot A _fwd	GGTTTGCTTCAGCGTTCCAAAAAGTCATAACC
HDT054	Turandot A _rev	ATTAAAACAATATTAACCAGTGAATAATTGAG
ZD123	Nora virus _fwd	AACCTCGTAGCAATCCTCTCAAG
ZD124	Nora virus _rev	TTCTTGTCCGGTGTATCCTGTATC

ZD119	DXV _fwd	GGAGTTGAAGCCACGGTTTG
ZD120	DXV _rev	GACGATCTTGCCAGTTGGCTCATCG
ZD121	Sigma virus _fwd	ATGTAACTCGGGTGTGACAG
ZD122	Sigma virus _rev	CCTTCGTTCATCCTCCTGAG
Diagnostic qPCR		
ZD245	A. pomorum fwd	TGTTTCCCGCAAGGGACCTCT
ZD246	A. pomorum rev	AGAGTGCCCAGCCCAACCTGA
ZD247	A. tropicalis fwd	TAGCTAACGCGATAAGCACA
ZD248	A. tropicalis rev	ACAGCCTACCCATACAAGCC
ZD249	L. fructivorans fwd	AACCTGCCCAGAAGAAGGGGA
ZD250	L. fructivorans rev	GCGCCGCGGATCCATCCAAA
ZD251	L. plantarum fwd	TGTCTCAGTCCCAATGTGGCCG
ZD252	L. plantarum rev	GGCTATCACTTTTGGATGGTCCCGC
Northern probe primers end oligonucleotides		
HD734	Dm $tRNA^{Asp}$_5’	CTAACCACTATACTATCGAG
HD040N	esi2.1	GGAGCGAACTTGTTGGAGTCAA
HD243	2s rRNA	TACAACCCTCAACCATATGTAGTCCAAGCA
HD242	5.8s rRNA	CAACACGCGGTGTTCCCAAGCCG
HD174	Rp49_fwd	CGGATCGATATGCTAAGCTGT
HD175	Rp49_rev	GCGCTTGTTCGATCCGTA
HD672	Drosocin _fwd	GTCCACCACTCCAAGCAC
HD673	Drosocin _rev	CTTTAGGCGGGCAGAATGGG
HD674	Metchnikowin _fwd	CGCCACCGAGCTAAGATGC
HD675	Metchnikowin _rev	GGTTAGGATTGAAGGGCGAC
HDT047	DCV _fwd	TCATCGGTATGCACATTGCT
HDT048	DCV _rev	CGCATAACCATGCTCTTCTG
Southern probe primers		
HDT021	Inv4 5’ LTR_fwd	TGTCGGAGCGCGACTCTTCG
HDT026	Inv4 5’ LTR_rev	TGGGCAAAGCTCTCTCCAGG
Inverse PCR primers		
HD90	5’IRRS-Element_fwd	GACTGTGCGTTAGGTCCTGTTCATTGTT
HD69	5’IRRS-Element_rev	ACACAACCTTTCCTCTCAACAA
In vitro transcription template primer		
ZD107	EGFP fwd	taatacgactcactatagggACCCTCGTGACCACCCTGACCTA
ZD108	EGFP rev	taatacgactcactatagggGACCATGTGATCGCGCTTCTCGT

ZD253	DCV IRES1 fwd	taatacgactcactatagggCGTGTGTACATATAAATATG
ZD126	DCV IRES1 rev	CAACCGCTTCCACATATCCTG
ZD257	DCV IRES2 fwd	taatacgactcactatagggGCGGACCCTTTGTACGACTTTTAG
ZD256	DCV IRES2 rev	GTACAATCTCTTTTTGCTCGGAAG
ZD166	DCV ctrl fwd	taatacgactcactatagggCAGAGATGTTTACTCAAT AC
ZD134	DCV ctrl rev	GTGTGCAGCATC ATCAGAAC
PCR primers for *in vitro* binding assay		
ZD125	DCV IRES1_fwd	TTTATATCGTGTGTACATAT AATATG
ZD126	DCV IRES1_rev	CAACCGCTTCCACATATCCTG
ZD255	DCV IRES2_fwd	GCGGACCCTTTGTACGACTTTTAG
ZD256	DCV IRES2_rev	GTACAATCTCTTTTTGCTCGGAAG
ZD133	DCV ctrl_fwd	CAGAGATGTTTACTCAATAC
ZD134	DCV ctrl_rev	GTGTGCAGCATCATCAGAAC
Stem loop RT primer		
HD649	tRNA-Asp rev	CTCAACTGGATTGGCTNNNNNGATAAATCCAGTTGAG TGGCTCCC
RIP primers		
HD254	tRNA-Asp fwd	TCCTCGATAGTATAGT
HD616	tRNA-Asp rev	CTCAACTGGATTGGCT
ZD127	DCV 698-1435fwd	GTGTATGATCTATACGCAC
ZD128	DCV 698-1435 rev	CAATCTTCATAATATCCTC
ZD137	DCV 4443-5163 fwd	GAAGAATATTTCCTCAC
ZD138	DCV 4443-5163 rev	GGCGAAATGCAACTACAAAATG
ZD149	DCV 8841-9264 fwd	CAATTAATAGTGTCTTGCGTG
ZD150	DCV 8841-9264 rev	AGAAAACAACTATTATTTTAATTC
PCR primers for RNA bisulfite sequencing		
HD267	tRNA-Asp fwd	AGTATAGTGGTGAGTATT
HD616	universal_rev (used for Asp)	CTCAACTGGATTGGCT
HD503	tRNA-Gly_fwd	GTGGTTTAGTGGTAGAATGT
HD502	tRNA-Gly_rev	TACATCAATCAAAAATCA

2.2 Fly Treatments

2.2.1 Fly Strains and Husbandry

w^{1118}, *yw*, *Dnmt2*^{99} (Schaefer et al., 2010), *w*^{1118}/Y-HA1925 and *w*^{1118}/Y-HA1925; *Dnmt2*^{149} (Phalke et al. 2009), *Dnmt2*^{99};pGeno::Dnmt2-EGFP (D2^{TG}) (Schaefer et al., 2008), *w*^{1118}; pUbq::Dnmt2-EFGP, *Dnmt2*^{99}; pUbq::Dnmt2-cat^{mutant}-FLAG (D2$^{cat\Delta}$), *w(*); ago2*^{414} (DGRC), *y*^{d2} *w*^{1118}; *Dcr-2*^{L811fsX} (Bloomington), Act5C-GAL4/CyO; Ubq-GFP (Bloomington 4888 and 4414). All flies were kept Standard *Drosophila* Medium at 25°C, 60% humidity, under a 12-h light–dark cycle.

2.2.2 Heat Shock and Recovery Experiments

All heat shock treatments of adult flies were performed at 37°C for 1 hour in a water bath. After the heat shock, flies were kept at 25 °C on standard *Drosophila* medium for the indicated time periods. All heat shock treatments of second to third instar wandering larvae were performed at 37°C for 45 minutes in a water bath, followed by a recovery phase at 25°C for 1 hour and another heat shock at 37 °C for 45 minutes. After this treatment larvae were kept till adulthood at 25°C on standard *Drosophila* medium.

2.2.3 Phenotype Analyses

Flies were maintained on standard medium at 25°C, 60% humidity, under a 12-h light–dark cycle. For culturing flies under sub-optimal (crowded) conditions, flies were allowed to hatch but were not removed from the vials. These flies laid more eggs and finally succumbed to the crowded conditions. Developing larvae were feeding not only on medium, but also on the carcasses of the parental generation. Larvae, pupae and adults arising from this generation were scored for melanotic inclusions. For the phenotypic analyses after heat shock, second to third instar larvae were heat shocked as described above. After developing at 25°C adult flies were scored for phenotypes. For eye color phenotypic analysis after stress exposure, male adult flies (w^{1118}/Y-HA1925 and w^{1118}/Y-HA1925; *Dnmt2*^{149}) were heat shocked as described above. After recovery heat shocked males were crossed with non-heat shocked virgin females. The F1 generation was scored for a change of eye color phenotype.

2.2.4 Virus Infection by Inoculation

Inoculation experiments were performed with crude extracts from ca. 200 µg of *w*^{1118}, *Dnmt2*^{99}, pGeno::*Dnmt2*-EGFP flies. Flies were homogenized in 500 µl H2O and mixed with 500 µl watery yeast paste. The homogenates were used for feeding of freshly hatched flies (1 day old). After 24 hours flies were transferred to standard *Drosophila* medium and RNA was isolated 1 day and 10 days after the inoculation.

2.3 Nucleic Acids Analyses

2.3.1 RNA Extraction

Total RNA was isolated either from whole flies or after separation of soma from germ line tissues. Whole flies or tissues were homogenized in 1 ml Trizol and incubated for 5 min at RT. After adding 200 µl Chloroform samples were centrifuged for 20 min at 12000g. Aqueous phase was transferred into new tube and 1 volume of Isopropanol was added. After precipitation for 10 min at RT samples were centrifuged for 30 min at 16000g. The pellets were washed with 70% Ethanol and resolved in 50-100 µl RNase-free water.

2.3.2 Reverse Transcription (RT)

Reverse transcription was performed using QuantiTect Reverse Transcription Kit (Qiagen) or SuperScript III (Invitrogen).

First strand cDNA synthesis using the QuantiTect Reverse Transcription Kit (Qiagen)

cDNA synthesis reaction

Reagents	Amount	Incubation
RNA	1 µg	
7x gDNA Wipeout Buffer	2 µl	5 min at 42°C
H_2O	to 14 µl	
5x Reverse Transcriptase Buffer	4 µl	
Primers (random hexamers)	1 µl	30 min at 42°C
Reverse Transcriptase	1µl	15 min at 95°C
Σ	20 µl	

First strand cDNA synthesis using SuperScript III (Invitrogen)

Before reverse transcription using SuperScript III samples were treated with 2 U Turbo^{TM}DNAse for 30 min at 37°C followed by Phenol/Chloroform purification and Ethanol precipitation.

cDNA synthesis reaction

Reagents	Amount	Incubation
RNA	1 µg	5 min at 70°C
Primers (random hexamers) (50 ng/µl)	1 µl	
dNTPs (10 mM)	2 µl	
H_2O	to 13 µl	
5x Reverse Transcriptase Buffer	4 µl	10 min at 25°C 50 min at 50°C 15 min at 95°C
DTT (0,1 mM)	1 µl	
RNaseOUT™ (40 U/µl)	1µl	
Reverse Transcriptase® (200 U/µl)	1 µl	
Σ	20 µl	

2.3.3 Quantitative Polymerase Chain Reaction (qPCR)

qPCR analyses were performed in 384-well plates using the ABsolute QPCR SYBR Green Mix (Thermo Scientific). Primers used for qPCRs are listed in Table 2.6.

qPCR reaction

Reagents	Amount
cDNA, gDNA or extra-chromosomal DNA	1 µl or X ng
2x QPCR SYBR Green Mix	5 µl
Forward Primer (10 µM)	0,2 µl
Reverse Primer (10 µM)	0,2 µl
H_2O	3,6 µl
Σ	10 µl

qPCR conditions

Steps	Temperature	Time	Cycles
Denaturating	95°C	15 min	1
Cycling	95°C 60°C	10 sec 30 sec	40
Melting	95°C	-	1
Cooling	40°C	10 min	1

2.3.4 Northern Blotting

RNA was separated on 15% Urea-PAGE (Table 2.3) or 2% Formaldehyde Gel (Table 2.3). RNA was transferred to Nylon membranes (Roche) using semi dry blotting with 0,5x TBE for 30 min at 5V or wet blotting with 5x SSC overnight (Thomas, 1980). Blotted RNA was immobilized by UV cross-linking (Stratalinker) and by incubation at 80°C for 1 hour.

Hybridization using DIG Northern Starter Kit (Roche)

The hybridization was performed overnight at 40ºC with DIG-labeled PCR probes in hybridization solution supplied in the Kit. After hybridization the membrane was washed 2 times at RT for 5 min in DIG-Wash 1 (Table X) and 2 times at 40°C for 15 min in DIG-Wash 2. After the incubation in Blocking Solution (Roche) at RT for 30 min membrane was incubated with DIG-antibodies (1:10000, supplied in the Kit) in Antibody Solution (Roche) at RT for 30 min. The membrane was washed 2 times at RT for 15 min in Washing Buffer (Roche) and incubated for 5 min in Detection Buffer (Roche) prior to the incubation with CDP-Star solution (Roche) and exposure to the X-ray film (Fujifilm).

Probe labeling with DIG-dUTP

PCR reaction

Reagents	Amount
Genomic DNA or cDNA	100 ng or 1 µl
10x Taq Polymerase Buffer	2,5 µl
dNTPs (10 mM)	1 µl
DIG-dUTP (1 mM)	1 µl
Forward Primer (10 µM)	1 µl
Reverse Primer (10 µM)	1µl
Taq Polymerase (5 U/µl)	0,5 µl
H_2O	to 25 µl
Σ	25 µl

PCR conditions

Temperature	Time	Cycles
95°C	5 min	1
95°C 55°C 72°C	30 sec 30 sec 30 sec	30
72°C 4°C	10 min ∞	1

PCR products have been purified using QIAquick Gel Extraction Kit (Qiagen) and denatured at 95°C for 5 min prior to the overnight hybridization.

Hybridization using radioactive labeled probe

The hybridization was performed overnight at 38ºC ^{32}P-end labeled oligonucleotides in Northern-Hybridization Solution (Table 2.3). After washing at 38ºC for 15 min with Northern-Wash 1 (Table 2.3) and with Northern-Wash 2 (Table 2.3) for 15 min at room temperature, membranes were exposed to film at -80 ºC.

Radioactive probe labeling

Radioactive probe labeling reaction

Reagents	Amount
Oligonucleotide (20 µM)	1.5 µl
10x T4 Polynucleotide Kinase Buffer	2 µl
T4 Polynucleotide Kinase (10 U/µl)	1 µl
^{32}P-γATP (500µCi)	5 µl
H_2O	10,5 µl
Σ	20 µl

PCR products have been purified using Micro BioSpin 6 Chromatography Columns (BioRad) prior to the overnight hybridization.

2.3.5 Isolation of Extra-Chromosomal DNA and qPCR Analysis

Extra-chromosomal DNA was isolated from 20 flies using a Mini Prep Kit (Qiagen). Flies were homogenized in buffer P1, followed by all further purification steps according to the manufacturer's recommendations. qPCR analysis was performed on 100 ng of extra-chromosomal DNA as described in 2.3.3. Primers used for qPCR are listed in Table 2.6.

2.3.6 Southern Blotting

1 µg of extra-chromosomal DNA was separated on a 1% TBE-Agarose gel (Table X). DNA was denaturated by soaking the gel in 1.5 M NaCl/0.5 N NaOH, followed by transfer onto a Nylon membrane (Roche) using wet blotting with 10X SSC overnight (Southern, 1975). Blotted DNA was immobilized by UV cross-linking (Stratalinker). Hybridization was performed overnight at 50°C in Southern-Hybridization Solution (Table 2.3) with radioactive labeled probe. After washing with Southern-Wash 1 for 15 min at RT, Southern-Wash 2 for 15 min at

37°C, Southern-Wash 3 for 15 min at 50°C (Table 2.3), the membrane was exposed to X-ray film (Fujifilm) for 5 days.

Radioactive probe labeling

The *Invader4* specific 5' LTR probe was radioactively labeled (^{32}P-γdCTP) using a Nick Translation Kit (Roche).

PCR reaction

Reagents	Amount
Genomic DNA	100 ng
10x Taq Polymerase Buffer	2,5 µl
dNTPs (10 mM)	1 µl
Forward Primer (10 µM)	1 µl
Reverse Primer (10 µM)	1µl
Taq Polymerase (5 U/µl)	0,5 µl
H_2O	to 25 µl
Σ	25 µl

PCR conditions

Temperature	Time	Cycles
95°C	5 min	1
95°C 55°C 72°C	30 sec 30 sec 30 sec	30
72°C 4°C	10 min ∞	1

After PCR amplification the probe was purified using QIAquick Gel Extraction Kit (Qiagen) .

Nick Translation Reaction (Roche)

Reagents	Amount	Incubation
DNA	100 ng	35 min at 15°C 10 min at 68°C
10x Nick Translation Buffer	2 µl	
dATP, dTTP, dGTP Mix (0,4 mM)	3 µl	
^{32}P-γdCTP 200µCi	2 µl	
Enzyme Mix	2 µl	
H_2O	to 20 µl	
Σ	20 µl	

Radioactive labeled probe has been denatured at 95°C for 5 min prior to the overnight hybridization.

2.3.7 Inverse PCR for Mapping of Transposon Insertions

Single fly genomic DNA preparations were performed as described in (Gloor et al. 1993). 500 ng of genomic DNA was used for restriction with 20 units *EcoRI*. Ligation of digested DNA fragments was performed using 400 units T4 Ligase (NEB) in a reaction volume of 100 µl for 7 days at 4°C. 5 µl of each ligation reaction was used for PCR amplification.

PCR reaction

Reagents	Amount
Ligation Reaction	5 µl
10x Taq Polymerase Buffer	2,5 µl
dNTPs (10 mM)	1 µl
Forward Primer (10 µM)	1 µl
Reverse Primer (10 µM)	1µl
Taq Polymerase (5 U/µl)	0,5 µl
H_2O	to 25 µl
Σ	25 µl

PCR conditions

Temperature	Time	Cycles
95°C	10 min	1
95°C 55°C 72°C	45 sec 45 sec 2 min	40
72°C 4°C	10 min ∞	1

PCR amplicons were purified using QIAquick Gel Extraction Kit (Qiagen) and commercially sequenced. Primers used for inverse PCR are listed in Table 2.6.

2.3.8 Diagnostic qPCR

Genomic DNA from whole flies was extracted using the DNeasy Blood and Tissue Kit (Qiagen). Diagnostic qPCR analyses were performed on 100 ng of genomic DNA per reaction as described in 2.3.3. Primers are listed in Table 2.6.

2.3.9 RNA Bisulfite Analysis

For tRNA methylation analysis, reactions and amplifications were performed as described in (Schaefer et al., 2009). Prior to bisulfite treatment samples were treated with 2 U Turbo^{TM}DNase (Ambion) for 30 min at 37°C followed by Phenol/Chloroform purification and Ethanol precipitation. For bisulfite treatment of RNAs the EpiTect Bisulfite Kit (Qiagen) was used. Conversions were carried out in a reaction volume of 70 µl. One microgram total RNA, dissolved in 20 µl RNase-free water was used.

Bisulfite reaction

Reagents	Amount
DNase-treated RNA (50 ng/µl)	20 µl
Bisulfite mix	42,5
DNA Protection Buffer	17,5
Σ	70 µl

Incubation conditions

Temperature	Time	Cycle
70°C	5 min	3
60°C	60 min	

The RNA was isolated from the bisulfite reaction mix with Micro BioSpin 6 Chromatography Columns (BioRad). RNA samples were treated with 0.5M Tris-HCl, pH 9,0 at 37°C for 1 h. The isolated RNA was Ethanol precipitated overnight at -80°C.

cDNA synthesis

Reverse transcription reactions were carried out on 1 µg of bisulfie treated RNA with the SuperScript III Reverse Transcriptase Kit (Invitrogen) as described in 2.3.2 using stem-loop primer or specific primer (Table 2.6).

PCR amplification of cDNA from bisulfite treated RNA

cDNA was PCR amplified using primers specific for deaminated sequences (Table 2.6).

PCR reaction

Reagents	Amount
cDNA	1 µl
10x Taq Polymerase Buffer	2,5 µl
dNTPs (10 mM)	1 µl
Forward Primer (10 µM)	1 µl
Reverse Primer (10 µM)	1µl
Taq Polymerase (5 U/µl)	0,5 µl
H_2O	to 25 µl
Σ	25 µl

PCR conditions

Temperature	Time	Cycles
95°C	5 min	1
95°C 55°C 72°C	30 sec 30 sec 30 min	30
72°C 4°C	10 min ∞	1

2,5 µl of the PCR reaction were used to re-amplify the amplicons and to add 454-sequencing adapters.

PCR reaction

Reagents	Amount
PCR Products	2,5 µl
10x Taq Polymerase Buffer	2,5 µl
dNTPs (10 mM)	1 µl
Forward Primer (10 µM)	1 µl
Reverse Primer (10 µM)	1µl
Taq Polymerase (5 U/µl)	0,5 µl
H_2O	to 25 µl
Σ	25 µl

PCR conditions

Temperature	Time	Cycles
95°C	5 min	1
95°C 50°C 72°C	30 sec 30 sec 30 min	15
72°C 4°C	10 min ∞	1

PCR products were purified using Micro BioSpin 6 Chromatography Columns (BioRad) and analyzed on a 454 sequencer (Roche).

2.3.10 Small RNA Sequencing by Illumina Technology

After heat shock treatment of adult flies and indicated recovery times, germ line was separated from soma and RNA was extracted from soma as described above. Total RNA was incubated with biotinylated DNA oligos complementary to the 2s rRNA sequence and Streptavidin Magnetic Beads (Promega) to decrease the levels of 2s rRNA. 10 µg RNA was separated on a 20% denaturing Urea-PAGE, followed by SYBR-Gold (Invitrogen) staining to visualize RNAs. Small RNAs (25-70 nucleotides) were extracted and eluted using 0,3 M NaCl. RNAs were precipitated with Ethanol and further processed for bar-coded RNA sequencing (6 barcodes) using the TrueSeq Small RNA Sample Preparation Kit (Illumina). Sequencing of samples was performed on a HighSeq platform (Illumina).

2.3.11 dsRNA Isolation and Analysis

RNaseOne™ (Promega) was used to selectively digest ssRNA in total RNA samples.

RNaseOne treatment

Reagents	Amount
Total RNA	100 µg
In vitro transcribed GFP dsRNA	20 ng
10x RNaseOne™ Buffer	10 µl
RNaseOne™ (10 U/µl)	2 µl
H_2O	to 100 µl
Σ	100 µl

dsRNA was purified by Phenol/Chloroform extraction and Ethanol precipitation. The obtained dsRNA was denatured at 95°C for 5 min prior to first strand cDNA synthesis.

cDNA synthesis reaction

Reagents	Amount	Incubation
Denaturated dsRNA	500 ng	
7x gDNA Wipeout Buffer	2 µl	5 min at 42°C
H_2O	to 14 µl	
5x Reverse Transcriptase Buffer	4 µl	
Primers (random hexamers)	1 µl	30 min at 42°C
Reverse Transcriptase	1µl	15 min at 95°C
Σ	20 µl	

qPCR analysis was performed on 1 µl cDNA as described in 2.3.3. Primers are listed in Table 2.6. PCR product levels were normalized using products from *in vitro* transcribed GFP control.

2.3.12 *In vitro* Transcription

For *in vitro* transcription of dsRNA and ssRNA PCR-amplified DNA-template was used (primers are listed in Table 2.6).

PCR reaction

Reagents	Amount
EGFP cont. gDNA or cDNA	2,5 µl
10x Taq Polymerase Buffer	2,5 µl
dNTPs (10 mM)	1 µl
Forward Primer (10 µM)	1 µl
Reverse Primer (10 µM)	1µl
Taq Polymerase (5 U/µl)	0,5 µl
H_2O	to 25 µl
Σ	25 µl

PCR conditions

Temperature	Time	Cycles
95°C	5 min	1
95°C	30 sec	
55°C	30 sec	30
72°C	30 min	
72°C	10 min	1
4°C	∞	

PCR products were purified using QIAquick Gel Extraction Kit (Qiagen). 1 µg of DNA-template was used for *in vitro* transcription.

In vitro transcription reaction

Reagents	Amount	Incubation
DNA-template	1 µg	
5x T7 Polymerase Buffer	8 µl	
5x Polyethylene-Glycol	8 µl	
10x Inorganic Pyrophosphate	4 µl	18 h at 37°C
RiboLock (40 U/µl)	0,2 µl	
T7 Polymerase (20 U/µl)	4 µl	
H_2O	to 40 µl	

Reactions were treated with 2 U Turbo™DNase for 30 minutes at 37°C. *In vitro* transcribed dsRNA was recovered using acidic Phenol-Chloroform extraction and Ethanol precipitation.

2.3.13 Dot Blot Analyses

2 µg of total RNA or dilution series of total RNA (1 µg, 0,5 µg, 0,25 µg, 0,125 µg) were transferred to Nylon membranes using 96-well Bio-Dot® Microfiltration Apparatus. Blotted RNA was immobilized by UV cross-linking and by incubation at 80°C for 1 hour. Membranes were blocked in Western-Blocking solution (Table 2.3) supplemented with 0,2 U RiboLock (Fermentas) for 30 min at RT and incubated with anti-dsRNA antibodies (1:2000) 2 h at RT or overnight at 4°C. After incubation with primary antibodies membranes were washed 3 times for 5 min at RT in Western-Blocking solution (Table 2.3) supplemented with 0,2 U RiboLock (Fermentas) followed by incubation with secondary antibodies anti-mouse-HRP (1:10000) for 30 min at RT. After washing with Western-Blocking solution (Table 2.3) supplemented with 0,2 U RiboLock (Fermentas) 3 times for 5 min at RT and once with 0,1 % PBST (Table 2.3) detection of chemiluminescence was performed using Immobilon™ Western Kit containing Luminol reagent and Peroxide solution. Signals were detected after exposure to the X-ray film (Fujifilm).

2.3.14 RNA Immunoprecipitation

Inoculation of D2-TG recipients was performed as described above but continuously for 72 hours. Adult flies were homogenized in Empigen Buffer followed by centrifugation for 30 minutes at 16000g. EGFP nanobodies (ChromoTek) were blocked with 0,5 µg/ml Myc-peptide for 1 hat 4°C prior to the incubation with 1,2 mg of total protein extracts for 1 hour at 4°C.

Paramagnetic beads were 5 time washed in Empigen Buffer, followed by Proteinase K digestion (0.2 mg/ml) for 30 minutes at 37°C and Phenol/Chloroform extraction of bound RNA.

cDNA synthesis

Reverse transcription reactions were carried out with the QuantiTect Reverse Transcription Kit (Quiagen) as described in 2.3.2.

PCR amplification of cDNA from RIP

Primers used in PCR reaction are listed in Table 2.6.

PCR reaction

Reagents	Amount
cDNA	1 µl
10x Taq Polymerase Buffer	2,5 µl
dNTPs (10 mM)	1 µl
Forward primer (10 µM)	1 µl
Reverse primer (10 µM)	1 µl
Taq Polymerase (5 U/µl)	0,5 µl
H_2O	to 25 µl
Σ	25 µl

PCR conditions

Temperature	Time	Cycles
95°C	5 min	1
95°C 55°C 72°C	30 sec 30 sec 30 min	35
72°C 4°C	10 min ∞	1

2.4 Protein analyses

2.4.1 Protein Extraction

For whole protein extracts of adult flies, around 20 flies were homogenized in 1 volume of Protein Extraction Buffer (Table 2.3). Samples were incubated at 4°C for 10 minutes under rotation, followed by two centrifugations, each 15 minutes at 16.000 g. Protein concentration were determined using Bradford dye assay (Bradford, 1976).

2.4.2 Western Blotting

50-100 µg of total protein extracts were solubilized in SDS-Sample Buffer (Table X) by boiling at 95°C for 5 minutes and analyzed by 10% or 15% SDS-PAGE (Laemmli, 1970). Proteins were transferred to cellulose membrane (Towbin et al., 1979) using wet blotting (BioRad) in Western-Blotting Buffer (Table 2.3) for 1 h at 400 mA. The membranes were blocked in Western-Blocking Solution (Table 2.3) for 30 min at RT and incubated with antibodies against Dnmt2 (1:250), DCV capsid (1:25000), Hsp70 (1:10000), Tubulin (1:10000), Dcr-2 (1: 500) (Table X) 2 h at RT or overnight at 4°C. After incubation with primary antibodies membranes were washed 3 times for 5 min at RT in Western-Blocking Solution (Table 2.3) followed by incubation with secondary antibodies anti-mouse-HRP, anti-rabbit-HRP or anti-chicken-HRP (Table X) (1:10000) for 30 min at RT. After washing with Western-Blocking Solution (Table 2.3) 3 times for 5 min at RT and once with 0,1% PBST (Table 2.3) detection of chemiluminescence was performed using Immobilon™ Western Kit containing Luminol reagent and Peroxide solution. Signals were detected after exposure to the X-ray film.

2.4.3 Immunoprecipitation and *In Vitro* Binding Assay

Adult flies (D2-TG and Ubq::EGFP) were homogenized in Empigen Buffer followed by centrifugation for 30 minutes at 16000g. EGFP nanobodies (ChromoTek) were blocked with 0,5 µg/ml Myc-peptide for 1 hat 4°C prior to the incubation with 1,2 mg of total protein extracts for 1 hour at 4°C. Paramagnetic beads were 3 time washed in Empigen Buffer, followed by 3 time equilibration in Dnmt2-Reaction Buffer. Immunoprecipitated were then incubated with 1 µg *in vitro* transcribed DCV RNAs at 37°C for 1h. Paramagnetic beads were 5 time washed in Empigen Buffer, followed by Proteinase K digestion (0.2 mg/ml) for 30 minutes at 37°C and Phenol/Chloroform extraction of bound RNA.

cDNA synthesis

Reverse transcription reactions were carried out with the QuantiTect Reverse Transcription Kit (Quiagen) as described in 2.3.2.

PCR amplification of cDNA from in vito binding assay

PCR amplification was performed as described in 2.3.14. Primers used in PCR reaction are listed in Table 2.6.

2.5 Bioinformatical Methods and Statistical Analyses

2.5.1 RNA Methylation Analyses

Bioinformatic analysis was performed using the BisQuID server and mapping script (Falckenhayn et al., 2012).

2.5.2 Small RNA Sequencing Analyses

Linkers and barcode sequences were extracted from the raw tags. Tags were imported into Galaxy (http://main.g2.bx.psu.edu/), converted into Sanger reads (groomer tool) and mapped to the Drosophila dm3 genome assembly using, Bowtie. Mapped reads were subsequently filtered for Drosophila tRNAs, rRNAs and mRNAs sequences using LASTZ pair-wise sequence alignment.

2.5.2 Statistical Analyses

All data are presented as arithmetic averages. Standard deviations were determined as measure of the statistical spread. The level of significance of differences between means of gene expression was analyzed with the Student's t-test. The required level of significance was defined to be 5 % ($p \leq 0.05$). The level of significance of differences between means of phenotypic eye color changes was analyzed with the test of hypothesis for two populations. The required level of significance was defined to be 5% ($p \leq 0,05$). The level of significance of differences between means of RNA fragmentation was analyzed with the Wilcoxon's matched pairs test. The required level of significance was defined to be 5 % ($p \leq 0,05$). The level of significance of differences in stress recovery between wild type and mutant flies was analyzed with long rank test. The required level of significance was defined to be 5 % ($p \leq 0,05$).

Chapter 3

Results

3.1 Dnmt2 Function in Biotic Stresses Responses

Efficient control of various biotic stressors is essential for the survival of the infected host. *Drosophila* use innate immunity systems for the suppression of the pathogen infections and employ small-interfering RNA mechanisms to limit the amplification of viruses. Preliminary work showed the increased expression of immune response genes in adult Dnmt2 mutant flies (Tim Pollex, Master thesis, 2010), which indicated the *Dnmt2* mutant flies were affected by biotic stressors and suggested that Dnmt2 function is involved in the suppression of unidentified pathogens.

3.1.1 Stress-Induced *Dnmt2* Mutant Phenotype

Since Dnmt2 function is connected to stress-conditions (Schaefer et al., 2010; Thiagarajan et al., 2011) *Dnmt2* mutants were analyzed for phenotypic changes under specific stress conditions.

Dnmt2 mutant flies display stress-induced morphological phenotypes

Heat shock of *Drosophila* larvae (second to third instar) caused morphological phenotypes in hatching adult flies (Figure 3.1A). For instance, a significant increase of black spots was detected in *Dnmt2* mutant flies (Figure 3.1B). These spots resembled melanotic lesions, which have been associated with increased immune responses in flies (Rodriguez et al., 1996; Watson et al., 1991). Also, when flies were cultured in population cages and under sub-optimal conditions (overcrowding), only *Dnmt2* mutant animals developed melanotic spots if compared to wild type and a Dnmt2 transgenic recue ($D2^{TG}$) line that carries a *Dnmt2*–EGFP construct in the *Dnmt2* mutant background (Figure 3.1C). Adults with melanotic lesions (Figure 3.1C) were inter-crossed and the resulting embryos were allowed to develop under optimal conditions. No incidence of melanotic spots could be detected, indicating the absence of genetic mutations in the parental generation and suggesting other factors (i.e. stress) as inducer of the melanization phenotype. These observations indicated that stress-induced signals caused increased immune responses in adult *Dnmt2* mutants.

A

B

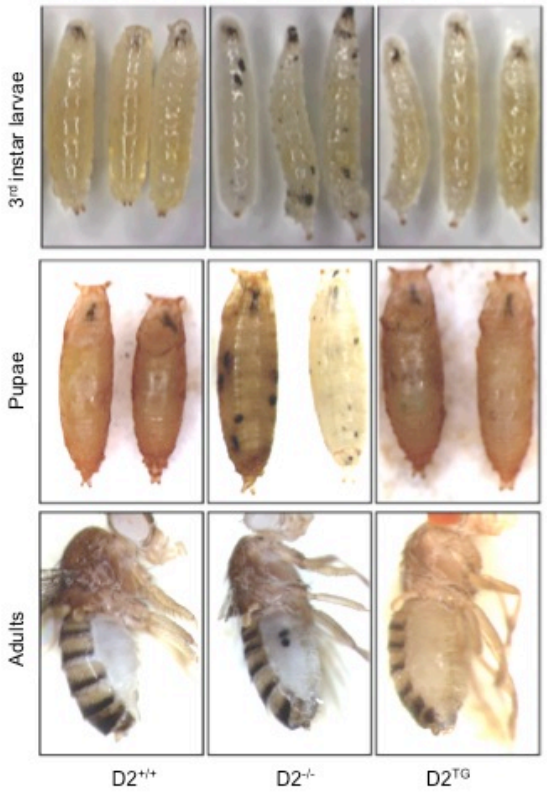

C

Genotype / Phenotype	D2+/+ F	D2+/+ M	D2-/- F	D2-/- M
Melanotic spots	1,9%	0	37,1%	30,0%
Leg malformation	5,7%	0	3,0%	2,3%
Compromised tergite fusion	0	0	1,4%	9,8%
Appendage overgrowth	0	0	0	3,9%

Figure 3.1: Stress induces mutant phenotypes in *Dnmt2* mutant animals.
(A) Phenotypic abnormalities in adult *Dnmt2* mutant flies can be induced by larval heat shock treatment. Melanotic spots (left), incomplete tergite fusion (middle, arrow) and appendage overgrowth (right, arrowhead). (B) Manifestation of melanotic spots in *Dnmt2* mutants ($D2^{-/-}$) after keeping flies under sub-optimal conditions. Wild type ($D2^{+/+}$), *Dnmt2* mutants ($D2^{-/-}$) and transgenic rescue ($D2^{TG}$) are shown. (C) Quantification of phenotypes after larval heat shock treatment.

Immune response genes are induced in Dnmt2 mutants

To test whether the appearance of melanotic spots correlated with increased immune responses, quantitative PCR analysis for selected immune response genes was performed. The results revealed significantly increased expression of various genes representing all immune response pathways in *Dnmt2* mutant flies. Importantly, the expression differences became more pronounced with the age of the flies (Figure 3.2A). Increased expression of antimicrobial peptide RNAs in *Dnmt2* mutants was also confirmed by Northern blotting (Figure 3.2B). Importantly, $D2^{TG}$ flies showed gene expression levels, which were similar to wild type controls (Figure 3.1A) indicating the rescue of the *Dnmt2* mutant phenotype. These results confirmed that stress-induced melanotic lesions in *Dnmt2* mutants were caused by increased innate immune responses and suggested that *Dnmt2* mutant animals were unable to control unidentified pathogens.

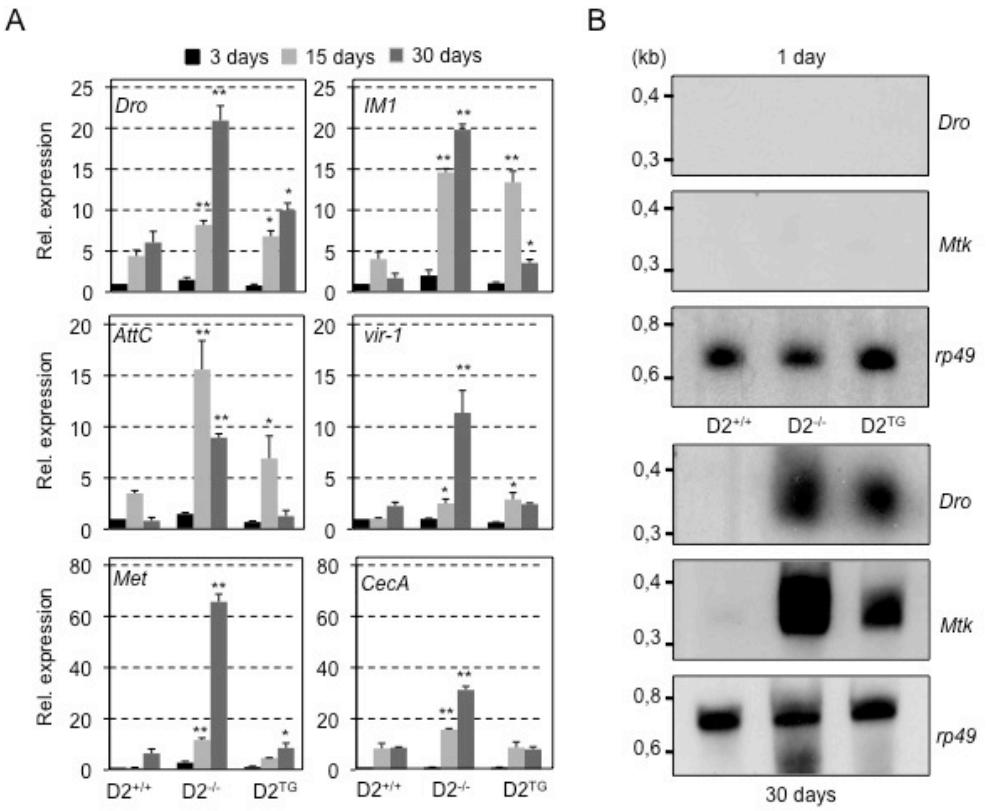

Figure 3.2: Stress induces innate immune responses in *Dnmt2* mutant animals.
(A) qPCR analysis for immune response genes in wild type ($D2^{+/+}$) *Dnmt2* mutant ($D2^{-/-}$) and transgenic rescue ($D2^{TG}$) flies at three time points after hatching (3, 15 and 30 days). (b) Northern blotting of RNA from freshly hatched (1 day) and aged (30 days) adult wild type ($D2^{+/+}$), *Dnmt2* mutant ($D2^{-/-}$) and transgenic rescue (D2-TG) flies for *Drosocin (Dro)* and *Metchnikowin (Met)*. *rp49* was used as loading control. RNA expression of genes in wild type ($D2^{+/+}$) was set to 1 and normalized to *rp49* messenger RNA in individual experiments. Error bars represent s.d.'s from three biological replicates. *p*-values were determined by Student's t-test (**p*=0.05; ***p*=0.01).

3.1.2 Pathogens in *Dnmt2* Mutant Flies

The elevated expression of various immune response genes in adult *Dnmt2* mutant flies (Figure 3.1A) indicated the presence of pathogens. Since the analyzed immune response genes were predominantly involved in the response to viruses and bacteria, the presence of these pathogens in *Dnmt2* mutant animals was determined.

Dnmt2 mutants contain high levels of specific RNA viruses

As DNA viruses have not been detected in *Drosophila* laboratory strains and *Dnmt2* is an RNA methyltransferase, the levels of naturally occurring RNA viruses were analyzed. While the RNA levels of double-stranded Drosophila X virus and single-stranded (-) Sigma virus were low and not affected by the *Dnmt2* mutation or age of the flies (Figure 3.3A) *Dnmt2* mutants contained high levels of single-stranded (+) RNA viruses. Compared to wild type flies, Nora virus and *Drosophila* C virus (DCV) levels were increased between 100 and 3.000-fold, respectively, particularly in older *Dnmt2* mutant animals (Figure 3.3A). Of note,

transgenic rescue flies ($D2^{TG}$) contained viral RNA levels that were similar to wild type flies (Figure 3.3A) confirming that the accumulation of RNA viruses in *Dnmt2* mutants was Dnmt2-dependent.

To investigate whether viruses in *Dnmt2* mutant flies were present as mature (replicable) virions, Northern and Western blotting was performed. Since DCV infection has been extensively studied in *Drosophila*, this virus was chosen for the further analyses. Northern blotting confirmed full-length DCV RNA genomes in 30-day-old *Dnmt2* mutant flies (Figure 3.3C), and Western blotting revealed significant amounts of DCV capsid proteins in *Dnmt2* mutants of this age (Figure 3.3D). These results confirmed the presence of DCV mature virions in *Dnmt2* mutant animals.

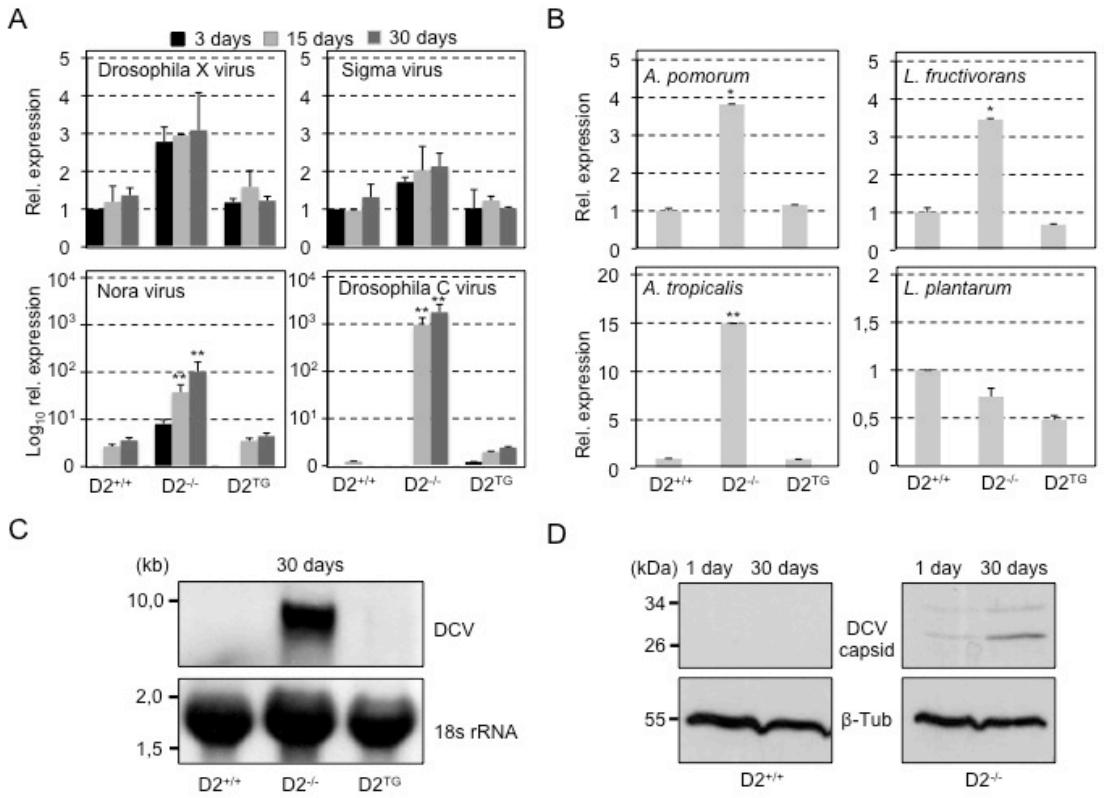

Figure 3.3: Levels of (+) RNA viruses and bacteria are increased in *Dnmt2* mutant flies.

(A) qPCR analysis for dsRNA *Drosophila* X virus, (-) RNA Sigma virus and (+) RNA (Nora and DCV) viruses in wild type ($D2^{+/+}$), *Dnmt2* mutant ($D2^{-/-}$) and transgenic rescue ($D2^{TG}$) and at various time points after hatching (3, 15, 30 days). (B) Diagnostic qPCR analysis for *Lactobacillus plantarum, Acetobacter tropicalis, Lactobacillus fructivorans* and *Acetobacter pomorum* in genotypes as in (A) flies 30 days after hatching. DNA content of bacteria in wild type was set to 1 and normalized to rp49 content in individual experiments. (C) Northern blotting for DCV genomes from aged (30 days) flies of the genotypes as in (A). Cross-hybridization of the DCV probe with 18s rRNA was used as loading control. (D) Western blotting for DCV capsid from young (1 day) and aged (30 days) wild type ($D2^{+/+}$) (left) and *Dnmt2* mutant ($D2^{-/-}$) flies (right). β-Tubulin was probed as loading control. RNA expression of genes in wild type ($D2^{+/+}$) was set to 1 and normalized to *rp49* messenger RNA in individual experiments. Error bars represent s.d.'s from three biological replicates. *p*-values were determined by Student's t-test (**p*=0.05; ***p*=0.01).

Levels of bacteria are moderately increased in Dnmt2 mutants

To determine the bacterial load of adult *Drosophila*, diagnostic qPCR was used. The analysis showed comparably moderate differences for three out of four dominant gut bacteria (Wong et al., 2011) between the tested genotypes (Figure 3.3B). These results indicated that highly increased levels of (+) RNA viruses rather than gut bacteria caused the up-regulation of innate immunity responses in *Dnmt2* mutant flies and suggested a role for *Dnmt2* in anti-viral defense mechanisms.

3.1.3 Dnmt2-Dependent Control of Virus Infections

DCV is a *Drosophila* virus that occurs naturally in flies without causing obvious symptoms. In contrast, if adult flies are inoculated with purified virions, replicating viruses cause lethality (Cherry and Perrimon, 2004). Since the natural route for many viruses (including DCV) includes the digestive and respiratory tracts, whole flies were used as virus source in infection experiments. To establish a natural infection system, fly carcasses of 30-day-old flies (donors) were fed to freshly hatched (recipient) flies (Figure 3.4A).

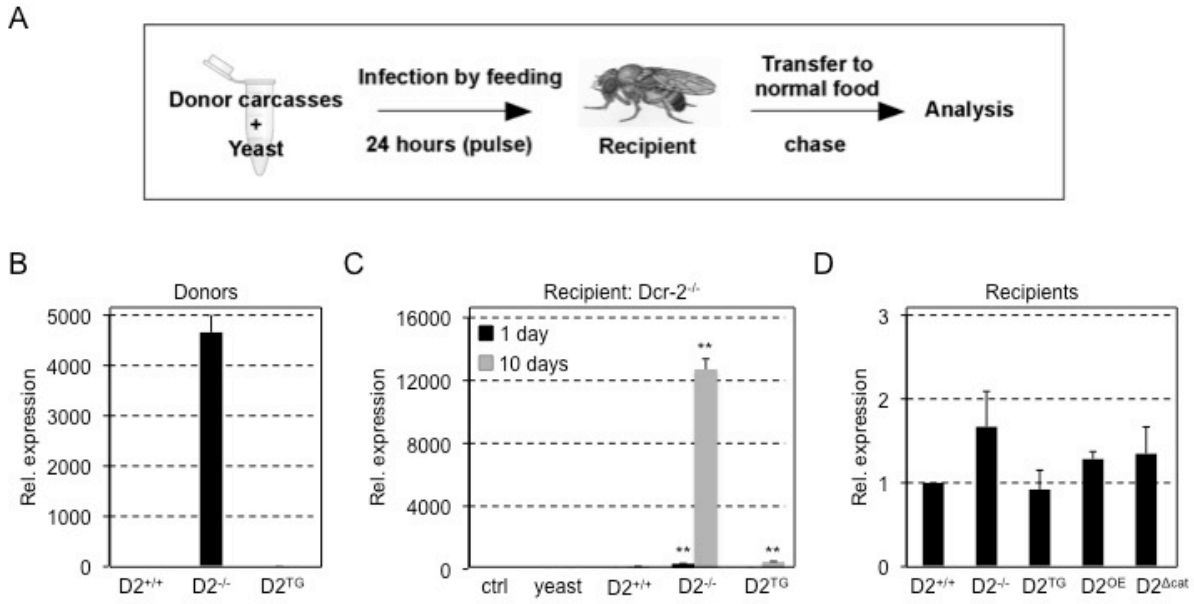

Figure 3.4: A virus infection-by-feeding paradigm.

(A) Schematic representation of an experiment designed to infect adult flies (recipients) with carcasses from donors containing virus particles. The feeding of recipients was carried out for a pulse period (24 hours) before infected flies were moved to normal food (chase) until analysis. (B) qPCR analysis for DCV in 30 days old wild type ($D2^{+/+}$), *Dnmt2* mutant ($D2^{-/-}$) and transgenic rescue ($D2^{TG}$) donors. (C) qPCR analysis for DCV in *Dicer-2* mutant recipients (*Dcr-2*$^{-/-}$) after feeding with donors as described in (B). Two time points after infection (1 and 10 days) were analyzed. (D) qPCR analysis for DCV in freshly hatched recipients. RNA levels of virus was set to 1 in non-infected (ctrl) and normalized to *rp49* messenger RNA in individual experiments. Error bars represent s.d.'s from three biological replicates. *p*-values were determined by Student's t-test (**p*=0.05; ***p*=0.01).

Feeding of fly carcasses resembles a natural virus Infection

To test whether the infection-by-feeding (oral infection) could be applied to transmit replication-competent virus to flies, *Dicer-2* mutant flies (Dcr-$2^{-/-}$) served as recipients. Dcr-2 function in siRNA pathways has been shown to be important for the restriction of viruses in *Drosophila* (Deddouche et al., 2008). Infection with DCV (Figure 3.4B) was monitored at two time points (1 and 10 days after feeding with donors) using qPCR. While infection with wild type and $D2^{TG}$ donors caused minor increases in DCV levels (Figure 3.4C), *Dnmt2* mutant donors caused a 250-fold increase of DCV RNA in *Dcr-2* mutants at day 1 after feeding (Figure 3.4C). Importantly, at day 10 after infection with *Dnmt2* mutant donors, *Dcr-2* mutant recipients had accumulated more than 12.000 times more DCV RNA than control recipients (Figure 3.4C). These results confirmed that oral infection can be used to propagate DCV in flies with compromised antiviral defense mechanisms.

Dnmt2 mutant flies are unable to suppress virus infection

To investigate whether *Dnmt2* was involved in the control of DCV infections, wild type, *Dnmt2* mutant and $D2^{TG}$ recipients were fed with *Dnmt2* mutant donors (Figure 3.4A,B). DCV levels in recipient flies were comparable at the time of hatching (Figure 3.4D). Wild type recipients suppressed DCV levels efficiently with only residual virus detectable after feeding with *Dnmt2* mutant donors (Figure 3.5A, left). In contrast, *Dnmt2* mutant recipients showed significantly increased DCV RNA levels (10.000 to 35.000-fold, Figure 3.5A, middle). DCV levels in $D2^{TG}$ recipients were similar to wild type controls (Figure 3.5A, right), thus confirming that DCV suppression was *Dnmt2*-dependent.

To test the presence of mature virions in infected flies Northern and Western blotting was performed. Northern blotting (10 days after infection) showed full-length DCV RNA genomes in *Dnmt2* mutant but not in wild type recipients (Figure 3.5B). Western blotting also confirmed that infected *Dnmt2* mutant recipients contained more viral capsid protein if compared to wild type recipients (Figure 3.5C). These results revealed that DCV was present as mature virions after oral infection. To confirm that observed effects were DCV-specific intra-thoracic injection of purified DCV virions was performed. The analyses confirmed the sensitivity of *Dnmt2* mutants to DCV infection (Durdevic et al., 2013). These results clearly showed that *Dnmt2* is required for the efficient control of DCV.

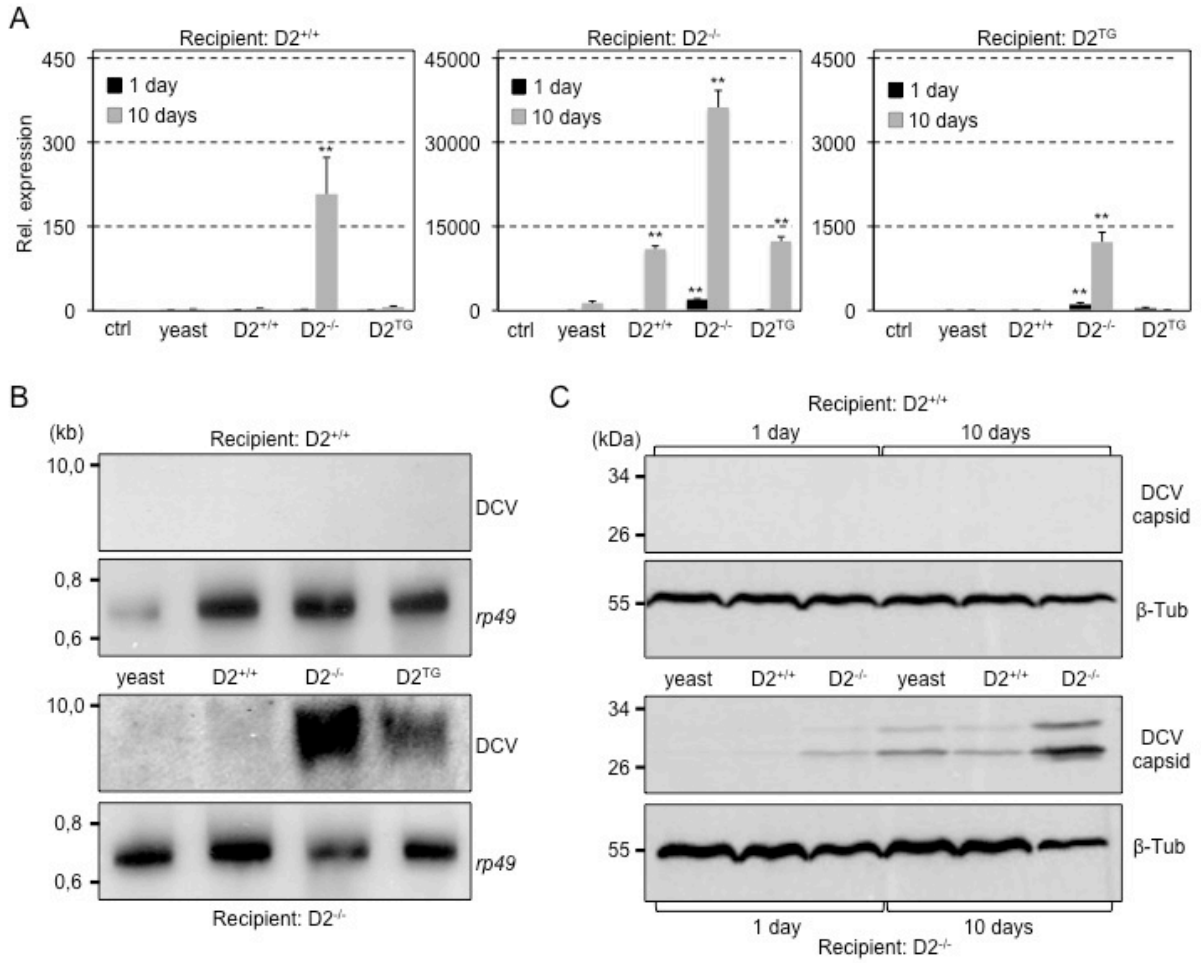

Figure 3.5: *Dnmt2* mutants fail to restrict DCV infections.

(A) qPCR analysis for DCV in wild type ($D2^{+/+}$) (left), *Dnmt2* mutant ($D2^{-/-}$) (middle) and transgenic rescue ($D2^{TG}$) recipients (right) after feeding with yeast alone or donors and two incubation periods (1 and 10 days). (B) Northern blotting of RNA for DCV genomes from wild type ($D2^{+/+}$) (upper) and *Dnmt2* mutant ($D2^{-/-}$) recipients (lower) after feeding with yeast or donors (10 days chase). *rp49* was used as loading control. (C) Western blotting for the DCV capsid protein from wild type ($D2^{+/+}$) (upper) and *Dnmt2* mutant ($D2^{-/-}$) recipients (lower) after feeding with yeast or donors (1 and 10 days chase). β-Tubulin was probed as loading control. RNA levels of virus was set to 1 in non-infected (ctrl) and normalized to *rp49* messenger RNA in individual experiments. Error bars represent s.d.'s from three biological replicates. *p*-values were determined by Student's t-test (**p*=0.05; ***p*=0.01).

Dnmt2 function is important during the acute phase of immune response

To test the induction of immune response in *Dnmt2* mutant animals during the DCV infection, immune response gene expression after oral infection was analyzed using qPCR. The results showed the rapid up-regulation of immune response genes in control recipients at day 1 after infection (Figure 3.6A, black bars, left). In contrast, immune response gene expression remained low in *Dnmt2* mutants at that time of infection (Figure 3.6A, black bars, middle), indicating the sensing and immediate response to the infection only in wild type control flies.

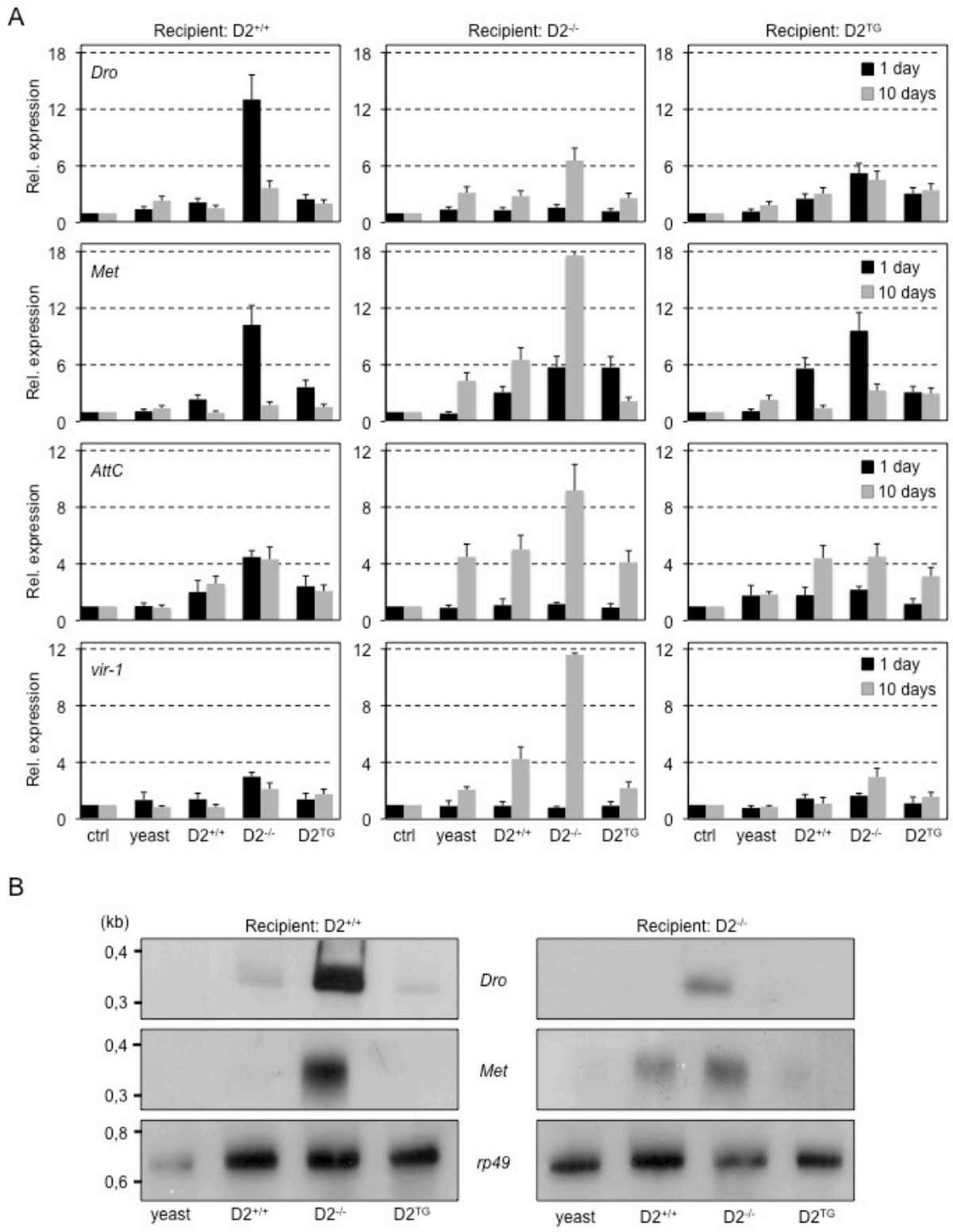

Figure 3.6: Acute immune response is impaired in *Dnmt2* mutants.

(A) qPCR analysis for immune response genes in adult wild type ($D2^{+/+}$) (left), *Dnmt2* mutant ($D2^{-/-}$) (middle) and transgenic rescue ($D2^{TG}$) recipients (right) after feeding with yeast or donors (1 and 10 days chase). (B) Northern blotting of RNA from adult wild type ($D2^{+/+}$) (left) and *Dnmt2* mutant ($D2^{-/-}$) recipients (right) after feeding with yeast or donors (1 day chase) for *Drosocin (Dro)* and *Metchnikowin (Met)*. *rp49* was used as loading control. RNA expression was set to 1 in non-infected (ctrl) and normalized to *rp49* messenger RNA in individual experiments. Error bars represent s.d.'s from three biological replicates.

Northern blotting confirmed that wild type but not *Dnmt2* mutant recipients expressed high RNA levels for the AMPs *Metchnikowin* and *Drosocin* at day 1 after infection (Figure 3.6B, left). In contrast, *Dnmt2* mutant recipients showed significantly increased immune responses only at day 10 after oral infection (Figure 3.6A, grey bars, middle) indicating a response to the accumulation of viruses in infected *Dnmt2* mutant flies. Importantly, at this time point, wild type and $D2^{TG}$ recipients had efficiently down-regulated the initial immune response (Figure 3.6A, grey bars, left and right). These results indicated that *Dnmt2* function was needed during the acute phase of immune system activation.

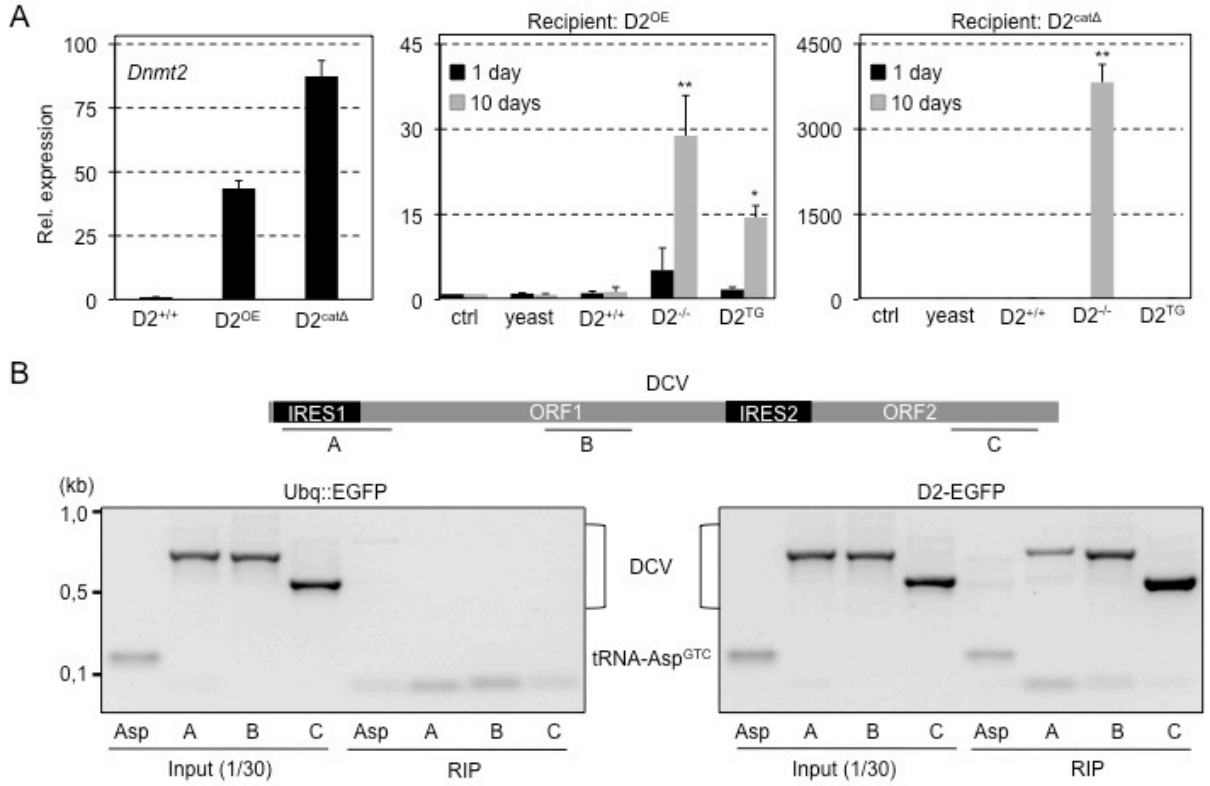

Figure 3.7: Catalytic activity of Dnmt2 contributes to the control of DCV and *Dnmt2* interacts with DCV genomic RNA.

(A) qPCR analysis for *Dnmt2* mRNA expression in wild type flies ($D2^{+/+}$), wild type flies that over-express *Dnmt2* ($D2^{OE}$) and *Dnmt2* mutant flies over-expressing a catalytically inactive *Dnmt2* ($D2^{catΔ}$) (left). qPCR analysis for DCV in *Dnmt2* over-expressing ($D2^{OE}$) (middle) and in recipients that over-express a catalytically inactive *Dnmt2* ($D2^{catΔ}$) (right) after feeding with yeast or donors (1 and 10 days chase). (B) Schematic illustration of the DCV RNA genome with three primer sets used for the analysis of RIPs. Agarose gels show the results of RIP from control (Ubq::EGFP) and $D2^{TG}$ (D2-EGFP) recipients after continuous feeding (72 h) with *Dnmt2* mutant donors. Both samples contained tRNA-Asp^{GTC} and DCV in the input fraction. After RIP, only Dnmt2–EGFP complexes contained tRNA-Asp^{GTC} and DCV. RNA expression of *Dnmt2* in wild type ($D2^{+/+}$) was set to 1 and RNA levels of virus was set to 1 in non-infected (ctrl), both were normalized to *rp49* messenger RNA in individual experiments. Error bars represent s.d.'s from three biological replicates. *p*-values were determined by Student's t-test (**p*=0.05; ***p*=0.01).

3.1.4 *Dnmt2* Catalytic Activity in the Control of Virus Infection

Since Dnmt2 is an RNA methyltransferase the catalytic activity of *Dnmt2* in the control of virus infection and the interaction between Dnmt2 and DCV were investigated in more detail.

The catalytic activity of Dnmt2 is required for the control of virus infection

To investigate if *Dnmt2* directly affected the accumulation of DCV, recipients that ectopically expressed *Dnmt2* were used in oral infection experiments. Expression of *Dnmt2* under the ubiquitin promoter in a wild type background ($D2^{OE}$, Figure 3.7A, left) efficiently suppressed DCV RNA levels during the infection with *Dnmt2* mutant donors (Figure 3.7A, middle). Importantly, recipients that expressed a catalytically inactive *Dnmt2* (PCQ motif mutated to AAQ) under the same promoter but in the *Dnmt2* mutant background ($D2^{catΔ}$, Figure 3.7A, left) failed to suppress DCV as efficiently (Figure 3.7, right). The analysis of DCV infection by intra-thoracic injection of purified DCV also indicated that the catalytic activity of Dnmt2 was required for the control of DCV infection (Durdevic et al., 2013). These results showed that *Dnmt2* was necessary and sufficient to suppress DCV levels and indicated that the cytosine-5-methyltransferase activity of *Dnmt2* contributed to *Dnmt2*-mediated DCV control.

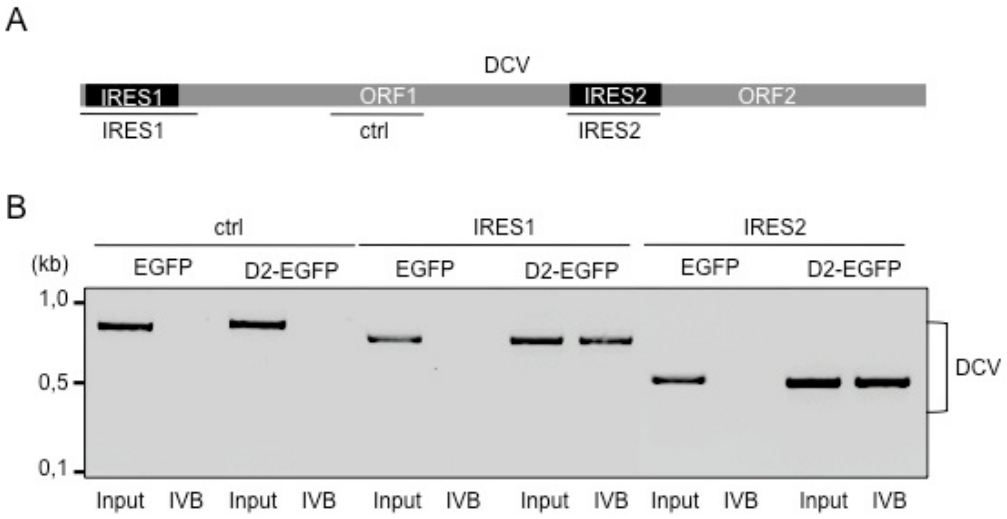

Figure 3.8: Dnmt2 bind specifically to IRES sequences of DCV genomic RNA.
(A) Schematic illustration of the DCV RNA genome with three *in vitro* transcribed regions (IRES1 and 2 and control region) used in *in vitro* binding assay. (B) Agarose gel shows the results of *in vitro* binding (IVB) assays. After incubation of immunoprecipitated EGFP (from Ubq::EGFP flies) and Dnmt2-EGFP (D2-EGFP from $D2^{TG}$ flies) with *in vitro* transcribed IRES1, IRES2 and control DCV region (ctrl) only Dnmt2-EGFP specifically bound to both IRES sequences.

Dnmt2 directly interacts with DCV genomic RNA

To test if Dnmt2 interacted with DCV RNA immunoprecipitation (RIP) were performed. Prior to RIP, Dnmt2 transgenic rescue ($D2^{TG}$) recipients and control recipients, that expressed EGFP from the ubiquitin promoter (Ubq::EGFP), were continuously (72 hours) fed with food that contained *Dnmt2* mutant donors (30 days old flies). The specificity of RIP was confirmed by analyzing the precipitate for *Dnmt2* substrate tRNA-Asp^{GTC}. The analysis showed that Dnmt2–EGFP complexes but not EGFP specifically interacted with tRNA-Asp^{GTC} and with at least three regions of the DCV RNA genome (Figure 3.7B). These results indicated the association of Dnmt2 with viral RNA and suggested direct interactions of Dnmt2 with DCV.

Dnmt2 specifically binds to IRES sequences

DCV genomic RNA possesses two IRESs that are important for the translation of viral proteins. Due to their structural features (Thompson, 2012), these sequences could potentially represent Dnmt2 binding sites. In order to determine whether Dnmt2 interacts with these or other regions of the DCV genome *in vitro* binding assays were performed. *In vitro* transcribed IRESs and a region in ORF1 from DCV genomic RNA (Figure 3.8A) were incubated with immunoprecipitated Dnmt2-EGFP. As a control immunoprecipitated EGFP was used. The analysis showed that Dnmt2 specifically interacted with both IRESs (Figure 3.8B). This result suggested that Dnmt2 could interact with DCV IRESs *in vivo* and that these sequences could represent targets of Dnmt2 methylation activity

3.2. Dnmt2 Function in Abiotic Stress Responses

The silencing of mobile genetic elements and repetitive regions in somatic tissues is mostly controlled by the formation of inactive chromatin (Talbert and Henikoff, 2006). In addition, small non-coding RNAs (e.g. siRNAs, piRNAs) contribute significantly to the regulation of transposons at the post-transcriptional level (Ghildiyal and Zamore, 2009). It is established that thermal stress induces chromatin change, which inadvertently lead to the mobilization of endogenous viruses (Ito et al., 2011; Tittel-Elmer et al., 2010; Vasilyeva et al., 1999). While mobile element control under standard laboratory conditions has been extensively studied, the processes that control the re-silencing of stress-induced mobile elements are not well understood. It was proposed that siRNA pathways are involved in these processes (Ito et al., 2011).

Genetic experiments in *Drosophila* indicated that transposon control was affected by Dnmt2 function (Phalke et al., 2009). In addition, the identification of a role for Dnmt2 in the regulation of exogenous mobile elements (viruses) suggested that an important biological function for Dnmt2 in *Drosophila* is be the control of mobile elements.

3.2.1 Dnmt2-Dependent Control of Stress-Induced Transposon RNA

Dnmt2 mutant display increased sensitivity to thermal and oxidative stress (Schaefer et al., 2010) and show stress-induced immune deficiencies in virus control (section 3.1). Since thermal stress is also an established paradigm that causes the mobilization of transposable elements (Tittel-Elmer et al., 2010; Vasilyeva et al., 1999), heat shock was used to test whether stress is a contributing factor to the *Dnmt2*-dependent transposon control.

Dnmt2 is required for the re-silencing of stress-induced transposon RNA

To investigate *Dnmt2* function in stress-induced transposon regulation, RNA levels after applying stress (heat shock, 1 hour at 37°C) and during the stress recovery phase were analyzed. To address this question, flies were heat-shocked (1 hour at 37°C) and the levels of transposon-derived RNA were monitored for several days during the recovery. Denaturing gel analysis of transposon RNA levels during the recovery from heat shock showed the appearance of high molecular weight (HMW) nucleic acids in *Dnmt2* mutant flies if compared to the wild type control (Figure 43.9A). In order to determine the identity of these RNAs, (HMW) RNA (hs + R1-R8) was extracted and sequencing on an Illumina platform was performed. The analysis showed that all of the (HMW) RNAs represented most of the mobile element families in *Drosophila* (Table 5.1) indicating that after heat shock and during the recovery phase almost all transposons became up-regulated in *Dnmt2* mutant flies.

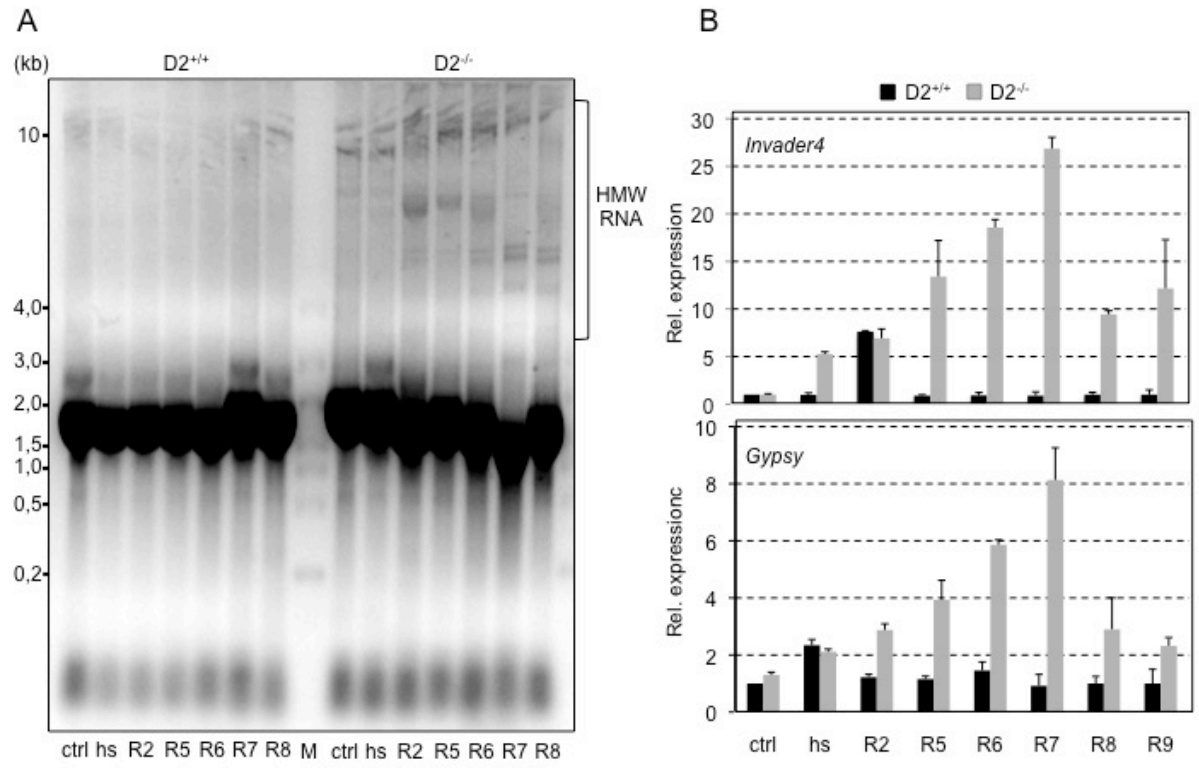

Figure 3.9: Dnmt2 fails to re-silence of stress-induced transposon RNAs.
(A) Ethidium bromide stained gel of RNAs from wild type ($D2^{+/+}$) and *Dnmt2* mutant flies ($D2^{-/-}$) before (ctrl) and after heat shock (hs, 37°C, 1 hour) and during days of recovery (R2-8) (HMW= high molecular weight). (B) qPCR analysis of transposon (*Invader4 and Gypsy*) expression in wild type ($D2^{+/+}$) and *Dnmt2* mutant flies ($D2^{-/-}$) before (ctrl) and after heat shock (hs, 37°C, 1 hour) and during days of recovery (R2-9). RNA expression of genes in wild type ($D2^{+/+}$) was set to 1 and normalized to *rp49* messenger RNA in individual experiments. Error bars represent s.d.'s from three biological replicates.

To quantify the extent of this de-regulation qPCR analysis for individual transposable elements was performed. Elevated levels of long-terminal-repeat (LTR) transposon RNA (*Gypsy* and *Invader4*) were detectable in control and *Dnmt2* mutant tissues after the heat shock (Figure 3.9B). Transposon levels decreased within two days after heat shock in wild type flies (Figure 3.9B). In contrast, *Dnmt2* mutant flies showed constantly increasing transposon levels for more than 5 days after the heat shock (Figure 3.9B). These results indicated that *Dnmt2* mutants failed to efficiently control stress-induced transposon RNA.

3.2.2 *Dnmt2*-Dependent Control of Transposon Mobility

LTR transposons use transposon-encoded reverse transcriptase for the synthesis of their double-stranded DNA intermediates (cDNA). Transposon cDNA becomes inserted into the genome by transposon-encoded integrase, which causes the multiplication and propagation of the respective element (Beauregard et al., 2008).

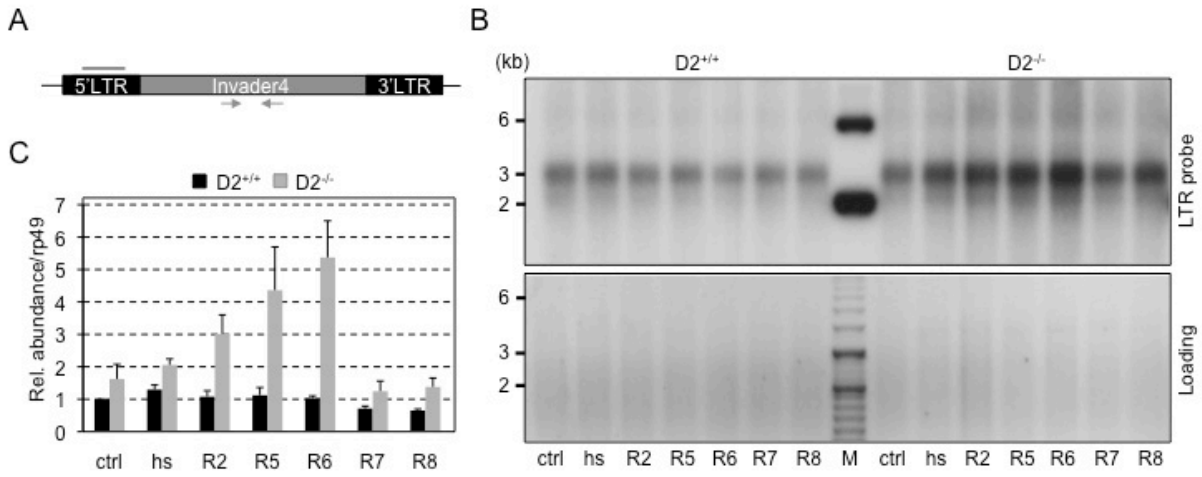

Figure 3.10: Transposon-derived cDNA is increased in *Dnmt2* mutants after heat shock.
(*A*) Schematic representation of *Invader4* element (ca. 3 kb) with localization of diagnostic PCR primer pair in the coding region (grey arrows) and LTR-specific probe for southern blotting (black line) (B) Southern blot of extra-chromosomal DNA preparations from wild type ($D2^{+/+}$) and *Dnmt2* mutant ($D2^{-/-}$) adult flies before (ctrl) and after heat shock (hs, 37°C, 1 hour) and during days of recovery (R2-8), hybridized with a 5' LTR-spanning probe. (C) Extra-chromosomal DNA quantification in wild type ($D2^{+/+}$) and *Dnmt2* mutant ($D2^{-/-}$) adult flies using qPCR analysis of *Invader4* cDNA before (ctrl) and after heat shock (hs, 37°C, 1 hour) and during days of recovery (R2-8). cDNA levels in wild type ($D2^{+/+}$) was set to 1 and normalized against single copy gene *rp49*. Error bars represent s.d.'s from three biological replicates.

Invader4 cDNA is increased in Dnmt2 mutants upon heat shock

To determine if increased transposon RNA levels in *Dnmt2* mutant flies gave rise to cDNA, extra-chromosomal DNA was isolated from wild type and *Dnmt2* mutant flies during a heat shock experiment. First, the copy number per cell and genome of *Invader4* elements was determined using qPCR. The results showed an increase of *Invader4*-derived extra-chromosomal DNA in *Dnmt2* mutant flies if compared to control flies (Figure 3.10C). Of note, extra-chromosomal DNA levels peaked at time points of highest *Invader4*-derived RNA expression (compare to Figure 3.9B). Secondly, Southern blotting of extra-chromosomal DNA preparations using an *Invader4* LTR-specific probe showed an increase of hybridization signals for full-length *Invader4* elements (ca. 3 kb) in *Dnmt2* mutant animals when compared to wild type controls (Figure 3.10B). Since the synthesis of cDNA is a prerequisite step for the genomic propagation of retrotransposons, these findings suggested mobilization of transposon in *Dnmt2* mutant flies after heat shock.

A

	(1) w^-	(2) w^{++}	(3) w^+
Phenotype			
Genotype	XX;AA YX;AA 0X;AA	$Y^{w+}X;A^{w+}A$	$Y^{w+}X;AA$ $Y^{w+}XX:AA$ $XX;A^{w+}A$

B

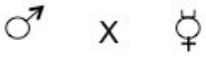

F1 of the crossing under standard laboratory conditions

Genotype / Phenotype	$D2^{+/+}$		$D2^{-/-}$	
	F	M	F	M
(1) w^-	3465	3	3881	32
(2) w^{++}	0	0	0	10
(3) w^+	1	3663	25	3864

C

F1 of heat shocked males and non-heat shocked females

Genotype / Phenotype	$D2^{+/+}$		$D2^{-/-}$	
	F	M	F	M
(1) w^-	791	1	634	7
(2) w^{++}	0	0	0	11
(3) w^+	0	809	5	683

D

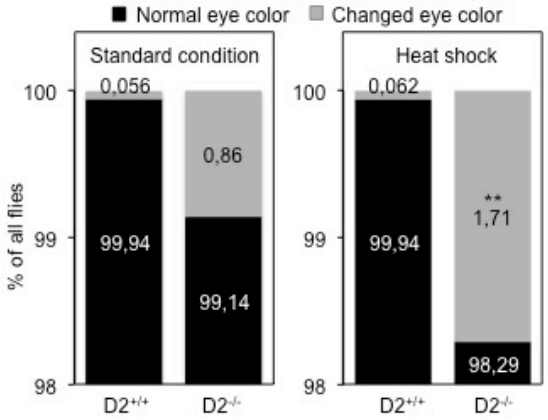

Figure 3.11: *Dnmt2* mutant flies display increased stress-induced transposition.

(A) Eye color variation of the P-element reporter line (HA-1925) (B) Eye color change in F1 generation single fly crosses under standard laboratory conditions and (C) in F1 of single fly crosses from heat shocked paternal generation line HA-1925. Homozygous stocks containing wild type ($D2^{+/+}$) or *Dnmt2* mutant ($D2^{-/-}$) chromosomes were phenotypically scored for changes in *white* reporter gene expression. w^-: loss of *white* expression (white eyes); w^{++}: increased *white* expression (red eyes); w^+: normal *white* expression (orange eyes) (D) Quantification of the mobility rate from (B) and (C). *p*-values were determined by the test of hypothesis for two populations: (**p=0,01)

Dnmt2 mutants display increased Invader4 mobility

To analyze *Invader4* mobility transgenic flies were used, which contain a male-specific P-element insertion in the 5' LTR of *Invader4* (tagged-*Invader4*) on the Y-chromosome (Phalke et al., 2009) (Figure 5.1). The insertion was analyzed in the wild type and *Dnmt2* mutant genetic backgrounds for the eye phenotypes (eye pigmentation changes), which were indicative of tagged-*Invader4* mobility. The following phenotypes were scored: (1) loss of *white* expression in males as consequence of recombination events or non-disjunction of X and Y chromosomes (w^-); (2) increased *white* expression in males, indicating reporter transposition in *cis* or *trans* (w^{++}); (4) expression of *white* in females, indicating transposition in *trans* or the presence of XXY females after non-disjunction of the sex chromosomes (w^+) (Figure 3.11A). Under standard laboratory conditions, all pigmentation changes in *Dnmt2* mutant flies amounted to 0.86 % (n=7812) and to 0.06 % (n=7142) in wild

type controls (Figure 3.11B and D, left). The difference could be attributed to females expressing *white* (0.014 % in wild type; 0.32 % in *Dnmt2* mutants), to males with increased *white* expression (0 % in wild type; 0,13 % in *Dnmt2* mutants) and to males, which lost *white* expression (0.042 % in wild type; 0.41 % in *Dnmt2* mutants). These results indicated the stochastic occurrence of transposition and chromosome non-disjunction in *Dnmt2* mutant flies under standard laboratory conditions.

To analyze the mobility of tagged-*Invader4* after heat shock adult male flies were heat shocked (1h at 37°C) and mated with non-stressed virgin females. Eye pigmentation changes in the F1 generation were scored as percentage of all offspring. The progeny of heat-shocked *Dnmt2* mutant males showed changes of 1.71 % (n=1340) if compared to 0.06 % (n=1601) in progeny from wild type males (Figure 3.11C and D, right). Comparison of the phenotypic changes before and after heat shock showed that the number of *Dnmt2* mutant male F1 progeny with increased *white* expression (w++, 0.13 % before heat shock; 0.81 % after heat shock) contributed most to these differences. These results supported the notion that heat shock caused an increase in the transposition of a tagged-*Invader4* element in *Dnmt2* mutant male flies.

Increased mobility of Invader4 flies leads to trans-generational insertional mutagenesis in Dnmt2 mutant flies

The observed changes in the eye pigmentation phenotypes in the F1 generation of *Dnmt2* mutant males indicated the mobilization of tagged-*Invader4* in the germ line leading to new insertion events into the genome. To test whether this stress-induced mobility of tagged-*Invader4* resulted in new insertions in *Dnmt2* mutant flies transposon mapping was performed. Individual F1 flies from crosses of heat-shocked males and non-heat-shocked females were phenotypically selected for eye pigmentation changes (Figure 3.11A). Single flies were processed for insertion mapping using unique P-element sequences in the transgene as anchor for inverse PCR analysis (Figure 5.1). This showed that F1 progeny that resembled parental males ($Y^{w+}X$;AA) produced the correct PCR product of ca. 500 bp whereas resembled parental females (XX;AA) as well as white-eyed F1 males (X0;AA or XY;AA) did not produce the correct PCR product when compared to the *white* expressing males ($Y^{w+}X$;AA; Figure 3.12A). In contrast, males with increased *white* expression (w++, $Y^{w+}X;A^{w+}A$) as well as females with *white* expression (w+, $XX;A^{w+}A$ or XXY^{w+};AA) showed additional PCR products of different lengths when compared to resembled parental males ($Y^{w+}X$;AA; Figure 3.12A). Sequence analysis revealed that new insertions of *Invader4* had occurred at different chromosomal locations (Figure 3.12B and C). These observations indicated that transposition of the Y-linked tagged-*Invader4* had occurred in heat-shocked paternal genomes, which had been inherited to the F1 generation. Since the 5'-inverted

repeat of the P-element in line HA-1925 was truncated (Figure 5.1), autonomous P-element excision as cause for the observed phenotypes was excluded. Taken together, these results demonstrated that loss of *Dnmt2* caused stress-induced *Invader4* elements to propagate throughout the genome.

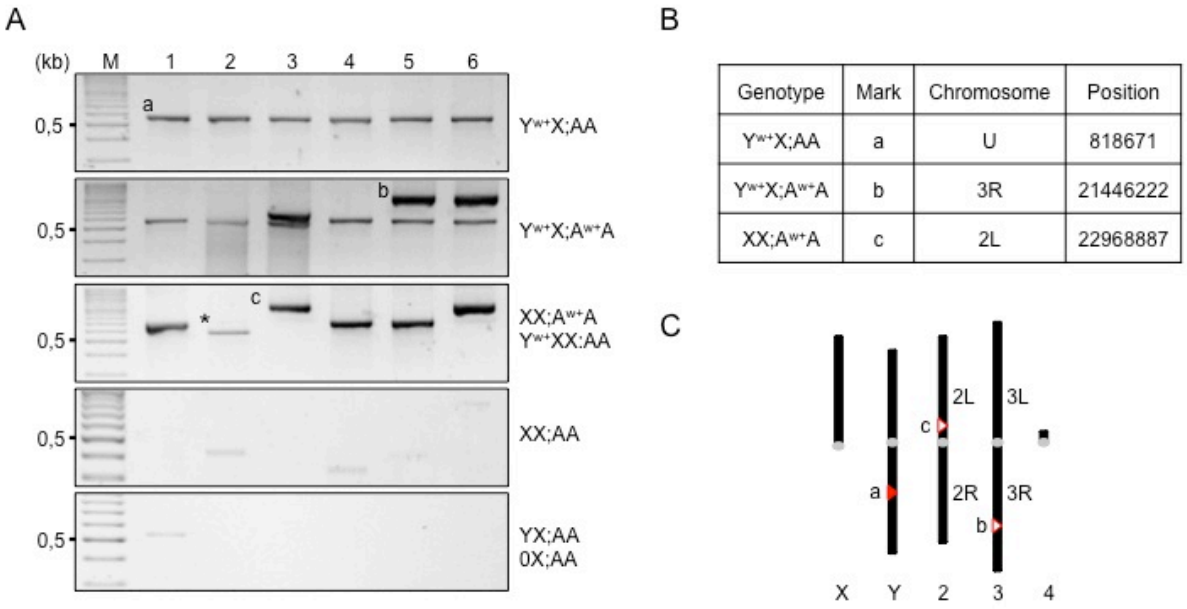

Genotype	Mark	Chromosome	Position
$Y^{w+}X;AA$	a	U	818671
$Y^{w+}X;A^{w+}A$	b	3R	21446222
$XX;A^{w+}A$	c	2L	22968887

Figure 3.12: Stress-induced phenotypic changes in *Dnmt2* mutants are a consequence of new *Invader4* insertions.

(A) Results of inverse PCR mapping of single fly progeny as visualized in Figure 4.4A. White^{+} founder males produced a specific PCR amplicon of 600 bp (marked as a, $Y^{w+}X;AA$). White^{-} founder females (without the Y-linked HA-1925) did not produce a specific PCR amplicon (XX;AA). Darker white^{+} males ($Y^{w+}X;A^{w+}A$) produced additional PCR amplicons (marked as b) while white^{+} females ($XX;A^{w+}A$) produced differently sized PCR amplicons (marked as c), representing additional or new P-element/transposon insertion sites. Of note, one white^{+} female (asterisk) produced a 600 bp product as founder males ($Y^{w+}X;AA$), indicating that this female carried a Y-chromosome as result of non-disjunction of XY. (B) Sequencing of inverse PCR amplicons from (A) resulted in the identification of new insertion sites in autosomal genomic DNA. (C) Schematic representation of identified original Y-chromosom linked insertion and new insertions in autosomes.

3.2.3 Catalytic Activity of *Dnmt2* in the Control of Stress-Induced Transposons

Although *Dnmt2* shows a week and distributive DNA methylation activity (Hermann *et al*., 2004, Fischer *et al*., 2004) it was proposed that *Dnmt2*-dependent DNA methylation is involved in the control of transposable elements in *Drosophila* (Phalke et al., 2009). However, these findings have been controversially discussed (Schaefer and Lyko, 2010). To address this problem, the involvement of the catalytic activity of Dnmt2 in the process of transposon silencing was investigated.

The catalytic activity of Dnmt2 is required for the regulation of stress-induced transposons

To confirm that the stress-induced increase of transposon RNA levels in *Dnmt2* mutants was due to Dnmt2 function, animals that ectopically expressed *Dnmt2* ($D2^{OE}$) were analyzed during a heat shock experiment. Adult flies carrying this construct did not show increased levels of *Invader4* and *Gypsy* RNA after heat shock (Figure 3.13, left) indicating that ectopic Dnmt2 quantitatively suppressed transposon-derived RNA levels. To test whether the catalytic activity of *Dnmt2* was involved adult flies expressing a catalytic inactive (PCQ motif mutated to AAQ) *Dnmt2* in the mutant background ($D2^{cat\Delta}$) were analyzed. The analysis showed a heat shock-dependent increase of *Invader4* and *Gypsy* RNAs (Figure 3.13, right) that was similar to the increase observed in *Dnmt2* mutants (Figure 3.9B). These results indicated that the methyltransferase activity of *Dnmt2* was required for efficient control of stress-induced transposon RNA.

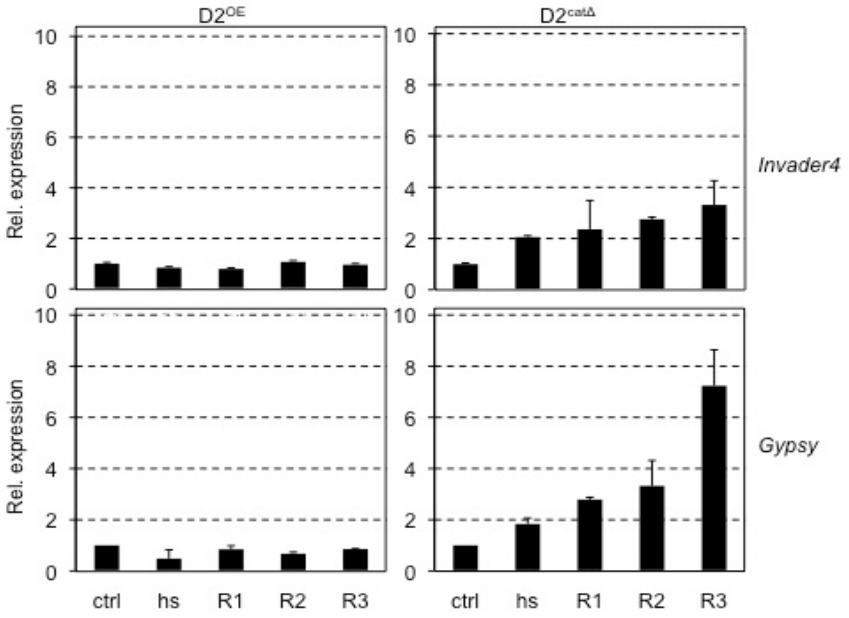

Figure 3.13: Transposon re-silencing requires catalytically active Dnmt2.
qPCR analysis of *Invader4*- and Gypsy-derived RNA *Dnmt2* over-expressing ($D2^{OE}$) (upper) and in recipients that over-express a catalytically inactive *Dnmt2* ($D2^{cat\Delta}$) (lower) before (ctrl) and after heat shock (hs, 37°C, 1 hour) and during days of recovery (R1-4). RNA expression of genes in wild type ($D2^{+/+}$) was set to 1 and normalized to *rp49* messenger RNA in individual experiments. Error bars represent s.d.'s from three biological replicates.

The 5' LTR of *Invader4* had been previously shown to be a substrate of *Dnmt2*-mediated DNA methylation (Phalke et al., 2009). However, later studies demonstrated lack of DNA methylation at this locus (Schaefer and Lyko, 2010) as well as lack of methylation in whole *Drosophila* genome (Radatz et al., 2013), suggesting alternative Dnmt2-dependent mechanism in the regulation of stress-induced transposons.

3.2.4 Dnmt2-Substrate tRNAs Methylation and Fragmentation upon Heat Shock

Instead of a reproducible DNA methylation activity, *Dnmt2* enzymes display a robust and specific tRNA methylation activity (Goll et al., 2006; Schaefer et al., 2010). Because the catalytic function of Dnmt2 appears to be involved in the control of stress-induced transposons *Dnmt2*-dependent tRNA methylation and fragmentation in adult *Drosophila* was analyzed during the heat shock response.

Heat shock causes specific loss of tRNA methylation and transient loss of Dnmt2 protein

To analyze the methylation patterns of *Dnmt2*-substrate tRNAs during the heat shock response, RNA bisulfite sequencing for tRNA-Asp^{GTC} and tRNA-Gly^{GCC} was performed. At standard laboratory conditions, C38 in tRNA-Asp^{GTC} and tRNA-Gly^{GCC} was almost completely methylated (>88%). Following heat shock, a substantial decrease of tRNA methylation at C38 could be observed (Figure 3.14A). tRNA methylation at this position decreased to ca. 60% for tRNA-Asp^{GTC} and for tRNA-Gly^{GCC} (Figure 3.14A). These results indicated that *Dnmt2*-dependent tRNA methylation at C38 is being suspended during the heat shock response whereas other target sites of the known tRNA methyltransferase Nsun2 (C47, C48, C49) remained unaffected.

To determine the cause of the temporary loss of tRNA methylation during the heat shock response, *Dnmt2* levels in adult animals were monitored using qPCR and Western blotting. While a single heat shock (1 hour at 37°C) caused only a moderate increase of *Dnmt2* mRNA levels during the recovery from stress, repeated heat shocks (daily 1 hour at 37°C) markedly increased *Dnmt2* mRNA levels (Figure 3.14B). Protein extracts from adult animals that were exposed to a single heat shock showed reduced Dnmt2 protein levels at the time of heat shock, which was followed by a modest increase of Dnmt2 protein during the recovery phase (Figure 3.14C). In contrast, *Dnmt2* protein was barely detectable in protein extracts upon repeated heat shocks (Figure 3.14C). Of note, a shorter polypeptide (ca. 30 kDa) became visible after heat shocks, which disappeared during the recovery phase as Dnmt2 full-length protein became detectable again (Figure 3.14C). These results indicated the existence of stress-induced pathways that degraded Dnmt2 protein, thereby creating temporary *Dnmt2*-mutant conditions. This was accompanied by the loss of the Dnmt2-substrate tRNA methylation. These findings suggested that the temporary degradation of Dnmt2 protein and the concomitant loss of C38 methylation are important parts of a normal heat shock response in *Drosophila*.

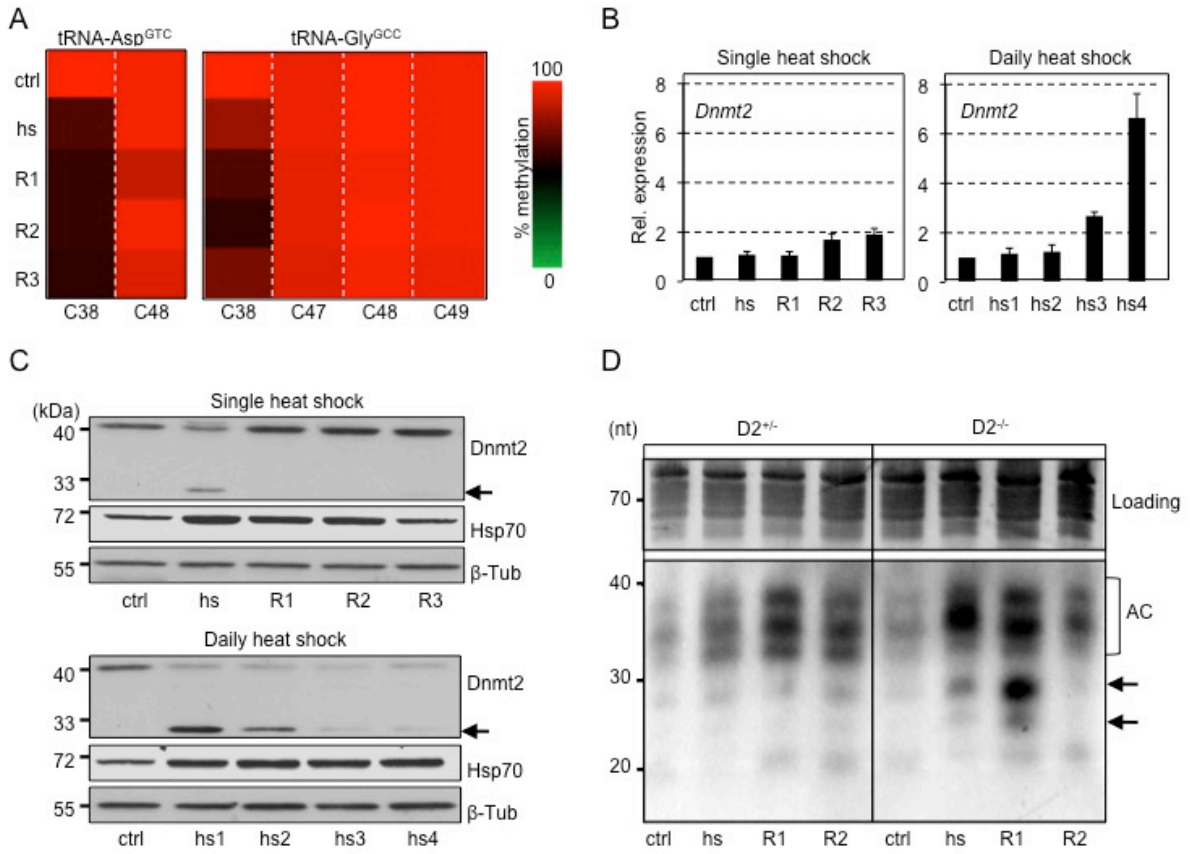

Figure 3.14: Heat shock causes loss of tRNA methylation and *Dnmt2* protein depletion.
(A) RNA bisulfite sequencing results for tRNA-Asp^{GTC} and tRNA-Gly^{GCC} in adult wild type tissues before (ctrl) and after heat shock (hs), followed by 3 days of recovery (R1-3). Methylation levels are represented as heat maps at two sites (C38, C48) in tRNA-Asp^{GTC} and at four sites (C38, C47, C48, C49) in tRNA-Gly^{GCC}. Heat map legend defines 100% methylation (red) and 0% methylation (green). (B) qPCR analysis of *Dnmt2* mRNA expression in wild type after single heat shock as in (A) (left) and after repeated heat shocks (hs1-4, 37°C, 1 hour) (right). (C) Western blotting for Dnmt2 and Hsp70 protein expression in wild type after single heat shock as in (A) (upper) and after repeated heat shocks (hs1-4, 37°C, 1 hour) (lower). β-Tubulin was probed as loading control. (D) Northern blot on RNA from adult heterozygous (D2$^{+/-}$) and *Dnmt2* mutant (D2$^{-/-}$) flies using a ^{32}P-labelled anti-sense DNA probe to visualize tRNA-Asp^{GTC}-derived 5'-halves before (ctrl) and after a single heat shock (hs, 37°C, 1 hour) and during recovery (R1-2) (AC= anticodon, *Dnmt2* mutant specific fragments are marked by arrows). RNA expression of genes in wild type (D2$^{+/+}$) was set to 1 and normalized to *rp49* messenger RNA in individual experiments. Error bars represent s.d.'s from three biological replicates.

Dnmt2 mutants display increased tRNA fragmentation upon heat shock

Because Dnmt2-dependent tRNA methylation affects the fragmentation of tRNAs (Schaefer et al., 2010), tRNA fragmentation in heat-shocked adult flies was analyzed using Northern blotting and RNA sequencing. Northern analysis showed substantially increased fragmentation of the known Dnmt2 substrate tRNA-Asp^{GTC} in *Dnmt2* mutant flies when compared to wild type flies (Figure 3.14D). In addition to tRNA fragments that were derived from anticodon cleavage and could also be observed in wild type flies *Dnmt2* mutant flies produced additional tRNA fragments (Figure 3.14D).

Small RNAs (25-70 nucleotides) from such an experiment were extracted and processed for RNA sequencing on an Illumina platform. After all reads that mapped to the *Drosophila* genome were extracted (Table 5.4) rRNA, mRNA and tRNA matches were further analyzed (Table 5.5). Analysis of reads from rRNA and mRNA showed that rRNA fragments were predominant (Figure 3.15A, C) and that the fragmentation was not significantly different in *Dnmt2* mutants when compared to the wild type flies (Figure 3.15B, D). Detailed analysis of mRNA fragmentation showed that several mRNAs (Table 5.6) were over-represented when compared to all reads from *Drosophila* protein coding genes (Figure 3.15C).

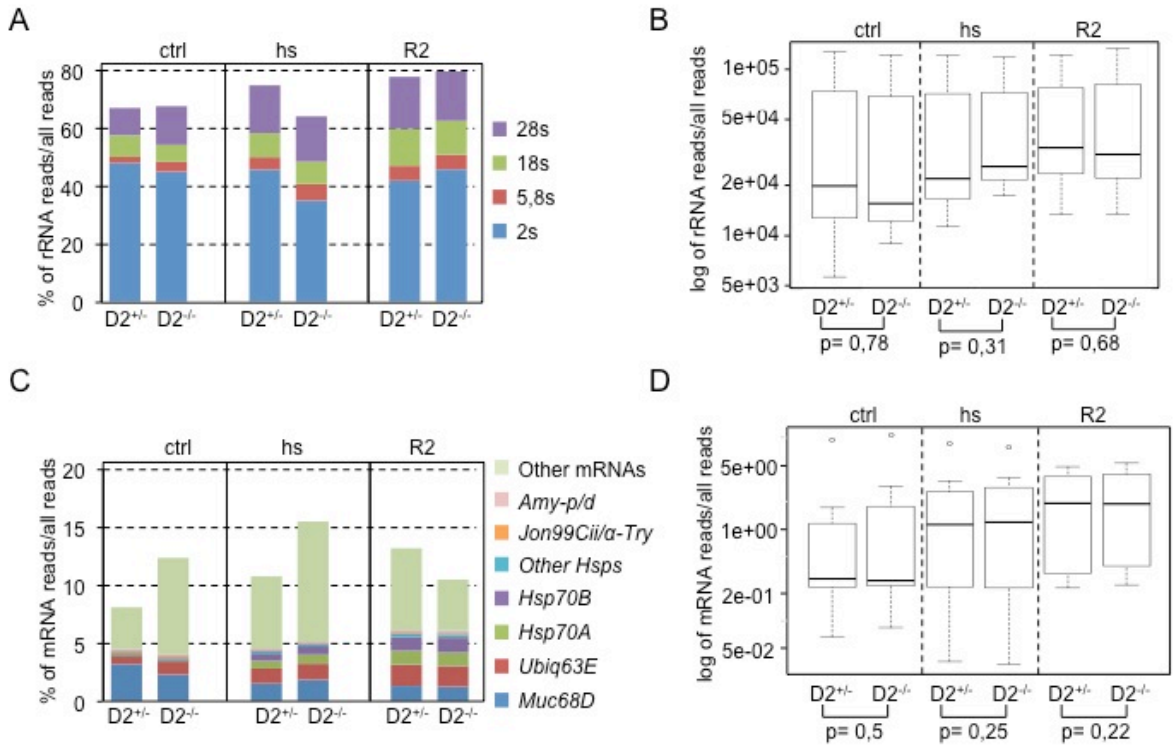

Figure 3.15: No difference in rRNA and mRNA fragmentation after heat shock.
(A) rRNA-derived reads extracted from RNA sequencing data of adult somatic heterozygous control ($D2^{+/-}$) and *Dnmt2* mutant ($D2^{-/-}$) tissues before (ctrl) and after a single heat shock (hs, 37°C, 1 hour) and during recovery (R2). Each sample is normalized to library size. (B) Box plots display rRNA fragment reads of individual experiments. Quantitative differences in rRNA fragmentation are presented in *p*-values calculated using Wilcoxon's matched pairs test. (C) mRNA-derived reads extracted from RNA sequencing data of adult somatic heterozygous control ($D2^{+/-}$) and *Dnmt2* mutant ($D2^{-/-}$) tissues during a heat shock experiment as in (A). Samples are normalized as in (A). (D) Box plots display mRNA fragment reads of individual experiments. Quantitative differences in mRNA fragmentation are presented in *p*-values calculated using Wilcoxon's matched pairs test.

The majority of tRNA-derived reads (>90 %) in all sequenced libraries originated from tRNA-$Gly^{GCC(TCC)}$, tRNA-$Glu^{CTC(TTC)}$, tRNA-$Lys^{CTT(TTT)}$, tRNA-Asp^{GTC}, tRNA-Cys^{GCA}, which indicated that these tRNAs were preferentially fragmented (Figure 3.16A, Table 5.7 and 5.8). For tRNAs that are represented by two isoacceptor types the acceptor type in parentheses indicates the lower and sometimes negligible contribution of the corresponding isoacceptor to

all reads (Table 5.9 and 5.10). Detailed analysis showed that the production of tRNA fragments after heat shock was substantially increased in *Dnmt2* mutant tissues (Figure 3.16A). Statistical analysis confirmed significant differences in tRNA fragmentation between wild type and *Dnmt2* mutant flies (Figure 3.16B). Among tRNAs, which contained a C38 (tRNA-Gly$^{GCC(TCC)}$, tRNA-Asp^{GTC} and tRNA-Glu$^{CTC(TTC)}$), only *Dnmt2* target tRNAs (tRNA-Gly$^{GCC(TCC)}$, tRNA-Asp^{GTC}) showed *Dnmt2*-dependent differences in the number of sequenced fragments (Figure 3.16C). Interestingly, also tRNAs which do not contain a cytosine at position 38 (tRNA-Lys$^{CTT(TTT)}$, tRNA-Cys^{GCA}) showed increased fragmentation in *Dnmt2* mutants (Figure 3.16C). Taken together, these data confirmed that *Dnmt2* function affected the fragmentation of *Dnmt2* substrate tRNAs. Additionally, the results also indicated that permanent loss of *Dnmt2* had an effect on the fragmentation of additional tRNAs, which are not known to be methylated by *Dnmt2*.

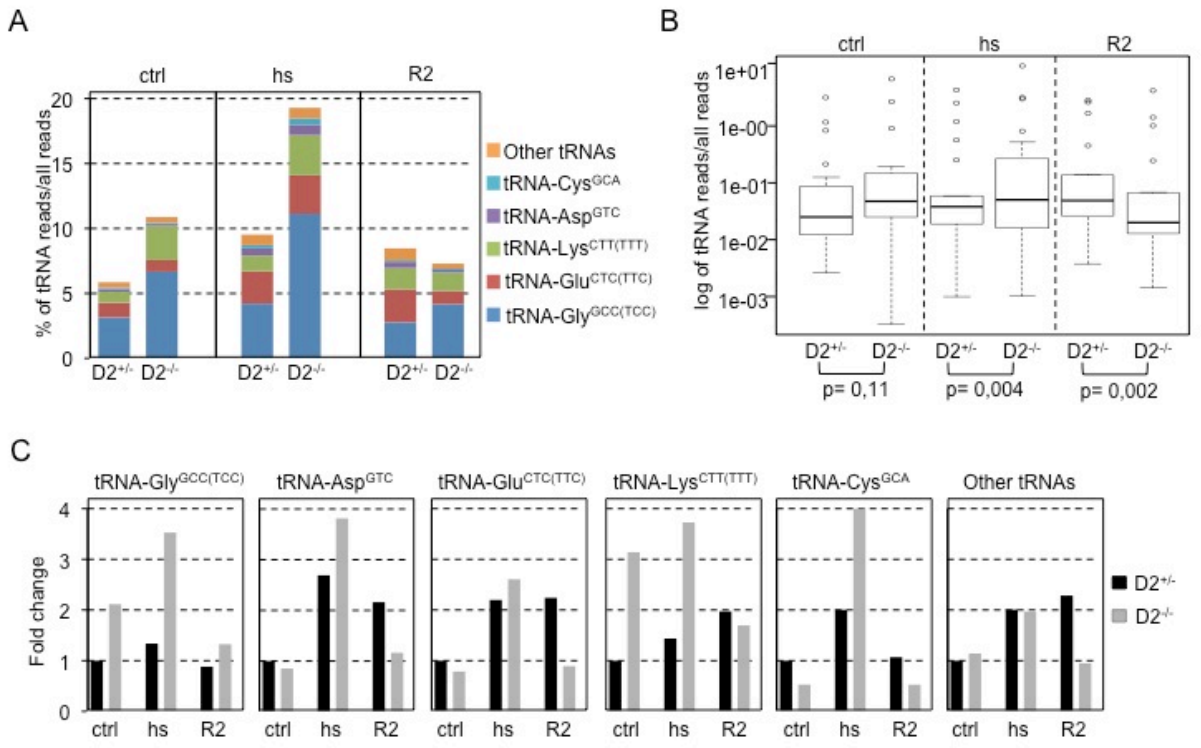

Figure 3.16: Heat shock causes increased tRNA fragmentation in *Dnmt2* mutants.
(A) tRNA-derived reads extracted from RNA sequencing data of adult somatic heterozygous control ($D2^{+/-}$) and *Dnmt2* mutant ($D2^{-/-}$) tissues during a heat shock experiment as in (A). Each sample is normalized to library size. (B) Box plots display tRNA fragment reads of individual experiments. Quantitative differences in tRNA fragmentation are presented in *p*-values calculated using Wilcoxon's matched pairs test. (C) Fold change of reads corresponding to abundant tRNAs and remaining tRNA reads (other) during the heat shock experiment. Reads were normalized to heterozygous control ($D2^{+/-}$).

Dnmt2 mutants produce tRNA fragments with different identities

To test whether tRNA-fragmentation in *Dnmt2* mutants displayed also qualitative differences, the length distribution of tRNA-Asp^{GTC}- and tRNA-Gly^{GCC}-derived fragments was

analyzed. All reads corresponding to tRNA-Asp^{GTC} and tRNA-Gly^{GCC} were filtered for matches to their respective 5' and 3'-ends. Under physiological conditions, 5'- and 3'-fragment reads from tRNA-Asp^{GTC} were equally represented in the sequenced libraries. Heat shock caused an increase of 5'-fragment reads (Figure 3.17A). Also, the majority of tRNA-Gly^{GCC}-derived fragments consisted of 5' matching reads (Figure 3.18A).

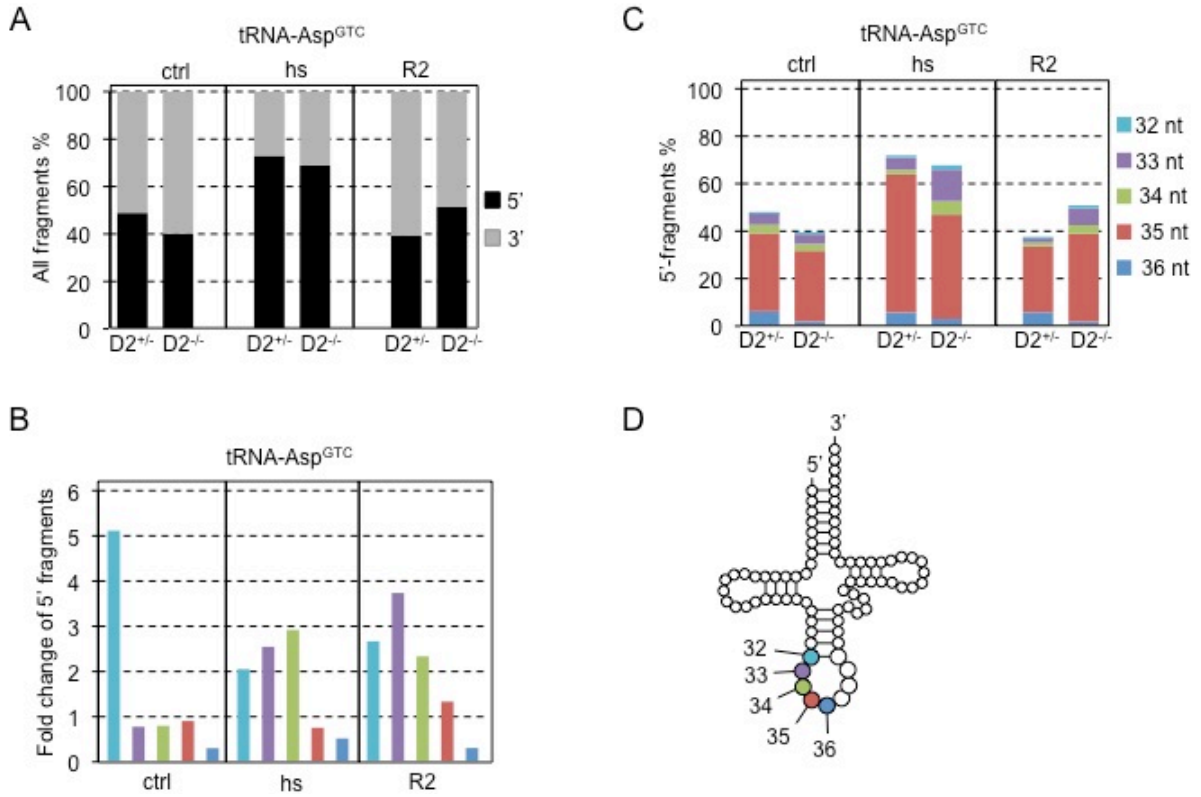

Figure 3.17: *Dnmt2* mutant somatic tissues contain tRNA-Asp^{GTC} fragments with different identities.
(A) Reads corresponding to tRNA-Asp^{GTC} were separated into 5' and 3'-derived fragments, based on break points of individual fragments. (B) Breakpoints in the anticodon loop of individual 5'-derived fragments of tRNA-Asp^{GTC} were mapped and visualized as percentage of all tRNA-Asp^{GTC} fragments. (C) Fold change of specific 5'-derived tRNA-Asp^{GTC} fragments in *Dnmt2* mutant (D2$^{-/-}$) tissues. Reads were normalized to heterozygous controls (D2$^{+/-}$) for each time point. (D) Cartoon introduces color-coding for individual fragments breaking at specific nucleotides.

Since 5'-derived tRNA fragments have been shown to be biologically effective (Emara *et al.*, 2010; Ivanov *et al.*, 2011), the length distribution of individual 5'-fragments was determined. This analysis showed a different length distribution for tRNA-Asp^{GTC} and tRNA-Gly^{GCC} fragments between wild type and *Dnmt2* mutant flies (Figure 3.17B and Figure 3.18B, Table 5.11, 5.12, 5.13 and 5.14). Especially after heat shock, *Dnmt2* mutant tissues accumulated shorter 5'-fragments (32-34 nucleotides long) indicating increased access to the anticodon loop of tRNA-Asp^{GTC} during the heat shock response (Figure 3.17C). In contrast, *Dnmt2* mutants accumulated longer fragments (47-51 nucleotides, variable loop) from tRNA-Gly^{GCC} than wild type flies (Figure 3.18C) indicating preferential cleavage in the variable loop of tRNA-Gly^{GCC}. These data supported the observed differences for tRNA-Asp^{GTC}-derived

fragments in *Dnmt2* mutants (Figure 3.14D) and suggested that, in addition to these quantitative differences, cleavage site accessibility or further processing of tRNA fragments could also be affected by the *Dnmt2* mutation.

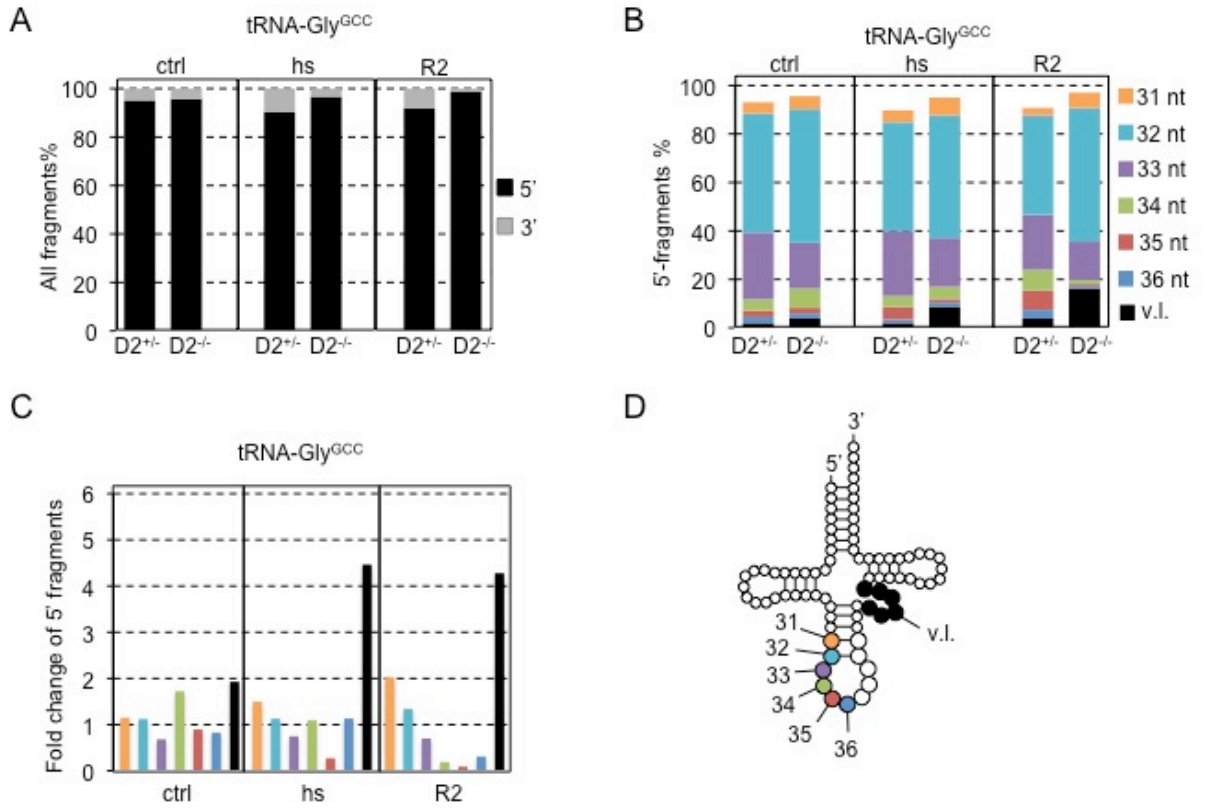

Figure 3.18: *Dnmt2* mutant somatic tissues contain tRNA-Gly^{GCC} fragments with different identities.
(A) Reads corresponding to tRNA-Gly^{GCC} were separated into 5' and 3'-derived fragments, based on break points of individual fragments. (B) Breakpoints in the anticodon loop of individual 5'-derived fragments of tRNA-Gly^{GCC} were mapped and visualized as percentage of all tRNA-Gly^{GCC} fragments. (C) Fold change of specific 5'-derived tRNA-Gly^{GCC} fragments in *Dnmt2* mutant (D2$^{-/-}$) tissues. Reads were normalized to heterozygous controls (D2$^{+/-}$) for each time point. (D) Cartoon introduces color-coding for individual fragments breaking at specific nucleotides; black bars represent the sum of break points in the variable loop (v.l.).

3.2.5 tRNA Fragments and their Effects on siRNA Pathways

tRNA-derived fragments have been found to potentially affect the function of siRNA pathways (Haussecker et al., 2010). Importantly, mobile element control in *Drosophila* relies on RNAi pathways. Therefore, the hypothesis that increased levels of stress-induced increased tRNA-derived fragments affected siRNA pathways in *Drosophila* was investigated.

Heat shock causes increased loading of tRNA fragments into Argonaute-2

To ask if heat shock affected the association of tRNA fragments with siRNA components, RNA sequencing data from a heat shock experiment in S2 cells was analyzed for the loading of tRNA fragments into Ago-2 (Cernilogar et al., 2011). Reads were filtered for tRNA matches and the results showed that after heat shock twice as many tRNA-derived

fragments associated with Ago-2 (Figure 3.19A). The majority of tRNA-derived fragments (>90%) in Ago-2 complexes consisted of five tRNAs including tRNA-Gly$^{GCC(TCC)}$, tRNA-Glu$^{CTC(TTC)}$, tRNA-Lys$^{CTT(TTT)}$, tRNA-Asp^{GTC}, tRNA-Cys^{GCA} (Figure 3.16A) and minor contribution of reads from tRNA-Ala$^{AGC(CGC/TGC)}$ and tRNA-Pro$^{AGG(CGG/TGG)}$ (Figure 3.19A, Table 5.15). Statistical analysis revealed significant differences in Ago-2 bound tRNA fragments between control and heat shock conditions (Figure 3.19B). The statistically relevant increase in Ago-2 bound tRNA-fragments could be attributed to only four tRNAs, including fragments from known *Dnmt2* substrate tRNAs (Figure 3.19D). To analyze the length distribution of loaded tRNAs, the identities of tRNA-Asp^{GTC} and tRNA-Gly$^{GCC(TCC)}$-derived fragments were determined. Interestingly, Ago-2 associated preferentially with 5'-derived fragments, which was independent of the heat shock (Figure 3.19C). These data confirmed that heat shock of S2 cells produced specific tRNA-derived fragments, which were increasingly loaded into Ago-2 complexes.

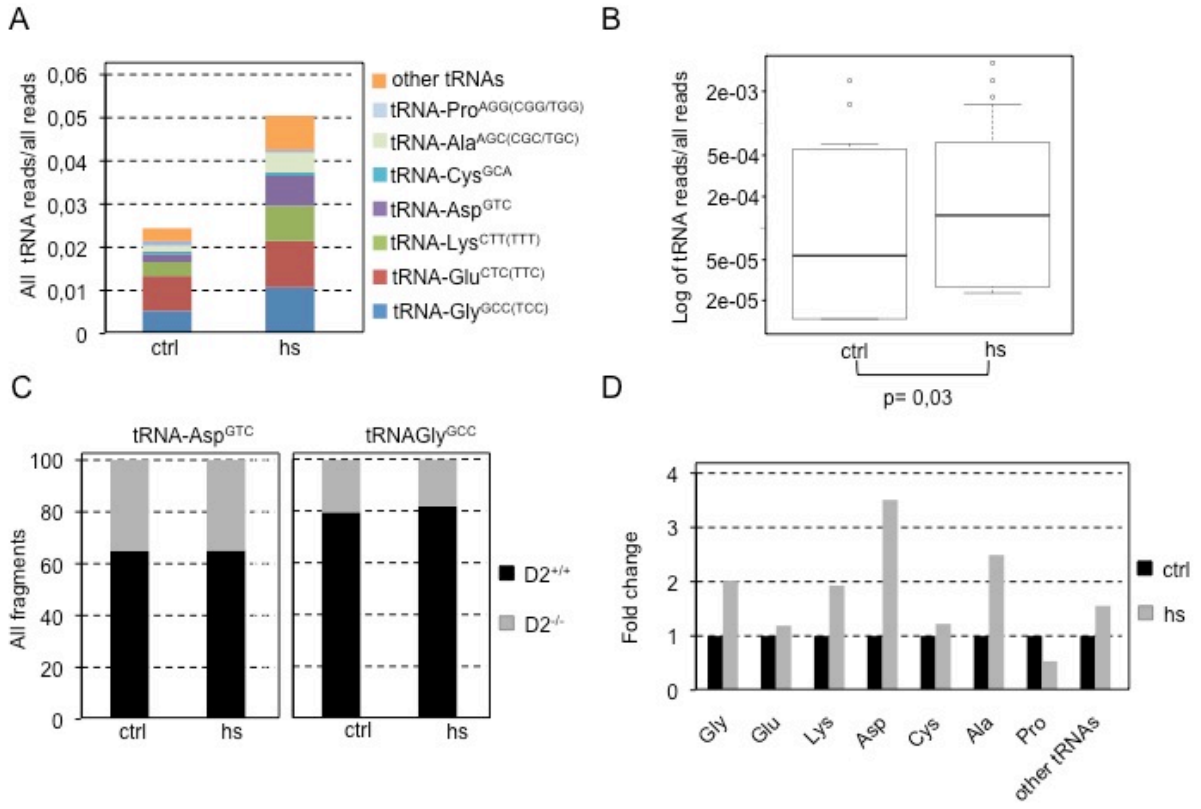

Figure 3.19: Heat shock induces loading of tRNA fragments into Argonaute-2.

(A) tRNA-derived small RNAs extracted from two data sets of Ago-2 immunoprecipitations (DNA Data Bank of Japan, accession: DRA000418) before (ctrl) and after heat shock (hs)). Each sample is normalized to library size. (B) Box plots display tRNA fragment reads of individual experiments. Quantitative differences in tRNA fragmentation are presented in *p*-values calculated using Wilcoxon's matched pairs test. (C) Ago-2 containing 5' and 3'-derived fragments of tRNA-Asp^{GTC} and tRNA-Gly^{GCC} (D) Fold change of reads corresponding to abundant tRNAs and remaining tRNA reads (other) in Ago-2 complexes after heat shock. Reads were normalized to tRNA reads under control conditions.

The expression of RNAi components is affected by heat shock but not by Dnmt2 mutation

To test whether RNAi pathways are mis-regulated in *Dnmt2* mutant flies, the expression of several small RNA factors was analyzed during a heat shock (1 hour at 37°C) experiment. These experiments showed the transcriptional induction of *Dcr-1* and *Dcr-2* but not *Ago-2* or *Piwi* upon heat shock (Figure 3.20A). In contrast to *Dcr-1*, *Dcr-2* showed increased transcript levels during the recovery phase in *Dnmt2* mutant flies if compared to the wild type flies (Figure 3.20A, right lower). In order to determine whether Dcr-2 protein levels were also increased in *Dnmt2* mutant flies Western blotting was performed. The results showed that shortly after heat shock Dcr-2 protein levels increased in both wild type and *Dnmt2* mutant flies, which corresponded to the transcriptional induction after heat shock (Figure 3.20B). In contrast, *Dnmt2* mutant flies did not show increased Dcr-2 protein levels during the recovery phase (compare Figures 3.20A, right lower and 3.20B, upper) if compared to the wild type flies (Figure 3.20B, lower). These results indicate that Dcr-2 expression responded to heat shock-induced cellular changes but was only transcriptionally mis-regulated in *Dnmt2* mutant flies.

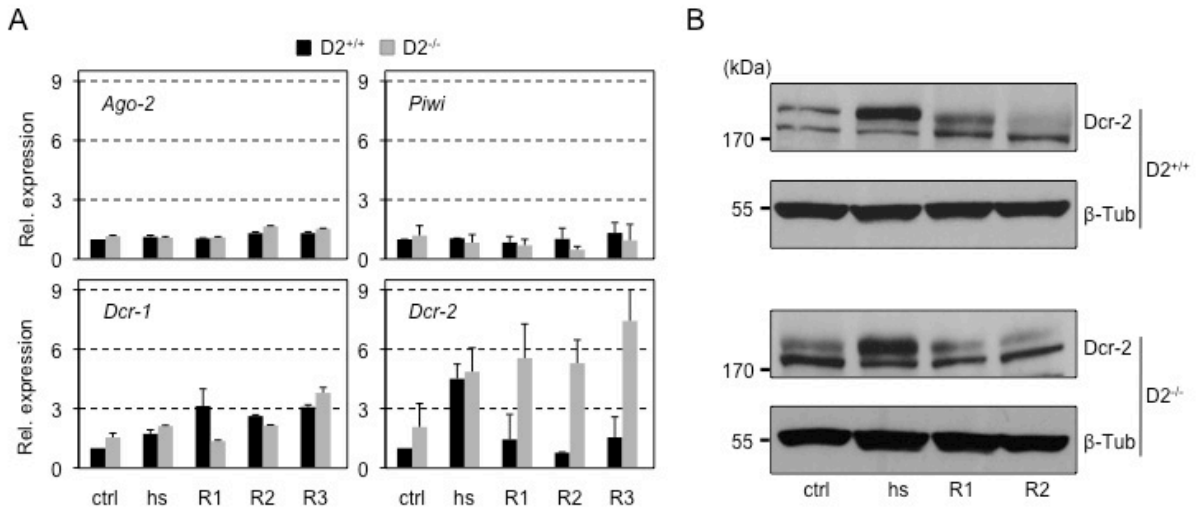

Figure 3.20: Dcr-2 responds to heat shock equally in wild type and *Dnmt2* mutants.
(A) qPCR analysis of RNAi components expression in wild type ($D2^{+/+}$) and *Dnmt2* mutant ($D2^{-/-}$) adult flies before (ctrl) and after heat shock (hs, 37°C, 1 hour) and during recovery (R1-3). (B) Dcr-2 protein expression in wild type ($D2^{+/+}$) and *Dnmt2* mutant ($D2^{-/-}$) adult flies before (ctrl) and after a single heat shock (hs, 37°C, 1 hour) followed by 2 days of recovery (R1-2). β-Tubulin was probed as loading control. RNA expression of genes in wild type ($D2^{+/+}$) was set to 1 and normalized to *rp49* messenger RNA in individual experiments. Error bars represent s.d.'s from three biological replicates.

Dnmt2 mutant and siRNA pathway mutant flies respond to heat shock in a similar fashion

To test the effects of heat shock on *Dnmt2* mutant, *Dcr-2* mutant and *Ago-2* mutant flies recovery rate from heat shock (1h at 37°C) was determined. Results and statistical analysis revealed that the recovery from heat shock was similar between all three mutants

but significantly different to wild type controls (Figure 3.21A), indicating involvement of siRNA pathway in the recovery from heat shock and supporting the notion that this pathway was impaired by *Dnmt2* mutation.

3.2.6 Efficiency of siRNA Pathway in *Dnmt2* Mutants

Prior to loading into Ago-2 complexes, endogenous siRNAs are produced by Dcr-2 activity on long dsRNA precursors. It has been shown that human DICER can bind tRNAs and process them into tRNA fragments (Cole et al., 2009). To investigate whether excessive tRNA fragmentation interfered with the efficiency of Dcr-2 activity, Dcr-2 substrates (dsRNAs), Dcr-2 products (siRNAs) and known candidate targets of Dcr-2-produced siRNAs (transposons, mRNAs and viruses) were analyzed during the heat shock response.

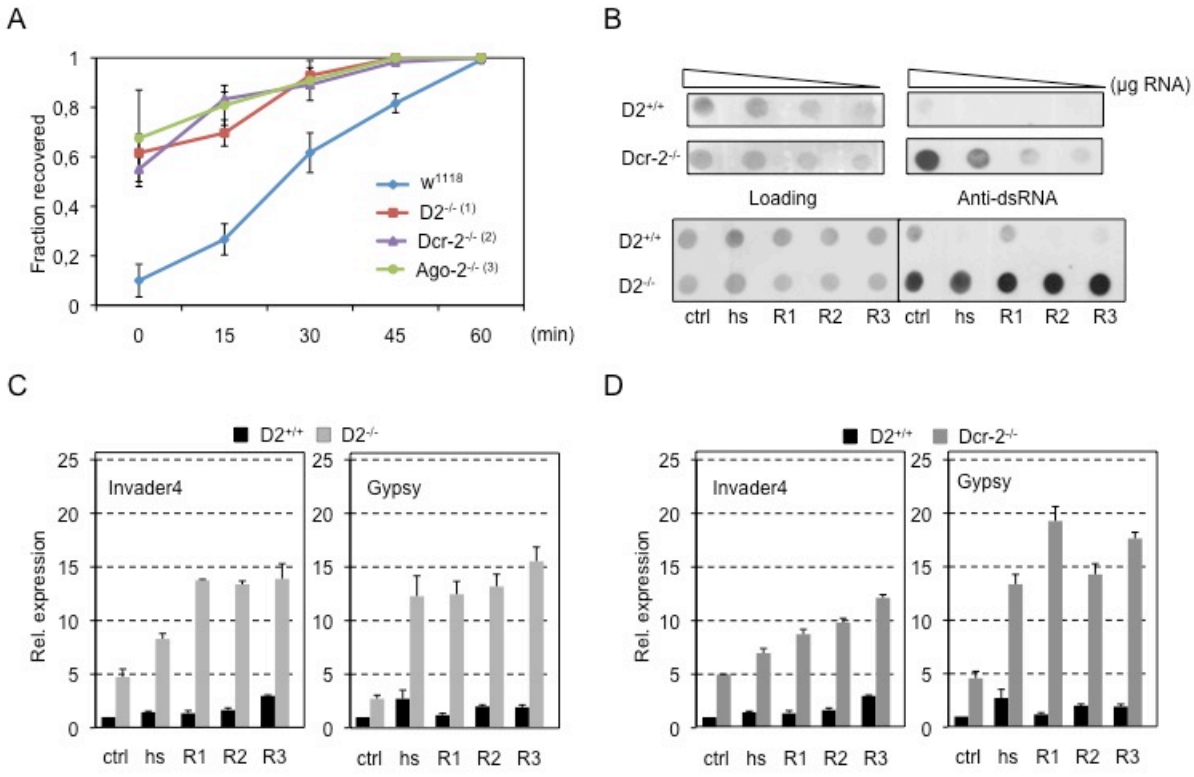

Figure 3.21: *Dnmt2* mutant flies response to heat shock is similar to that of RNAi mutants and heat shock causes increased dsRNA precursor levels in *Dnmt2* mutants.

(A) Recovery rate from heat shock of wild type (w^{1118}), *Dnmt2* mutant ($D2^{-/-}$), Dicer-2 mutant ($Dcr\text{-}2^{-/-}$) and Argoanute-2 mutant ($Ago\text{-}2^{-/-}$) flies. A mean of three experiments is shown with error bars representing s.d.'s. *p*-values calculated by log-rank test represent difference in recovery rate between wild type and each of the three mutants ((1) $p= 2{,}62 \times 10^{-6}$,(2) $p= 2{,}8 \times 10^{-6}$, (3) $p= 6{,}79 \times 10^{-7}$). (B) Dot blot analysis of dsRNA in dilution series of total RNA from wild type ($D2^{+/+}$) and *Dicer-2* mutant ($Dcr\text{-}2^{-/-}$) flies (upper). Dot blot analysis of dsRNA levels from ($D2^{+/+}$) and *Dnmt2* mutant ($D2^{-/-}$) flies before (ctrl) and after heat shock and during recovery (R1-3). (C) qPCR analysis of Invader4- and Gypsy-specific dsRNA from wild type ($D2^{+/+}$), *Dnmt2* mutant ($D2^{-/-}$) and (D) in Dicer-2 mutant ($Dcr\text{-}2^{-/-}$) flies before (ctrl) and after heat shock and during recovery (R1-3). dsRNA expression of genes in wild type ($D2^{+/+}$) was set to 1 and normalized to *in vitro* transcribed EGFP RNA in individual experiments. Error bars represent s.d.'s from three biological replicates.

Dnmt2 mutants accumulate double-stranded RNA precursors

To determine whether Dcr-2 activity was disturbed in *Dnmt2* mutants, the global levels of dsRNA upon heat shock (1 hour at 37°C) in wild type and *Dnmt2* mutant flies was analyzed using Dot blotting and qPCR. Dot blot analysis using antibodies against dsRNA revealed that *Dcr-2* mutant flies showed elevated levels of dsRNAs when compared to the wild type controls (Figure 3.21B, upper), which confirmed antibody specificity. Also *Dnmt2* mutant flies showed increased dsRNAs levels, which increased even more after heat shock while dsRNA levels in wild type flies did not change significantly (Figure 3.21B, lower). qPCR analysis on preparations of dsRNA showed that transposon-specific dsRNA precursors were elevated in *Dcr-2* mutants. Similar to *Dcr-2* mutants (Figure 3.21C, right), *Dnmt2* mutants showed also a significant increase of dsRNA precursors for the transposons *297* and *Invader4* after heat shock (Figure 3.21C, left). The elevated levels of dsRNAs indicated that Dcr-2 activity is impaired in *Dnmt2* mutant flies suggesting deficiencies in siRNA production.

Loss of Dnmt2 negatively affects siRNA production

To test whether the *Dnmt2* mutation affected the production of siRNAs, RNA from adult flies was probed for a strongly expressed endo-siRNA, esi-2.1 by Northern analysis. Animals with loss of function mutations in *Dcr-2* or *Ago-2* showed clearly reduced esi-2.1 abundance. *Dnmt2* mutants also showed reduced levels for esi-2.1 (Figure 3.22A) suggesting incomplete production of this specific siRNA under standard laboratory conditions. To test whether heat shock effected esi-2.1 production, RNA from heat-shocked (1 hour at 37°C) adult flies was probed for esi-2.1 levels. This showed that heat shock caused a strong and persistent reduction of esi-2.1 abundance in *Dnmt2* mutant animals (Figure 3.22B). These results supported the notion that heat shock reduced the production of siRNAs. Importantly, the observation that *Dcr-2* was unable to efficiently process dsRNA precursors into mature siRNAs indicated reduced Dcr-2 activity, especially in heat-shocked *Dnmt2* mutant flies.

Heat shock cause deregulation of siRNA targets in Dnmt2 mutant flies

To investigate whether reduced Dcr-2 function in *Dnmt2* mutant flies was also affecting the abundance of siRNA target RNAs the expression levels of various known siRNA targets was determined using qPCR and Northern blotting. The results showed that all tested RNA targets were increased in *Dnmt2* mutant animals after heat shock (Figure 3.22C-E). In agreement with general de-repression of transposons after heat shock (Figure 3.9 and Table 5.1) qPCR analysis showed that retrotransposons *297* and *Rover* were also deregulated (Figure 3.22C). Also, the expression of the mRNA target of esi-2.1, *mus408* mRNA, was up-regulated after heat shock of *Dnmt2* mutant flies, which was similar to *Dcr-2* mutant flies (Figure 3.22D). Furthermore, RNA levels of a persistent exogenous mobile element,

Drosophila C virus, increased dramatically in *Dnmt2* mutant flies after heat shock (Figure 3.22E). Taken together, these results indicated that the inefficient turnover of dsRNA precursors (Figure 3.22B and C) and decrease in siRNA production (Figure 3.22A and B) in *Dnmt2* mutants caused the deregulation not only of transposons but also of other siRNA targets.

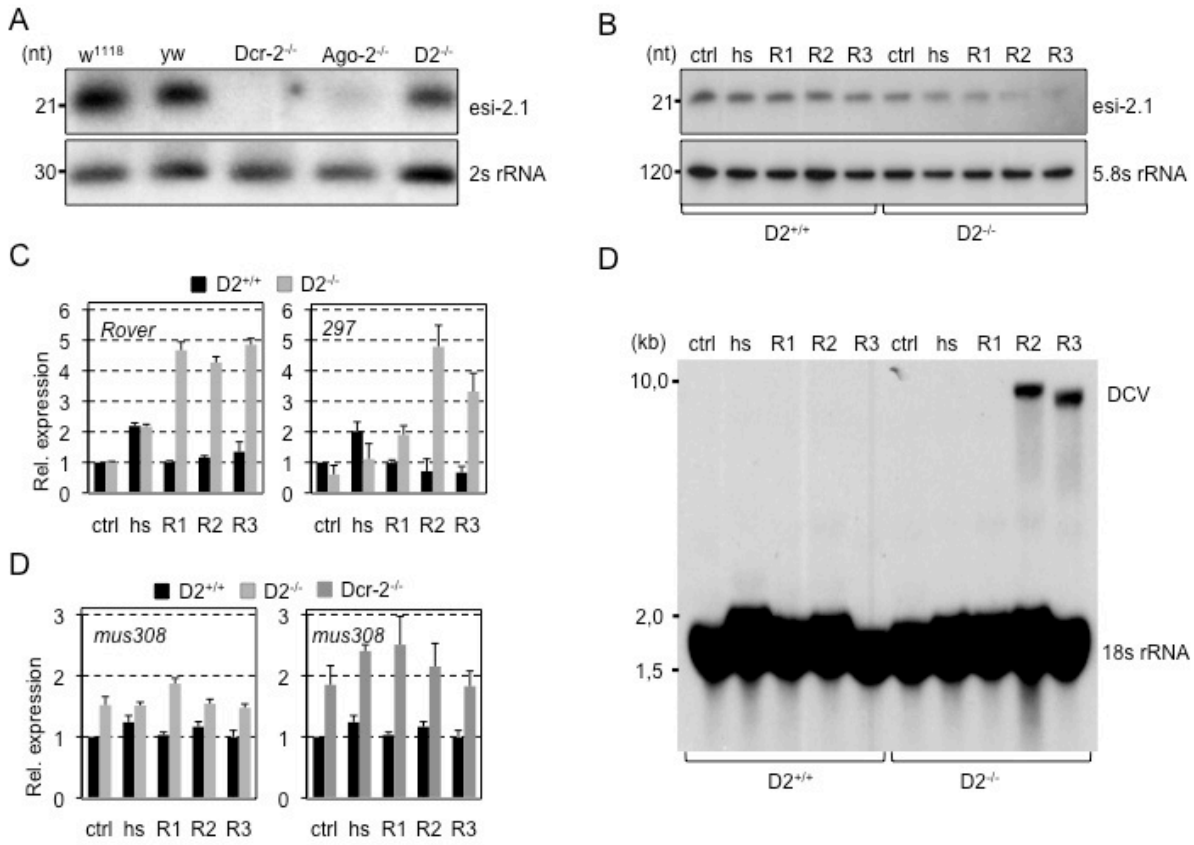

Figure 3.22: The efficiency of Dcr-2 activity is impaired in *Dnmt2* mutants after heat shock.
(A) Northern blot for esi-2.1 RNA from wild type (w^{1118} and *yw*), *Dicer-2* mutant (Dcr-$2^{-/-}$), *Argonaute-2* mutant (Ago-$2^{-/-}$) and *Dnmt2* mutant ($D2^{-/-}$) flies under standard laboratory conditions. 2S rRNA was probed as loading control. (B) Northern blot for esi-2.1 RNA from wild type ($D2^{+/+}$) and *Dnmt2* mutant ($D2^{-/-}$) flies before (ctrl) and after heat shock and during recovery (R1-3). 5,8S rRNA was probed as loading control. (C) qPCR of *Rover*- and *297*-derived RNAs from wild type ($D2^{+/+}$) and *Dnmt2* mutant ($D2^{-/-}$) flies in a heat shock experiment as in (B). (D) qPCR analysis of *mus308* mRNA from wild type ($D2^{+/+}$), *Dnmt2* mutant ($D2^{-/-}$) and *Dicer-2* mutant (Dcr-$2^{-/-}$) in heat shock experiment as in (B). Northern blot analysis of *Drosophila* C virus (DCV) genomic RNA from freshly hatched (3 days old) wild type ($D2^{+/+}$) and *Dnmt2* mutant ($D2^{-/-}$) flies in heat shock experiment as in (B). Cross-hybridization of the DCV probe with 18s rRNA was used as loading control. RNA expression of genes and level of the virus RNA in wild type ($D2^{+/+}$) was set to 1 and normalized to *rp49* messenger RNA in individual experiments. Error bars represent s.d.'s from three biological replicates.

Chapter 4

Discussion

Research on *Dnmt2* was challenged with contradicting findings for a long time. Dnmt2 enzymes show strong evolutionary conservation but *Dnmt2* mutant organisms do not develop any obvious phenotypes (Goll et al., 2006; Kunert et al., 2003; Wilkinson et al., 1995). Dnmt2 proteins have a *bona fide* DNA methyltransferase structure with conserved catalytic motives (Okano et al., 1998; Yoder and Bestor, 1998) but these enzymes do not methylate DNA (Radatz et al., 2013). The discovery that the enzymes are multi-substrate tRNA methyltransferases (Goll et al., 2006; Schaefer et al., 2010) and that their function is connected to cellular stress responses (Becker et al., 2012; Schaefer et al., 2010; Thiagarajan et al., 2011) provided new and important impulses to *Dnmt2*-related research. The findings presented in this study contribute additional information to Dnmt2 function and show that Dnmt2 in *Drosophila* is involved in the cellular response mechanisms to biotic and abiotic stresses.

4.1 Dnmt2 Function in the Cellular Responses to Biotic Stresses

Studies in various species revealed that organisms have evolved highly efficient mechanisms to cope with various intrinsic and extrinsic stresses. In recent years important roles for non-coding RNAs (ncRNAs), especially small ncRNAs (e.g. siRNAs, miRNA) for stress responses have been elucidated (Borsani et al., 2005; Cernilogar et al., 2011; Deddouche et al., 2008; Lucchetta et al., 2009; Woolcock et al., 2012) but their exact mode of action in these processes is still unclear.

4.1.1 Dnmt2-Mediated Methylation of Viral RNA Could Interfere with Viral Replication

The finding that the methyltransferase activity of Dnmt2 was required for the efficient restriction of viral replication suggests that RNA methylation affects viral replication. This conclusion is supported by the observation that high levels of non-functional Dnmt2 were unable to efficiently suppress DCV infections after oral infection (Figure 3.7A, right). A direct interaction between Dnmt2 complexes and DCV genomic RNA (Figure 3.7B) further indicates that Dnmt2-dependent methylation of viral RNA is involved in virus suppression. The observation that Dnmt2 complexes bind specifically to internal ribosomal entry sites (IRES) of the DCV RNA genome (Figure 3.8B) suggests specific regional binding and

methylation of viral RNA. Thus, binding or RNA methylation of IRES sequences might interfere with translation of viral proteins and reduce virus amplification. Attempts to analyze the RNA methylation status of DCV genomes are compromised by methodological limitations. Bisulfite treatment causes the random fragmentation of RNAs, which obstructs PCR-based amplification of large regions prior to sequencing. Additionally, the efficient suppression of viral RNA accumulation in wild type flies complicates a robust RNA methylation analysis of the DCV genome since Dnmt2 presence correlates with the loss of DCV sequences, thereby reducing the chances to detect the potential RNA methylation. Therefore, the analysis of Dnmt2-dependent methylation of viral RNA genomes needs to be addressed in future studies.

4.1.2 Dnmt2 Could Present Viral RNA to Cell Internal Sensors of Viral Infection

The observation that immune peptides are induced in wild type but not in *Dnmt2* mutants after acute infection with DCV containing donor flies (Figure 3.6A and B) suggests a role for Dnmt2 in the activation of the immune responses upon infection. Dcr-2 is important for the induction of antiviral activity in *Drosophila* (Deddouche et al., 2008). Importantly, the DExD/H-box helicase domain of Dcr-2 proteins is also found in other helicase families such as in mammalian retinoic acid-inducible gene I (RIG-I)-like receptors (Deddouche et al., 2008). This indicated that these helicase domains represent evolutionary conserved sensors of viral infection. Importantly, the observation that immune response genes can also be induced in a Dcr-2-independent fashion (Deddouche et al., 2008) indicated the existence of other viral sensors in *Drosophila*, which also participate in the detection of viral infections. It has been demonstrated that Dnmt2 enzymes can bind tightly to DNA without methylating its sequence (Dong et al., 2001). It is therefore also conceivable that Dnmt2 binding to DCV genomic RNA (Figure 3.7B) is necessary to present this RNA to innate immunity receptors such as Dcr-2. Such a molecular function of Dnmt2 would place Dnmt2 upstream of Dcr-2 and other sensors of viral infection. Consistent with this notion is the observation that *Dnmt2* mutants fail to restrict the propagation of DCV (Figure 3.5A, middle and 3.5B and C, lower) although *Dnmt2* mutant flies contain normal levels of Dcr-2 (Figure 4.13B). Therefore, Dnmt2 might bind viral RNA an act as facilitator of coordinated cellular antiviral responses.

4.1.3 A Role for Dnmt2 in the Systemic Spread of Antiviral Silencing

Sub-cellular membranes are important for viral entry and replication (Cherry and Perrimon, 2004; Cherry et al., 2006). Viruses also induce the formation of stress granules (SG) and interfere with the integrity of P bodies (PB) in infected cells (Lloyd, 2013). Argonaute proteins localize to PB and SG (Leung et al., 2006; Pare et al., 2009) and small interfering RNA

pathway activity has been linked to membranes of multivesicular bodies (Lee et al., 2009b). These observations indicated that cells use compartmentalization to organize antiviral response mechanisms. This concept is also supported by the observation in *Drosophila* that RNAi silencing of viruses requires receptor-mediated endocytosis (Saleh et al., 2006). The observation that Dnmt2 associates with SG (Schaefer et al., 2010) and that the protein re-localizes to distinctive macromolecular foci after virus infection (Durdevic et al., 2013) support the notion that compartmentalization of Dnmt2 function contributes to the sequestration of invading pathogens in order to mount siRNA-mediated defenses. The interconnections of SG, PB and GW bodies and their interaction with multivesicular bodies, which also give rise to exosomes (Siomi and Siomi, 2009), suggest that Dnmt2 might play a role in the dsRNA-dependent systemic spread of antiviral silencing in *Drosophila* (Saleh et al., 2009) and remains to be addressed in the future.

These findings indicate that Dnmt2 plays, in addition to the well-described role in tRNA methylation during the cellular stress response (Becker et al., 2012; Schaefer et al., 2010; Thiagarajan et al., 2011), additional roles in the response to biotic stressors. Even though the exact molecular mechanisms of Dnmt2-dependent virus control remain to be established, the presented data imply that Dnmt2 plays a central role in the activation of antiviral immune responses and in the efficient suppression of viral infection in *Drosophila*. A potential mode of action for Dnmt2 during virus-induced immune responses in *Drosophila* is presented in Figure 5.1.

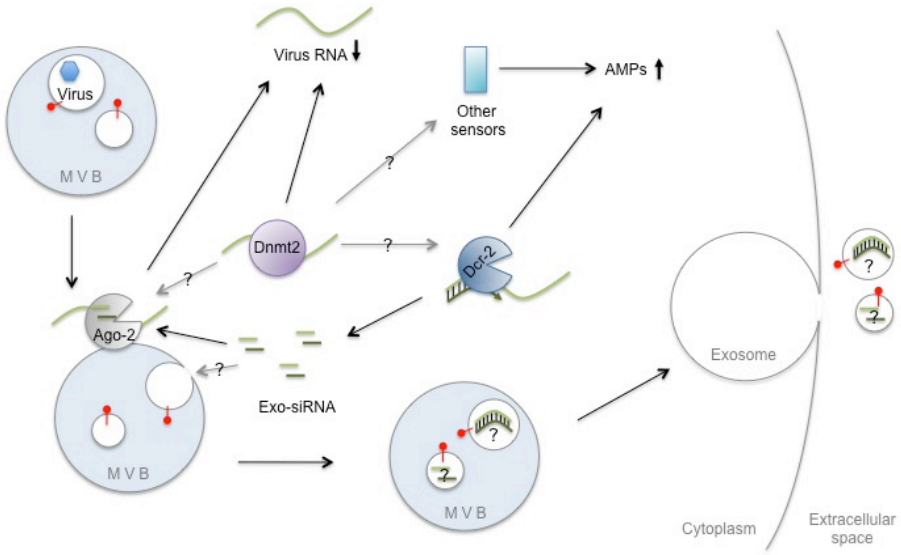

Figure 4.1: Illustration of the hypothetical mode of action of Dnmt2 during virus-induced immune responses in *Drosophila*.

Dnmt2 binding and potential methylation of viral RNA might be required to present the viral RNA to internal sensors of viral infection such as Dcr-2 and activate immune response. Dnmt2 might also contribute to mount the siRNA-mediated defense by directing viral RNAs to specific cellular foci. This compartmentalization might play a role in the dsRNA-dependent systemic spread of antiviral silencing in *Drosophila*. MVB= Multivesicular body, AMPs= Antimicrobial peptides.

4.2 Dnmt2 Function in General Stress Responses

Transfer RNAs are fundamental components of the translational machinery but recent work has also suggested additional roles for tRNAs in the modulation of various stress responses. Endonucleolytic cleavage of tRNAs has been found to be an evolutionary conserved response do stress (Thompson et al., 2008). Furthermore, it was suggested that tRNA-derived fragments could potentially act as modulators of siRNA pathways (Haussecker et al., 2010). However, while it is not clear how tRNA fragmentation is controlled and limited during cellular stress responses the exact functions for stress-induced tRNA fragments remain to be defined.

4.2.1 Stress-Induced Temporary Dnmt2-Depletion is Necessary for Efficient Cellular Stress Response

Dnmt2 enzymes have been associated with cellular stress responses in several species (Becker et al., 2012; Schaefer et al., 2010; Thiagarajan et al., 2011). Mostly on the basis of biochemical assays it was concluded that Dnmt2-mediated tRNA methylation in the anticodon protects tRNAs from endonucleolytic cleavage in *Drosophila* and mouse (Schaefer et al., 2010). This raised the question why many organisms, including flies, which contained functional Dnmt2, show stress-induced tRNA fragmentation of Dnmt2-substrate tRNAs (Figure 3.14D).

The observation that heat shock induced both a specific loss of RNA methylation in Dnmt2 substrate tRNAs (Figure 3.14A) and the depletion of full-length Dnmt2 (Figure 3.14C) can now explain the increased tRNA fragmentation of Dnmt2 substrates in wild type cells. The loss of tRNA methylation was measurable only at C38 but not at cytosines that were methylated by another RNA methyltransferase (Figure 3.14A). It is established that the reprogramming of tRNA modifications contributes to cellular responses during different stress conditions (Chan et al., 2010). Importantly, different stresses cause stress-specific changes in tRNA modifications (Chan et al., 2010). While the function of such stress-induced changes is connected to the enhanced translation of stress-specific mRNAs via codon usage bias (Chan et al., 2012; Novoa and Ribas de Pouplana, 2012), the mechanisms facilitating these changes are not clear. It was proposed that changes in the levels of tRNA modifications are linked to the activity of the respective modification enzymes (Chan et al., 2010; Chan et al., 2012). This notion is supported by the observation that Dnmt2 activity is inhibited by depletion of the protein, which enables remodeling of 5mC at position 38 during the stress response (Figure 3.14A and C). The possible effects of tRNA modifications on stress-induced tRNA fragmentation has been suggested (Chan et al., 2010; Chan et al., 2012; Schaefer et al., 2010; Tuorto et al 2012) but not well explored. The impact of stress-induced

decrease of Dnmt2-dependent tRNA methylation on protein synthesis is intriguing (Tuorto et al., 2012) and the exact mechanisms have to be addressed in the future. This study now provides new insights in the role of tRNA modifications possibly reprogramming stress-induced tRNA fragmentation.

Loss of tRNA methylation was closely followed by increased tRNA fragmentation (Figure 3.14D and 3.16A) indicating increased accessibility of stress-induced endonucleases to the anticodon stem loop of these tRNAs. These observations not only confirm the previous notion that Dnmt2-dependent methylation of tRNAs interferes with uncontrolled tRNA fragmentation but also suggest that the transient loss of functional Dnmt2 and the fragmentation of Dnmt2-substrate tRNAs is an important part of the physiological response to stress. Importantly, *Dnmt2* mutants show significantly higher levels for tRNA fragments (Figure 3.16B) if compared to the fragmentation of rRNAs and mRNAs (Figure 3.15) thereby linking Dnmt2 specifically to the tRNA fragmentation process. Additionally, Dnmt2 mutants showed different tRNA fragmentation patterns (Figure 3.16C). While the fragmentation of tRNA-Gly$^{GCC(TCC)}$ and tRNA-Asp^{GTC} (Figure 3.16C) confirms that Dnmt2-dependent methylation interferes with their processing by stress-induced ribonucleases, the increased fragmentation of non-substrate tRNAs tRNA-Lys$^{CTT(TTT)}$ and tRNA-Cys^{GCA} (Figure 3.16C) indicates a methylation-independent function of Dnmt2 on tRNA stability. Recent studies described the formation of tRNA granules in response to heat stress (Miyagawa et al., 2012) indicating that tRNAs are actively transported to specific cellular foci during stress responses. Considering the observed stress-induced re-localization of Dnmt2 to stress granules (Schaefer et al., 2010) it is intriguing to speculate that a methylation-independent function of Dnmt2 exists. This would be the re-localization of tRNAs to specific cellular foci during the stress response.

In addition to different tRNA fragmentation patterns, length distribution and terminal identity of individual tRNA fragments from Dnmt2-substrates tRNAs (tRNA-Gly^{GCC} and tRNA-Asp^{GTC}) was different in Dnmt2 mutants (Figure 3.17 and 3.18), suggesting also defects in further processing of these fragments that could be caused by the alteration in the accessibility to endo- and exonucleases. Of note, the 5'-end of tRNA-Gly^{GCC} acted as a potent inhibitor of protein translation (Ivanov et al., 2011) indicating that correct tRNA-Gly^{GCC} fragmentation might be important for the proper cellular stress response.

Taken together, these new findings support the notion that Dnmt2-mediated RNA processing modulates the general outcome of stress-induced tRNA fragmentation in *Drosophila*. Furthermore, the involvement of RNA cytosine methylation in tRNA fragmentation raises the possibility that also other tRNA modification systems could be involved in the control of tRNA fragmentation during stress responses.

4.2.2 Stress-Induced tRNA Fragments Interfere with siRNA Pathways to Facilitate Correct Stress Responses

The association of tRNA fragments with small RNA pathway components was recently demonstrated (Burroughs et al., 2011; Cole et al., 2009; Czech et al., 2008; Haussecker et al., 2010). Since the main function of siRNA pathways is to interfere with RNA expression on a post-transcriptional level these interactions were interpreted as indication that also tRNA fragments could act as siRNA and therefore might be used to target mRNAs (Burroughs et al., 2011; Cole et al., 2009; Haussecker et al., 2010). Alternatively, it was postulated that tRNA fragments could modulate RNAi pathways by interference with Argonaute protein binding to small RNAs (Durdevic and Schaefer, 2013; Haussecker et al., 2010). The increased loading of small tRNA-derived fragments into *Drosophila* Ago-2 after heat shock (Figure 3.19A and B) supports the notion that dynamic changes in small RNA binding to Ago-2 occur during the heat shock response and suggest that tRNA-derived fragments could compete with other small RNAs for Ago-2 binding. Importantly, stress leads to the accumulation of Ago-2 in SG and results in decreased small RNA-mediated gene silencing (Detzer et al., 2011). One possible role for such an Ago-2 sequestration could be to allow the rapid de-repression of stress response genes that are controlled by Ago-2-mediated silencing. Since tRNA fragments can induce the formation of SG (Ivanov et al., 2011), it is conceivable that tRNA fragments play a role in the re-localization of Ago-2 to SG during stress. Of note, Dnmt2 associates also with SG during the heat shock response (Schaefer et al., 2010) indicating that re-localization of Dnmt2 to these structures is relevant for its function on tRNAs during the stress conditions. However, how stress-induced tRNA fragments affect the re-localization of Ago-2 to SG or if Dnmt2 function is required in SG for correct stress responses remains to be investigated in future studies.

4.3 Dnmt2-Dependent Regulation of Stress-Induced Transposons

While mobile element control has been extensively studied under standard laboratory conditions, the mechanisms that regulate mobile elements during stress are still unclear. Heat shock causes changes in chromatin structure to accommodate specific stress-related transcriptional responses. Due to these transcriptional responses mobile elements, which are inserted in stress-regulated genomic regions become co-transcribed (Tittel-Elmer et al., 2010; Vasilyeva et al., 1999). While cells cannot efficiently suppress the transcription of stress-induced elements, the re-silencing of these elements, especially at the post-transcriptional level has to be controlled to avoid mobile element propagation.

4.3.1 Dnmt2-Dependent tRNA Fragmentation and Efficient RNAi-Mediated Transposon Control during Stress Response

In contrast to a previous report (Phalke et al., 2009), this work uncovered that transposon expression in *Dnmt2* mutant flies was not de-regulated under standard laboratory conditions but after heat shock treatment (Figure 3.9). Importantly, a general de-regulation of transposable elements could be observed in *Dnmt2* mutant flies after heat shock (Figure 3.9, Table 5.1). These data indicate that Dnmt2 exerts its function in mobile element control on a post-transcriptional level where its methyltransferase activity was needed to contribute to the efficient re-silencing of stress-induced mobile element RNA or cDNA (Figure 3.10B).

The methyltransferase activity of Dnmt2 was required for this function (Figure 3.13), suggesting a role for Dnmt2-mediated RNA methylation in transposon control. It is not known whether, similarly to Drosophila C virus, Dnmt2 can bind and potentially methylate transposon-derived RNAs. Yet, the relatively narrow substrate specificity of Dnmt2 enzymes for only few tRNAs argues against RNA methylation of all classes and families of *Drosophila* mobile elements and favors alternative explanations for its involvement in transposon control.

Recent observations link tRNA fragmentation to small RNA silencing pathways (Burroughs et al., 2011; Cole et al., 2009; Couvillion et al., 2010; Czech et al., 2008; Haussecker et al., 2010). tRNA-derived fragments were found in RNAi effector molecules, such as Ago-2 (Cole et al., 2009; Czech et al., 2008) and Piwi (Couvillion et al., 2010). Transposon silencing in *Drosophila* relies on siRNA pathways in somatic tissues and recent studies linked these pathways to the re-silencing of stress-induced transposons in plants (Ito et al., 2011). Although the expression of RNAi components in *Dnmt2* mutant flies was not significantly different from wild type flies (Figure 3.20) the observation that heat-shocked *Dnmt2* mutant flies phenotypically resembled RNAi mutant flies (Table 5.2 and 5.3, Figure 3.21A) indicated a connection between Dnmt2 and siRNA pathways.

In *Drosophila*, Dcr-2 is pivotal for the processing of dsRNA precursors into siRNAs. Importantly, the ability of human DICER to cleave tRNA-derived sequences into small RNAs was recently shown (Babiarz et al., 2008; Cole et al., 2009). *Drosophila* harbor two Dicer genes, *Dcr-1* and *Dcr-2*, but only Dcr-2 was identified to bind and cleave tRNA sequences (B. Mobin, Master Thesis, 2012). Interestingly, Dcr-2-mediated tRNA cleavage activity was shown to be stress-dependent (B. Mobin, Master Thesis, 2012). Since overall Dcr-2 protein levels were not affected in *Dnmt2* mutants (Figure 3.20B) but Dcr-2 output was reduced, excessive tRNA fragmentation in *Dnmt2* mutants (Figure 3.14D and 3.16A) could be causal for the reduced Dcr-2 activity. Indeed, a global accumulation of dsRNA (Dcr-2 substrates) could be observed in *Dnmt2* mutant flies, which was similar to the accumulation in *Dcr-2* mutant flies (Figure 3.21B). Heat shock caused even higher levels of dsRNA in *Dnmt2*

mutant flies (Figure 3.21B, lower), even though Dcr-2 protein levels were increased upon heat shock (Figure 3.20B), which again indicates impaired Dcr-2 function. These findings are substantiated by the heat shock-induced accumulation of transposon-derived dsRNAs in *Dnmt2* mutant flies (Figure 3.21C and D). Inefficient processing of dsRNA including precursors for exo-siRNA and endo-siRNAs led to decreased levels of a mature siRNA (esi-2.1) (Figure 3.22A and B) and the de-repression of its mRNA target *mus308* as well as to the accumulation of viruses in *Dnmt2* mutants (Figure 3.22C-E).

While the exact function of stress-induced and tRNA-derived fragments in small RNAi components remains to be investigated, their loading into RNA processing (Dcr-2) and RNAi effector (Ago-2) components suggests biological activity for these abundant RNA fragments. An intriguing mode of action would be to modulate the activity of RNAi components during the recovery from stress. Importantly, a decrease of small RNA-mediated gene silencing was observed during stress responses of human cells (Detzer et al., 2011). In such a scenario tRNA-fragments might compete with dsRNA precursors and/or siRNAs for their loading into Dcr-2 and Ago-2, respectively. Such tRNA-based competition mechanism could constitute a rapid means to de-repress the inhibitory effects of endo-siRNAs on various mRNAs during the stress response. While this process is transient in wild type animals (Figure 3.9B and 3.22C-E), the *Dnmt2* mutation increases the production of such inhibitory tRNA-derived small RNAs. As a result inhibition of siRNA pathways will be prolonged and downstream consequences will amplify such as the propagation and new insertions of mobile elements in *Dnmt2* mutant genomes (Figure 3.11 and 3.12). The presented data suggest that transient tRNA fragmentation in wild type cells is not only required to inhibit protein synthesis but also contributes to the transient inhibition of siRNA pathways during the heat shock response. These findings indicate that Dnmt2-mediated tRNA methylation is necessary to prevent the excessive production of tRNA-derived fragments, which could have lasting effects on siRNA pathways during the recovery from stress. It is therefore intriguing to speculate that the biological function of the highly conserved RNA methyltransferase Dnmt2 is founded in the regulated processing of equally well conserved tRNA molecules, which can influence not only protein translation but also ancient cellular mechanisms such as stress responses and mobile element control. Figure 5.2 illustrates the contribution of Dnmt2 to these processes during the cellular stress response and the stress recovery in *Drosophila*.

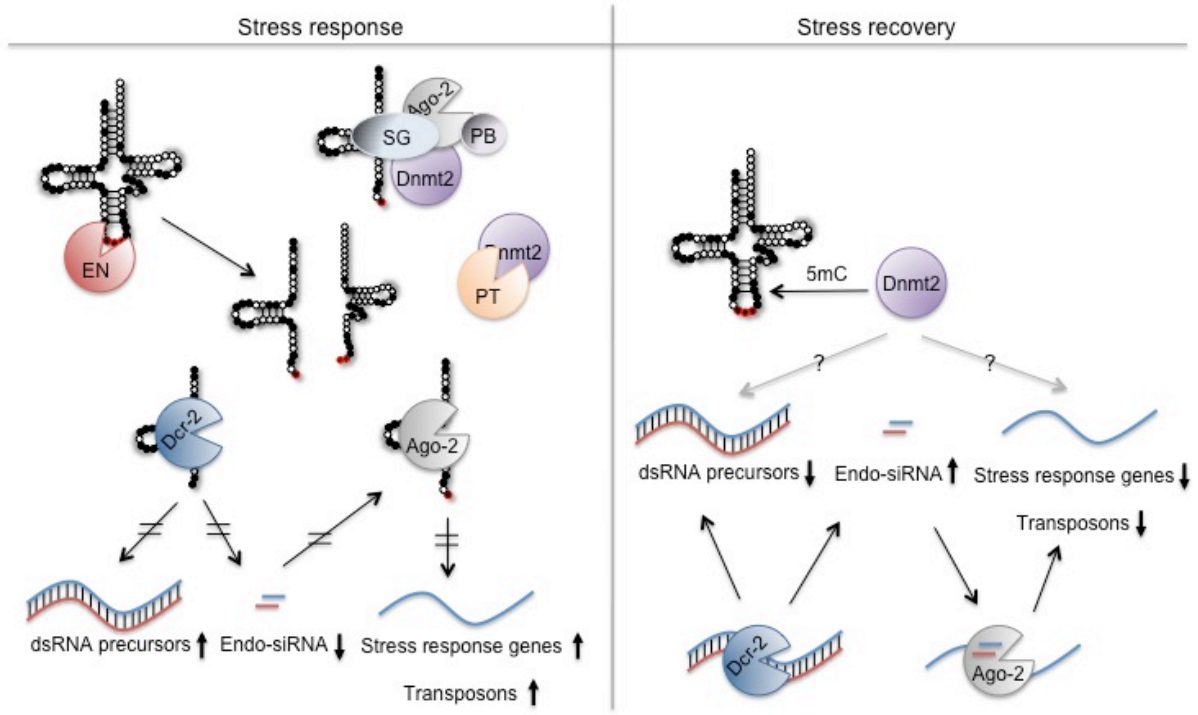

Figure 4.2: Schematic representation of Dnmt2 contribution to the processes during cellular stress response and stress recovery in Drosophila.

tRNA fragmentation is evolutionary conserved process in cellular stress response that coincide with stress-induced depletion of Dnmt2. tRNA fragments interfere with RNAi mediated PTGS and transposon control that lead to de-repression of stress response genes and transposons. During the recovery phase Dnmt2 proteins levels are restored and Dnmt2-mediated tRNA methylation prevents excessive tRNA fragmentation and ensures correct function of RNAi silencing. EN= RNA Endonuclease, PT=Protease, SG=Stress granules, PB=P bodies.

4.3.2 tRNA Fragments Could Enhance Transposon cDNA Synthesis

An intriguing aspect of LTR transposon propagation is the use of host tRNAs as primers for reverse transcription of mobile element RNA. Specifically, tRNAs are being used to prime the minus strong-stop DNA that is prerequisite for transposon cDNA synthesis (Arkhipova et al., 1986). Only for few LTR transposons corresponding tRNA-primers are identified. A fragment of tRNA-iMet^{ATG}, terminating in the anticodon stem is usually used to prime the reverse transcription of copia-group retroelements whereas gypsy-group uses tRNA-Lys, tRNA-Arg, tRNA-Leu, tRNA-Ser (Marquet et al., 1995), suggesting the possibility that other tRNA fragments could be used for similar purposes. Of note, the Dnmt2 substrate tRNA-Gly has been implicated in priming a murine LTR-retrotransposon (Hodgson et al., 1983). It remains to be investigated whether excessive fragmentation of Dnmt2-substrate tRNAs (Figure 3.14D and 3.16A) could contribute to the increased transposon propagation (Figure 3.11 and 3.12) by serving as primers for reverse transcription of mobile elements.

4.3.3 Dnmt2 and a Role in “Canalization”

Increased expression of transposon RNAs leads to the production of transposon-derived cDNA (Figure 3.10B and C), causing new integration events of functional transposons in both somatic and germ line cells (Figure 3.11 and 3.12). The observed transient up-regulation of transposon expression (Figure 3.9B) together with the observed albeit low mobilization of transposons in wild type tissues (Figure 3.11) indicates that stress could facilitates mutator mechanisms that result in genetic variability by transposon mutagenesis (Beauregard et al., 2008; Böhne et al., 2008; Oliver and Greene, 2012; Werren, 2011). In response to severe or repetive environmental changes such mechanisms are thought to allow the selection for advantageous genetic and epigenetic mutations. For instance, the preferential integration of retrotransposons into regulatory regions of stress response genes has been shown to enhance their expression (Feng et al., 2013). The stress-induced depletion of Dnmt2, especially after repeated heat shocks (Figure 3.14C, upper), could be interpreted as facilitator of transposon-induced mutations. However, in order to avoid disadvantageous insertional mutagenesis and to preserve genome stability, these processes have to be tightly regulated as noticeable by the rapid re-silencing of retrotransposon in wild type tissues (Figure 3.9B), which coincides with recurrence and even up-regulation of Dnmt2 during the stress recovery (Figure 3.14C, upper). Therefore it is tempting to speculate that Dnmt2 might be involved in the process of “canalization”, which is a concept that was proposed in 1942 (Waddington, 1942) and argues that newly induced genetic variation can be genetically assimilated over many generations to increase the fitness of the population (Gangaraju et al., 2011; Specchia et al., 2010). The development of adaptive mechanisms to prolonged environmental changes is essential for the survival of the species.

4.4 Phenotypic Robustness and Evolvability: Dnmt2 Perspective

Managing interactions between gene expression and the environment is of fundamental importance for successful evolution. Depending on the intensity and recurrence of environmental changes, responses might range from the development of alternative phenotypes without changes in the genotype (phenotypic plasticity, adaptive evolution), rapid appearance of novel genetic variations (non-adaptive evolution) or extinction at the population level.

Organisms are constantly challenged by environmental stresses, which trigger plastic responses in the range of genomic reaction norms (Aubin-Horth and Renn, 2009) including alterations in physiology, behavior and morphology. In contrast, extreme and persistent environmental changes often increase genetic variation because of elevated mutation and

recombination rates (Hoffmann and Merilä, 1999; Wright, 2004). A balance between phenotypic plasticity and genetic change is crucial for optimal fitness in variable environments and Dnmt2 enzymes could represent a link between these two processes. In this scenario Dnmt2-dependent RNA processing contributes to the correct response to environmental changes and therefore might facilitate plastic adaptation to the new environmental conditions. The findings that *Dnmt2* mutant flies show increased recombination events at repetitive genomic loci (Phalke et al., 2009) and the observed increased rate of stress-induced transposon-mediated mutagenesis in *Dnmt2* mutants (Figure 3.11) suggest that loss of Dnmt2 might enable the development of novel genetic variations, which would remain hidden or silent in case environmental pressure is temporary or could became “directional”, i.e. when certain genetic changes become advantageous under selection pressure of persisting environmental changes. Therefore, Dnmt2-dependent processes might represent “pre-adaptation“ mechanisms, which, depending on the intensity of environmental changes, may remain in the scope of phenotypic plasticity and genomic reaction norms (phenotypic robustness) or would promote genetic rearrangements to increase the fitness of the population in the context of adaptive responses to new environments (evolvability). Clarifying the involvement of Dnmt2 in such fundamental properties, which are important for every biological system, could contribute to the clarification of the strong evolutionary conservation of these enzymes.

4.5 Conclusions

Taken together, the findings presented in this doctoral thesis indicate that Dnmt2 enzymes play important role in cellular responses to biotic and abiotic stresses. Although the exact molecular mechanisms of Dnmt2 function in these processes remain to be established, the biological functions described here could explain the strong evolutionary conservation and wide phylogenetic distribution of Dnmt2 enzymes. Facilitating proper stress response by regulating tRNA-fragmentation, support of genome stability during stress responses by efficient control of stress-induced endogenous mobile elements, and effective defense against ancient exogenous invaders such are viruses represent crucial tasks for the survival of all living organisms. In light of the strong evolutionary conservation of Dnmt2 enzymes, it is intriguing to speculate that this biological function is a common denominator for all Dnmt2 family members.

Chapter 5

Appendix

Schematic representation P-element insertion in the 5' LTR of Invader4 on Y chromosome and inverse PCR method

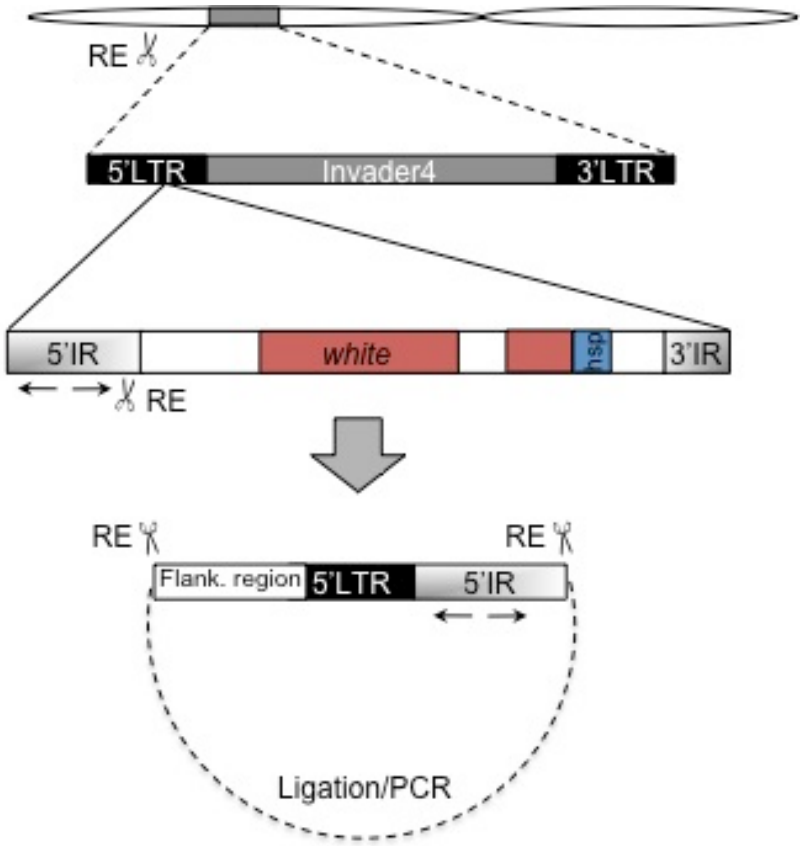

Figure 5.1: Schematic representation of mapping approach by inverse PCR and illustration of P-element insertion in the 5' LTR of Invader4 on Y chromosome.

Schematic drawing of the P-element insertion at *Invader4* on the Y-chromosome (HA-1925). Truncated 3' IR is represented as shorter bar. Mapping approach by inverse PCR. Restriction (RE) within the 5'-end of the *Invader4* LTR and at an unknown genomic site creates genomic DNA fragments suitable for ligation and inverse PCR mapping. PCR was carried out with primers from within the 5' IR (arrows).

Summary of de-regulated transposons in Dnmt2 mutant fllies indentified by the sequencing on Illumina platform.

Table 5.1: De-regulated transposons in *Dnmt2* mutant flies after heat hock and during the recovery phase, indentified by the sequencing on Illumina platform.

LTR			**Non-LTR**		
Name	Size	$D2^{-/-}$	Name	Size	$D2^{-/-}$
17,6	7439bp	+	baggins	5453bp	+
1731	4648bp	+	BS	5142bp	+
297	6995bp	+	BS3	1790bp	+
3S18	6126bp	+	BS4	754bp	-
412	7567bp	+	Cr1a	4470bp	+
accord	7404bp	+	Doc	4725bp	+
accord2	7650bp	+	Doc2	4789bp	+
aurora	4263bp	-	Doc3	4740bp	+
blood	7410bp	+	Doc4	2791bp	+
Burdock	6411bp	+	F-element	4708bp	+
Circe	7450bp	-	Fw2	3961bp	+
copia	5143bp	+	Fw3	3132bp	+
diver	6112bp	-	G-element	4346bp	+
diver2	4917bp	+	G2	3102bp	+
Dm88	4558bp	+	G3	4605bp	+
flea	5034bp	+	G4	3856bp	+
frogger	2483bp	-	G5	4856bp	+
GATE	8507bp	+	G5A	2841bp	+
gtwin	7411bp	+	G6	2042bp	+
gypsy	7469bp	+	G7	1192bp	-
gypsy2	6841bp	+	Helena	1318bp	+
gypsy3	6973bp	+	HeT-A	6083bp	+
gypsy4	7369bp	+	I-element	5371bp	-
gypsy5	6852bp	+	Ivk	5402bp	+
gypsy6	7826bp	+	Juan	4236bp	+
gypsy7	5486bp	+	jockey	5020bp	+
gypsy8	4955bp	+	jockey2	3428bp	+
gypsy9	5349bp	+	Penelope	804bp	-
gypsy10	6006bp	+	Porto1	4682bp	+
gypsy11	4428bp	-	Q-element	759bp	+
gypsy12	10218bp	+	R1A1	5356bp	+
HMS-Beagle	7062bp	+	R1-2	3216bp	+
HMS-Beagle2	7220bp	+	R2-element	3607bp	-
Idefix	7411bp	+	Rt1a	5108bp	+
invader1	4032bp	+	Rt1c	5443bp	+
invader2	5124bp	+	Rt1b	5171bp	+
invader3	5484bp	+	TAHRE	10463bp	-
invader4	3105bp	+	TART-A	13424bp	+
invader5	4038bp	+	TART-B	10654bp	-
invader6	4885bp	-	TART-C	11124bp	-
Max-element	8556bp	+	X-element	4740bp	+
McClintock	6450bp	+			

mdg1	7480bp	+
mdg3	5519bp	+
micropia	5461bp	+
opus	7521bp	+
Osvaldo	1543bp	-
Quasimodo	7387bp	+
roo	9092bp	+
rooA	7621bp	+
rover	7318bp	+
springer	7546bp	+
Stalker	7256bp	-
Stalker2	7672bp	+
Stalker3	372bp	-
Stalker4	7359bp	+
Tabor	7345bp	-
Tirant	8526bp	+
Tom1	410bp	-
Transpac	5249bp	+
ZAM	8435bp	-

SINE-like		
Name	Size	$D2^{-/-}$
INE-1	611bp	+

IR-elements		
Name	Size	D2-/-
1360	3409bp	+
Bari1	1728bp	+
Bari2	1064bp	+
HB	1653bp	+
hobo	2959bp	-
hopper	1435bp	+
hopper2	1593bp	+
looper1	1881bp	+
mariner2	912bp	+
NOF	4347bp	+
P-element	2907bp	-
pogo	2121bp	+
S-element	1736bp	+
S2	1735bp	+
Tc1	1666bp	+
Tc1-2	1644bp	+
Tc3	1743bp	+
transib1	2167bp	+
transib2	2844bp	+
transib3	2883bp	+
transib4	2656bp	+

Comparison of phenotypes of Ago2, Dcr-2 and Dnmt2 mutant flies

Table 5.2: Comparison of the degree of transposons de-repression between *Drosophila* RNAi mutants and heat shocked *Dnmt2* mutants.

Mutants analyzed	De-repressed transposon (%)	Number analyzed	Fold de-repression	Method of analysis	Transposon type	Reference
Ago-2$^{-/-}$ (heads)	100	5	2-5	qPCR	LTR, Non-LTR	{Chung:2008bj}
Ago-2$^{-/-}$ (ovaries,)	100	12	1,5-9	qPCR	LTR, Non-LTR	{Czech:2008ii}
Dcr-2$^{-/-}$ (heads,)	40	5	3,5	qPCR	LTR	{Chung:2008bj}
Dcr-2$^{-/-}$ (soma)	71	7	1,5-7	qPCR	LTR	{Kawamura:2008ei}
Dnmt2$^{-/-}$ (whole flies)	100	4	2-25	qPCR	LTR	Figures 3.9 and 3.22
Dnmt2$^{-/-}$ (whole flies)	82	124	-	Sequencing on Illumina platform	LTR, Non-LTR, DNA	Table5.1

Table 5.3: Comparison of phenotypes between *Drosophila* RNAi mutants and *Dnmt2* mutants.

Mutants analyzed	Ago-2$^{-/-}$	Dcr-2$^{-/-}$	Dnmt2$^{-/-}$
Viability	viable	viable	viable
Fertility	fertile	fertile	fertile
Transposon de-repression	yes	yes	Stress-induced
Recovery from heat stress (ca. 50% of wild type flies recover after time point 30 min)	>50% of the flies after time point 0	>50% of the flies after time point 0	>50% of the flies after time point 0

Summary of small RNA sequencing analyses

Table 5.4: Summary of the statistics of the six sequenced libraries of small RNAs.

Genotype	Experimental condition	Total extracted	Total mapping
Dnmt2 (+/-)	Control (ctrl)	4976019	264250
Dnmt2 (+/-)	Heat shock (hs)	6508750	504092
Dnmt2 (+/-)	2 day recovery (2R)	5699885	345423
Dnmt2 (-/-)	Control (ctrl)	8410307	605611
Dnmt2 (-/-)	Heat shock (hs)	4107107	197113
Dnmt2 (-/-)	2 day recovery (2R)	1738215	70310

Table 5.5: Summary of the percentage of reads corresponding to rRNAs, mRNAs, tRNAs and other (bacteria, viruses etc.).

	ctrl		hs		2R	
	$D2^{+/-}$	$D2^{-/-}$	$D2^{+/-}$	$D2^{+/-}$	$D2^{-/-}$	$D2^{+/-}$
rRNA	67,1	67,7	74,9	64,2	77,8	79,7
tRNA	6	11,3	9,4	19,9	8,5	7,4
mRNA	8,1	12,4	10,8	15,5	13,2	10,5
other	18,8	8,6	4,9	0,4	0,5	2,4

Table 5.6: Summary of the number of reads corresponding to mRNAs.

	ctrl		hs		2R	
mRNA	$D2^{+/-}$	$D2^{-/-}$	$D2^{+/-}$	$D2^{-/-}$	$D2^{+/-}$	$D2^{-/-}$
Muc68D	8561	6189	4129	4987	3596	3385
Ubi-p63E	1737	2951	3403	3646	4812	4724
Hsp70A	299	252	1749	2089	3186	3081
Hsp70B	275	252	1678	1850	3082	3303
other Hsps	67	84	581	555	781	695
Jon99Cii/α-Try	586	584	322	303	331	402
LysB	221	229	36	34	228	248
Amy-d/Amy-p	244	298	152	158	335	395
other mRNAs	9496	21912	16488	27406	18587	11549

Table 5.7: Mapped tRNA fragments from control ($D2^{+/-}$) *Drosophila* somatic tissue.
(ctrl= no heat shock; hs= 37 C, one hour plus 5 hours recovery; 2R = 2 days recovery after heat shock).

Heterozygous control: $D2^{+/-}$															
tRNA	Sense						Antisense						Total number of tRNA reads		
	Number of tRNA reads			% of total tRNA reads			Number of tRNA reads			% of total tRNA reads					
	ctrl	hs	2R	ctrl	hs	2R	ctrl	hs	2R	ctrl	hs	2R	ctrl	hs	2R
Gly	417	1063	480	54,51	45,96	35,29	7922	20196	9124	53,72	45,95	33,17	8339	21259	9604
Glu	150	629	408	19,61	27,19	30,00	2847	11942	8370	19,31	27,17	30,43	2997	12571	8778
Lys	110	301	250	14,38	13,01	18,38	2086	5720	5414	14,15	13,01	19,68	2196	6021	5664
Asp	29	141	58	3,79	6,10	4,26	552	2694	1502	3,75	6,11	5,46	582	2835	1560
Cys	6	63	23	0,78	2,72	1,69	322	1195	437	2,18	2,72	1,59	328	1258	460
Gln	7	12	23	0,92	0,52	1,69	136	227	447	0,92	0,52	1,62	143	239	470
Met	8	13	18	1,05	0,56	1,32	155	250	355	1,05	0,57	1,29	163	263	373
Pro	11	13	13	1,44	0,56	0,96	217	253	465	1,47	0,58	1,69	228	266	478
Val	4	15	8	0,52	0,65	0,59	71	279	154	0,48	0,63	0,56	75	294	162
Trp	4	11	11	0,52	0,48	0,81	69	199	210	0,47	0,45	0,76	73	210	221
His	3	9	6	0,39	0,39	0,44	62	167	128	0,42	0,38	0,47	65	176	134
Arg	2	9	12	0,26	0,39	0,88	45	179	217	0,31	0,41	0,79	47	188	229
Ser	2	5	4	0,26	0,22	0,29	46	104	88	0,31	0,24	0,32	48	109	92
Asn	2	3	5	0,26	0,13	0,37	30	50	74	0,20	0,11	0,27	32	53	79
Ala	2	4	15	0,26	0,17	1,10	40	76	115	0,27	0,17	0,42	42	80	130
SeC	2	8	12	0,26	0,35	0,88	46	149	154	0,31	0,34	0,56	48	157	166
Thr	2	5	8	0,26	0,22	0,59	29	89	86	0,20	0,20	0,31	31	94	94
Ile	1	5	1	0,13	0,22	0,07	25	99	71	0,17	0,23	0,26	26	104	72
Leu	2	3	0	0,26	0,13	0,00	29	65	52	0,20	0,15	0,19	31	68	52
Phe	0	0	0	0,00	0,00	0,00	7	5	13	0,05	0,01	0,05	7	5	13
Tyr	1	1	5	0,13	0,04	0,37	10	22	34	0,07	0,05	0,12	11	23	39
Σ	**765**	**2313**	**1360**				**14747**	**43960**	**27510**				**15512**	**46273**	**28870**

Table 5.8: Mapped tRNA fragments from *Dnmt2* mutant ($D2^{-/-}$) *Drosophila* somatic tissue. (ctrl= no heat shock; hs= 37 C, one hour plus 5 hours recovery; 2R = 2 days recovery after heat shock).

Dnmt2 mutant: $D2^{-/-}$															
tRNA	**Sense**						**Antisense**						**Total number of tRNA reads**		
	Number of tRNA reads			**% of total tRNA reads**			**Number of tRNA reads**			**% of total tRNA reads**					
	ctrl	**hs**	**2R**	**ctrl**	**hs**	**2R**	**ctrl**	**hs**	**2R**	**ctrl**	**hs**	**2R**	**ctrl**	**hs**	**2R**
Gly	2020	1097	147	59,50	59,04	56,98	38388	20850	2792	59,50	57,71	57,30	40408	21947	2939
Glu	270	291	36	7,95	15,66	13,95	5124	5534	676	7,94	15,32	13,89	5394	5825	712
Lys	790	255	50	23,27	13,72	19,38	15016	4852	941	23,27	16,20	19,31	15806	5107	991
Asp	54	69	9	1,59	4,04	3,49	744	1202	158	1,59	3,34	3,32	798	1271	167
Cys	20	50	2	0,59	2,69	0,78	378	956	44	0,59	2,65	0,90	398	1006	46
Gln	57	26	2	1,68	1,40	0,78	1091	490	33	1,69	1,36	0,68	1148	516	35
Met	45	10	2	1,33	0,54	0,78	846	196	45	1,31	0,54	0,92	891	206	47
Pro	35	9	2	1,03	0,48	0,78	673	163	35	1,04	0,45	0,72	708	172	37
Val	7	5	1	0,21	0,27	0,39	142	93	22	0,22	0,26	0,45	149	98	23
Trp	15	3	0	0,44	0,16	0,00	283	61	5	0,44	0,17	0,10	298	64	5
His	26	17	2	0,77	0,91	0,78	490	323	30	0,76	0,89	0,62	516	340	32
Arg	14	5	1	0,41	0,27	0,39	269	101	12	0,42	0,28	0,25	283	106	13
Ser	10	4	1	0,29	0,22	0,39	188	84	13	0,29	0,23	0,27	198	88	14
Asn	8	1	0	0,24	0,05	0,00	154	23	9	0,24	0,06	0,18	162	24	9
Ala	8	3	1	0,24	0,16	0,39	153	61	13	0,24	0,17	0,27	161	64	14
SeC	9	2	1	0,27	0,11	0,39	167	29	10	0,26	0,08	0,21	176	31	11
Thr	3	1	0	0,09	0,05	0,00	51	25	7	0,08	0,07	0,14	54	26	7
Ile	2	1	0	0,06	0,05	0,00	33	20	8	0,05	0,06	0,16	35	21	8
Leu	1	2	1	0,03	0,11	0,39	20	35	12	0,03	0,10	0,25	21	37	13
Phe	0	0	0	0,00	0,00	0,00	2	2	1	0,00	0,01	0,02	2	2	1
Tyr	1	1	0	0,03	0,05	0,00	24	26	2	0,04	0,07	0,04	25	27	2
Σ	**3395**	**1852**	**258**				**64236**	**35126**	**4868**				**67631**	**36978**	**5126**

Table 5.9: tRNA fragments from control ($D2^{+/-}$) *Drosophila* somatic tissue originating from 5 tRNAs (>90% of all tRNA fragments) separated according to the isoacceptor type. (ctrl= no heat shock; hs= 37°C, one hour plus 5 hours recovery; 2R = 2 days recovery after heat shock).

$D2^{+/-}$ adult *Drosophila* male somatic tissue			
tRNA	**Number of tRNA reads**		
	ctrl	**hs**	**2R**
tRNA-Gly^{GCC}	8204	21073	9451
tRNA-Gly^{TCC}	135	186	153
tRNA-Glu^{CTC}	2798	11773	8125
tRNA-Glu^{TTC}	199	798	653
tRNA-Lys^{CTT}	1452	4345	4031
tRNA-Lys^{TTT}	744	1676	1633
tRNA-Asp^{GTC}	582	2835	1560
tRNA-Cys^{GCA}	328	1258	460

Table 5.10: tRNA fragments from *Dnmt2* mutant ($D2^{-/-}$) *Drosophila* somatic tissue originating from 5 tRNAs (>90% of all tRNA fragments) separated according to the isoacceptor type. (ctrl= no heat shock; hs= 37°C, one hour plus 5 hours recovery; 2R = 2 days recovery after heat shock).

$D2^{-/-}$ adult *Drosophila* male somatic tissue			
tRNA	**Number of tRNA reads**		
	ctrl	**hs**	**2R**
tRNA-Gly^{GCC}	39824	21312	2880
tRNA-Gly^{TCC}	584	635	59
tRNA-Glu^{CTC}	4656	5144	701
tRNA-Glu^{TTC}	738	681	11
tRNA-Lys^{CTT}	13581	3513	568
tRNA-Lys^{TTT}	2225	1594	423
tRNA-Asp^{GTC}	798	1271	167
tRNA-Cys^{GCA}	398	1006	46

Table 5.11: tRNA-Asp^{GTC} fragment identities corresponding to the 5' end of tRNA-Asp^{GTC} from control (D2$^{+/-}$) and *Dnmt2* mutant (D2$^{-/-}$) *Drosophila* somatic tissue.

Three time points were analyzed: ctrl= no heat shock; hs= 5 hours after heat shock; 2R= 2 days recovery.

tRNA-Asp^{GTC}				TCCTCGATAGTATAGTGGTTAGTATCCCCGCCTGTCACGCGGGAGACCGGGGTTCAATTCCCCGTCGGGGAG
Control (ctrl)	**D2$^{+/-}$**	51 nt	1	TCCTCGATAGTATAGTGGTTAGTATCCCCGCCTGTCACGTGGGAGACCGGG
		37 nt	3	TCCTCGATAGTATAGTGGTTAGTATCCCCGCCTGTCA
		36 nt	36	TCCTCGATAGTATAGTGGTTAGTATCCCCGCCTGTC
		35 nt	192	TCCTCGATAGTATAGTGGTTAGTATCCCCGCCTGT
		34 nt	21	TCCTCGATAGTATAGTGGTTAGTATCCCCGCCTG
		33 nt	30	TCCTCGATAGTATAGTGGTTAGTATCCCCGCCT
		32 nt	1	TCCTCGATAGTATAGTGGTTAGTATCCCCGCC
		30 nt	1	TCCTCGATAGTATAGTGGTTAGTATCCCCG
	D2$^{-/-}$	37nt	5	TCCTCGATAGTATAGTGGTTAGTATCCCCGCCTGTCA
		36 nt	15	TCCTCGATAGTATAGTGGTTAGTATCCCCGCCTGTC
		35 nt	238	TCCTCGATAGTATAGTGGTTAGTATCCCCGCCTGT
		34 nt	23	TCCTCGATAGTATAGTGGTTAGTATCCCCGCCTG
		33 nt	32	TCCTCGATAGTATAGTGGTTAGTATCCCCGCCT
		32 nt	7	TCCTCGATAGTATAGTGGTTAGTATCCCCGCC
Heat shock (hs)	**D2$^{+/-}$**	51 nt	2	TCCTCGATAGTATAGTGGTTAGTATCCCCGCCTGTCACGTGGGAGACCGGG
		49 nt	2	TCCTCGATAGTATAGTGGTTAGTATCCCCGCCTGTCACGCGGGAGACCG
		45 nt	1	TCCTCGATAGTATAGTGGTTAGTATCCCCGCCTGTCACCCGGGAG
		41 nt	1	TCCTCGATAGTATAGTGGTTAGTATCTCCGCCTGTCACGCG
		40 nt	1	TCCTCGATAGTATAGTGGTTAGTATCCCCGCCTGTCACGC
		39 nt	2	TCCTCGATAGTATAGTGGTTAGTATCCCCGCTTGTCACG
		38 nt	2	TCCTCGATAGTATAGTGGTTAGTATCCCCGCCTGTCAC
		37 nt	8	TCCTCGATAGTATAGTGGTTAGTATCCCCGCCTGTCA
		36 nt	163	TCCTCGATAGTATAGTGGTTAGTATCCCCGCCTGTC
		35 nt	1649	TCCTCGATAGTATAGTGGTTAGTATCCCCGCCTGT
		34 nt	55	TCCTCGATAGTATAGTGGTTAGTATCCCCGCCTG
		33 nt	148	TCCTCGATAGTATAGTGGTTAGTATCCCCGCCT
		32 nt	25	TCCTCGATAGTATAGTGGTTAGTATCCCCGCC
		31 nt	7	TCCTCGATAGTATAGTGGTTAGTATCCCCGC
		30 nt	3	TCCTCGATAGTATAGTGGTTAGTATCCCCG
	D2$^{-/-}$	50 nt	2	TCCTCGATAGTATAGTGGTTAGTATCCCCGCCTGTCACGCGGGAGACCGG
		47 nt	1	TCCTCGATAGTATAGTGGTTAGTATCCCCGCCTGTCACGCGGGAGAC
		45 nt	1	TCCTCGCTAGTATAGTGGTTAGTCTCCCCGCCTGTCACGCGGGAG
		40 nt	1	TCCTCGATAGTATAGTGGTTAGTCTCCCCGCCTGTCACGC
		37 nt	7	TCCTCGATAGTATAGTGGTTAGTATCCCCGCCTGTCA
		36 nt	38	TCCTCGATAGTATAGTGGTTAGTATCCCCGCCTGTC
		35 nt	559	TCCTCGATAGTATAGTGGTTAGTATCCCCGCCTGT
		34 nt	72	TCCTCGATAGTATAGTGGTTAGTATCCCCGCCTG
		33 nt	169	TCCTCGATAGTATAGTGGTTAGTATCCCCGCCT
		32 nt	23	TCCTCGATAGTATAGTGGTTAGTATCCCCGCC
		31 nt	1	TCCTCGATAGTATAGTGGTTAGTATCCCCGC
		30 nt	2	TCCTCGATAGTATAGTGGTTAGTATCCCCG
2 Days recovery (2R)	**D2$^{+/-}$**	48 nt	1	TCCTCGATAGTATAGTGGTTAGTATCCCCGCCTGTCACGCGGGAGACC
		47 nt	1	TCCTCGATAGTATAGTGGTTAGTATCCCCGCCTGTCACGCGGGAGAC
		40 nt	1	TCCTCGATAGTATAGTGGTTAGTATCCCCGCCTGTCACGC
		39 nt	2	TCCTCGATAGTATAGTGGTTAGTATCCCCGCCTGTCACG
		37 nt	7	TCCTCGATAGTATAGTGGTTAGTATCCCCGCCTGTCA
		36 nt	91	TCCTCGATAGTATAGTGGTTAGTATCCCCGCCTGTC
		35 nt	434	TCCTCGATAGTATAGTGGTTAGTATCCCCGCCTGT
		34 nt	24	TCCTCGATAGTATAGTGGTTAGTATCCCCGCCTG
		33 nt	30	TCCTCGATAGTATAGTGGTTAGTATCCCCGCCT
		32 nt	7	TCCTCGATAGTATAGTGGTTAGTATCCCCGCC
		31 nt	1	TCCTCGATAGTATAGTGGTTAGTATCCCCGC
	D2$^{-/-}$	37 nt	1	TCCTCGATAGTATAGTGGTTAGTCTCCCCGCCTGTCA
		36 nt	3	TCCTCGATAGTATAGTGGTTAGTATCCCCGCCTGTC
		35 nt	62	TCCTCGATAGTATAGTGGTTAGTATCCCCGCCTGT
		34 nt	4	TCCTCGATAGTATAGTGGTTAGTATCCCCGCCTG
		33 nt	11	TCCTCGATAGTATAGTGGTTAGTATCCCCGCCT
		32 nt	1	TCCTCGATAGTATAGTGGTTAGTATCCCCGCC
		Read length	N° of reads	**5' fragments**

Table 5.12: tRNA-Gly^{GCC} fragment identities corresponding to the 5' end of tRNA-Gly^{GCC} from control (D2$^{+/-}$) and *Dnmt2* mutant (D2$^{-/-}$) *Drosophila* somatic tissue.
Time point ctrl = no heat shock.

		tRNA-Gly^{GCC}		GCATCGGTGGTTCAGTGGTAGAATGCTCGCCTGCCACGCGGGCGGCCCGGGTTCGATTCCCGGCCGATGCA
Control (ctrl)	D2$^{+/-}$	53 nt	12	GCATCGGTGGTTCAGTGGTAGAATGCTCGCCTGCCACGCGGGCGGCCCGGGTT
		52 nt	3	GCATCGGTGGTTCAGTGGTAGAATGCTCGCCTGCCACGCGGGCGGCCCGGGT
		51 nt	38	GCATCGGTGGTTCAGTGGTAGAATGCTCGCCTGCCACGCGGGCGGCCCGGG
		50 nt	45	GCATCGGTGGTTCAGTGGTAGAATGCTCGCCTGCCACGCGGGCGGCCCGG
		47 nt	67	GCATCGGTGGTTCAGTGGTAGAATGCTCGCCTGCCACGCGGGCGGCC
		46 nt	6	GCATCGGTGGTTCAGTGGTAGAATGCTCGCCTGCCACGCGGGCGGC
		40 nt	2	GCATCGGTGGTTCAGTGGTAGAATGCTCGCCTGCCACGCG
		39 nt	6	GCATCGGTGGTTCAGTGGTAGAATGCTCGCCTGCCACGC
		38 nt	3	GCATCGGTGGTTCAGTGGTAGAATGCTCGCCTGCCACG
		37nt	2	GCATCGGTGGTTCAGTGGTAGAATGCTCGCCTGCCAC
		36 nt	219	GCATCGGTGGTTCAGTGGTAGAATGCTCGCCTGCCA
		35 nt	213	GCATCGGTGGTTCAGTGGTAGAATGCTCGCCTGCC
		34 nt	386	GCATCGGTGGTTCAGTGGTAGAATGCTCGCCTGC
		33 nt	2296	GCATCGGTGGTTCAGTGGTAGAATGCTCGCCTG
		32 nt	4099	GCATCGGTGGTTCAGTGGTAGAATGCTCGCCT
		31 nt	386	GCATCGGTGGTTCAGTGGTAGAATGCTCGCC
		30 nt	19	GCATCGGTGGTTCAGTGGTAGAATGCTCG
	D2$^{-/-}$	53 nt	61	GCATCGGTGGTTCAGTGGTAGAATGCTCGCCTGCCACGCGGGCGGCCCGGGTT
		52 nt	17	GCATCGGTGGTTCAGTGGTAGAATGCTCGCCTGCCACGCGGGCGGCCCGGGT
		51 nt	322	GCATCGGTGGTTCAGTGGTAGAATGCTCGCCTGCCACGCGGGCGGCCCGGG
		50 nt	639	GCATCGGTGGTTCAGTGGTAGAATGCTCGCCTGCCACGCGGGCGGCCCGG
		48 nt	5	GCATCGGTGGTTCAGTGGTAGAATGCTCGCCTGCCACGCGGGCGGCCC
		47 nt	503	GCATCGGTGGTTCAGTGGTAGAATGCTCGCCTGCCACGCGGGCGGCC
		45 nt	2	GCATCGGTGGTTCAGTGGTAGAATGCTCGCCTGCCACGCGGGCGG
		43 nt	4	GCATCGGTGGTTCAGTGGTAGAATGCTCGCCTGCCACGCGGGC
		42 nt	7	GCATCGGTGGTTCAGTGGTAGAATGCTCGCCTGCCACGCGGG
		41 nt	4	GCATCGGTGGTTCAGTGGTAGAATGCTCGCCTGCCACGCGG
		40 nt	4	GCATCGGTGGTTCAGTGGTAGAATGCTCGCCTGCCACGCG
		39 nt	2	GCATCGGTGGTTCAGTGGTAGAATGCTCGCCTGCCACGC
		38 nt	1	GCATCGGTGGTTCAGTGGTAGAATGCTCGCCTGCCACG
		37nt	5	GCATCGGTGGTTCAGTGGTAGAATGCTCGCCTGCCAC
		36 nt	878	GCATCGGTGGTTCAGTGGTAGAATGCTCGCCTGCCA
		35 nt	925	GCATCGGTGGTTCAGTGGTAGAATGCTCGCCTGCC
		34 nt	3223	GCATCGGTGGTTCAGTGGTAGAATGCTCGCCTGC
		33 nt	7608	GCATCGGTGGTTCAGTGGTAGAATGCTCGCCTG
		32 nt	22308	GCATCGGTGGTTCAGTGGTAGAATGCTCGCCT
		31 nt	2155	GCATCGGTGGTTCAGTGGTAGAATGCTCGCC
		30 nt	47	GCATCGGTGGTTCAGTGGTAGAATGCTCG
		Read length	N° of reads	**5' fragments**

Table 5.13: tRNA-Gly^{GCC} fragment identities corresponding to the 5' end of tRNA-Gly^{GCC} from control (D2$^{+/-}$) and *Dnmt2* mutant (D2$^{-/-}$) *Drosophila* somatic tissue .

Time points hs= 5 hours after heat shock.

tRNA-Gly^{GCC}				GCATCGGTGGTTCAGTGGTAGAATGCTCGCCTGCCACGCGGGCGGCCCGGGTTCGATTCCCGGCCGATGCA
Heat shock (hs)	**D2$^{+/-}$**	53 nt	26	GCATCGGTGGTTCAGTGGTAGAATGCTCGCCTGCCACGCGGGCGGCCCGGGTT
		52 nt	9	GCATCGGTGGTTCAGTGGTAGAATGCTCGCCTGCCACGCGGGCGGCCCGGGT
		51 nt	101	GCATCGGTGGTTCAGTGGTAGAATGCTCGCCTGCCACGCGGGCGGCCCGGG
		50 nt	101	GCATCGGTGGTTCAGTGGTAGAATGCTCGCCTGCCACGCGGGCGGCCCGG
		47 nt	181	GCATCGGTGGTTCAGTGGTAGAATGCTCGCCTGCCACGCGGGCGGCC
		46 nt	47	GCATCGGTGGTTCAGTGGTAGAATGCTCGCCTGCCACGCGGGCGGC
		41 nt	7	GCATCGGTGGTTCAGTGGTAGAATGCTCGCCTGCCACGCGG
		40 nt	8	GCATCGGTGGTTCAGTGGTAGAATGCTCGCCTGCCACGCG
		39 nt	3	GCATCGGTGGTTCAGTGGTAGAATGCTCGCCTGCCACGC
		37 nt	3	GCATCGGTGGTTCAGTGGTAGAATGCTCGCCTGCCAC
		36 nt	329	GCATCGGTGGTTCAGTGGTAGAATGCTCGCCTGCCA
		35 nt	1064	GCATCGGTGGTTCAGTGGTAGAATGCTCGCCTGCC
		34 nt	987	GCATCGGTGGTTCAGTGGTAGAATGCTCGCCTGC
		33 nt	5724	GCATCGGTGGTTCAGTGGTAGAATGCTCGCCTG
		32 nt	9522	GCATCGGTGGTTCAGTGGTAGAATGCTCGCCT
		31 nt	1038	GCATCGGTGGTTCAGTGGTAGAATGCTCGCC
		30 nt	18	GCATCGGTGGTTCAGTGGTAGAATGCTCG
	D2$^{-/-}$	53 nt	28	GCATCGGTGGTTCAGTGGTAGAATGCTCGCCTGCCACGCGGGCGGCCCGGGTT
		52 nt	3	GCATCGGTGGTTCAGTGGTAGAATGCTCGCCTGCCACGCGGGCGGCCCGGGT
		51 nt	704	GCATCGGTGGTTCAGTGGTAGAATGCTCGCCTGCCACGCGGGCGGCCCGGG
		50 nt	389	GCATCGGTGGTTCAGTGGTAGAATGCTCGCCTGCCACGCGGGCGGCCCGG
		48 nt	2	GCATCGGTGGTTCAGTGGTAGAATGCTCGCCTGCCACGCGGGCGGCCC
		47 nt	803	GCATCGGTGGTTCAGTGGTAGAATGCTCGCCTGCCACGCGGGCGGCC
		46 nt	344	GCATCGGTGGTTCAGTGGTAGAATGCTCGCCTGCCACGCGGGCGGC
		40 nt	3	GCATCGGTGGTTCAGTGGTAGAATGCTCGCCTGCCACGCG
		38 nt	3	GCATCGGTGGTTCAGTGGTAGAATGCTCGCCTGCCACG
		36 nt	385	GCATCGGTGGTTCAGTGGTAGAATGCTCGCCTGCCA
		35 nt	300	GCATCGGTGGTTCAGTGGTAGAATGCTCGCCTGCC
		34 nt	1115	GCATCGGTGGTTCAGTGGTAGAATGCTCGCCTGC
		33 nt	4417	GCATCGGTGGTTCAGTGGTAGAATGCTCGCCTG
		32 nt	11103	GCATCGGTGGTTCAGTGGTAGAATGCTCGCCT
		31 nt	1605	GCATCGGTGGTTCAGTGGTAGAATGCTCGCC
		30 nt	7	GCATCGGTGGTTCAGTGGTAGAATGCTCG
		Read length	N° of reads	**5' fragments**

Table 5.14: tRNA-Gly^{GCC} fragment identities corresponding to the 5' end of tRNA-Gly^{GCC} from control (D2$^{+/-}$) and *Dnmt2* mutant (D2$^{-/-}$) *Drosophila* male somatic tissue.

Time point 2R= 2 days recovery

tRNA-Gly^{GCC}				GCATCGGTGGTTCAGTGGTAGAATGCTCGCCTGCCACGCGGGCGGCCCGGGTTCGATTCCCGGCCGATGCA
2 days recovery (2R)	D2$^{+/-}$	53 nt	14	GCATCGGTGGTTCAGTGGTAGAATGCTCGCCTGCCACGCGGGCGGCCCGGGTT
		52 nt	6	GCATCGGTGGTTCAGTGGTAGAATGCTCGCCTGCCACGCGGGCGGCCCGGGT
		51 nt	105	GCATCGGTGGTTCAGTGGTAGAATGCTCGCCTGCCACGCGGGCGGCCCGGG
		50 nt	81	GCATCGGTGGTTCAGTGGTAGAATGCTCGCCTGCCACGCGGGCGGCCCGG
		49 nt	1	GCATCGGTGGTTCAGTGGTAGAATGCTCGCCTGCCACGCGGGCGGCCCG
		48 nt	2	GCATCGGTGGTTCAGTGGTAGAATGCTCGCCTGCCACGCGGGCGGCCC
		47 nt	161	GCATCGGTGGTTCAGTGGTAGAATGCTCGCCTGCCACGCGGGCGGCC
		46 nt	1	GCATCGGTGGTTCAGTGGTAGAATGCTCGCCTGCCACGCGGGCGGC
		45 nt	30	GCATCGGTGGTTCAGTGGTAGAATGCTCGCCTGCCACGCGGGCGG
		43 nt	11	GCATCGGTGGTTCAGTGGTAGAATGCTCGCCTGCCACGCGGGC
		42 nt	6	GCATCGGTGGTTCAGTGGTAGAATGCTCGCCTGCCACGCGGG
		41 nt	2	GCATCGGTGGTTCAGTGGTAGAATGCTCGCCTGCCACGCGG
		40 nt	14	GCATCGGTGGTTCAGTGGTAGAATGCTCGCCTGCCACGCG
		39 nt	14	GCATCGGTGGTTCAGTGGTAGAATGCTCGCCTGCCACGC
		38 nt	4	GCATCGGTGGTTCAGTGGTAGAATGCTCGCCTGCCACG
		37 nt	3	GCATCGGTGGTTCAGTGGTAGAATGCTCGCCTGCCAC
		36 nt	359	GCATCGGTGGTTCAGTGGTAGAATGCTCGCCTGCCA
		35 nt	753	GCATCGGTGGTTCAGTGGTAGAATGCTCGCCTGCC
		34 nt	823	GCATCGGTGGTTCAGTGGTAGAATGCTCGCCTGC
		33 nt	2178	GCATCGGTGGTTCAGTGGTAGAATGCTCGCCTG
		32 nt	3937	GCATCGGTGGTTCAGTGGTAGAATGCTCGCCT
		31 nt	302	GCATCGGTGGTTCAGTGGTAGAATGCTCGCC
		30 nt	30	GCATCGGTGGTTCAGTGGTAGAATGCTCG
	D2$^{-/-}$	53 nt	3	GCATCGGTGGTTCAGTGGTAGAATGCTCGCCTGCCACGCGGGCGGCCCGGGTT
		51 nt	237	GCATCGGTGGTTCAGTGGTAGAATGCTCGCCTGCCACGCGGGCGGCCCGGG
		47 nt	35	GCATCGGTGGTTCAGTGGTAGAATGCTCGCCTGCCACGCGGGCGGCC
		40 nt	203	GCATCGGTGGTTCAGTGGTAGAATGCTCGCCTGCCACGCG
		39 nt	35	GCATCGGTGGTTCAGTGGTAGAATGCTCGCCTGCCACGC
		36 nt	34	GCATCGGTGGTTCAGTGGTAGAATGCTCGCCTGCCA
		35 nt	21	GCATCGGTGGTTCAGTGGTAGAATGCTCGCCTGCC
		34 nt	48	GCATCGGTGGTTCAGTGGTAGAATGCTCGCCTGC
		33 nt	467	GCATCGGTGGTTCAGTGGTAGAATGCTCGCCTG
		32 nt	1618	GCATCGGTGGTTCAGTGGTAGAATGCTCGCCT
		31 nt	187	GCATCGGTGGTTCAGTGGTAGAATGCTCGCC
		30 nt	10	GCATCGGTGGTTCAGTGGTAGAATGCTCG
		Read length	N° of reads	**5' fragments**

Table 5.15: tRNA fragments in Ago2-complexes from wild type *Drosophila* S2 cells. Two time points were analyzed (ctrl= no heat shock; hs= heat shock).

Ago2-IP from wild type *Drosophila* S2 cells										
tRNA	Sense				Antisense				Total number of tRNA reads	
	Number of tRNA reads		% of total tRNA reads		Number of tRNA reads		% of total tRNA reads			
	ctrl	hs	ctrl	hs	ctrl	hs	ctrl	hs	ctrl	hs
Gly	120	159	19,29	23,56	274	298	21,29	23,24	394	457
Glu	190	76	30,55	11,26	408	333	31,70	25,98	598	409
Lys	112	161	18,01	23,85	149	128	11,58	9,98	261	289
Asp	47	110	7,56	16,30	90	166	6,99	12,95	137	276
Cys	42	28	6,75	4,15	5	5	0,39	0,39	47	33
Gln	42	65	6,75	9,63	74	101	5,75	7,88	116	166
Met	33	17	5,31	2,52	55	10	4,27	0,78	88	27
Pro	2	0	0,32	0,00	13	9	1,01	0,70	15	9
Val	0	1	0,00	0,15	2	28	0,16	2,18	2	29
Trp	3	1	0,48	0,15	15	29	1,17	2,26	18	30
His	0	0	0,00	0,00	28	23	2,18	1,79	28	23
Arg	0	0	0,00	0,00	5	3	0,39	0,23	5	3
Ser	1	1	0,16	0,15	92	44	7,15	3,43	93	45
Asn	0	0	0,00	0,00	4	0	0,31	0,00	4	0
Ala	0	0	0,00	0,00	0	0	0,00	0,00	0	0
SeC	1	22	0,16	3,26	2	1	0,16	0,08	3	23
Thr	5	1	0,80	0,15	16	5	1,24	0,39	21	6
Ile	1	1	0,16	0,15	20	0	1,55	0,00	21	1
Leu	22	8	3,54	1,19	19	24	1,48	1,87	41	32
Phe	0	10	0,00	1,48	4	28	0,31	2,18	4	38
Tyr	1	14	0,16	2,07	12	47	0,93	3,67	13	61
Σ	622	675			1287	1282			1909	1957

List of Publications

Durdevic, Z., Hanna, K., Gold, B., Pollex, T., Cherry, S., Lyko, F., and Schaefer, M. (2013). Efficient RNA virus control in Drosophila requires the RNA methyltransferase Dnmt2. EMBO Rep. *14*, 269–275.

Durdevic, Z., and Schaefer, M. (2013). tRNA modifications: Necessary for correct tRNA-derived fragments during the recovery from stress? Bioessays *35*, 323–327.

References

Agaisse, H., Petersen, U.M., Boutros, M., Mathey-Prevot, B., and Perrimon, N. (2003). Signaling role of hemocytes in Drosophila JAK/STAT-dependent response to septic injury. Dev. Cell *5*, 441–450.

Ambros, V., Lee, R.C., Lavanway, A., Williams, P.T., and Jewell, D. (2003). MicroRNAs and other tiny endogenous RNAs in C. elegans. Curr. Biol. *13*, 807–818.

Ardelt, W., Mikulski, S.M., and Shogen, K. (1991). Amino acid sequence of an anti-tumor protein from Rana pipiens oocytes and early embryos. Homology to pancreatic ribonucleases. J. Biol. Chem. *266*, 245–251.

Arkhipova, I.R., Mazo, A.M., Cherkasova, V.A., Gorelova, T.V., Schuppe, N.G., and Llyin, Y.V. (1986). The steps of reverse transcription of Drosophila mobile dispersed genetic elements and U3-R-U5 structure of their LTRs. Cell *44*, 555–563.

Aström, S.U., and Byström, A.S. (1994). Rit1, a tRNA backbone-modifying enzyme that mediates initiator and elongator tRNA discrimination. Cell *79*, 535–546.

Aubin-Horth, N., and Renn, S.C.P. (2009). Genomic reaction norms: using integrative biology to understand molecular mechanisms of phenotypic plasticity. Mol. Ecol. *18*, 3763–3780.

Babiarz, J.E., Ruby, J.G., Wang, Y., Bartel, D.P., and Blelloch, R. (2008). Mouse ES cells express endogenous shRNAs, siRNAs, and other Microprocessor-independent, Dicer-dependent small RNAs. Genes & Development *22*, 2773–2785.

Balagy Mobin, M. (2011). Heat-shock Induced Fragmentation of Dnmt2-Substrate tRNA-Asp in Drosophila melanogaster. Master Thesis, Heidelberg University.

Beauregard, A., Curcio, M.J., and Belfort, M. (2008). The take and give between retrotransposable elements and their hosts. Annu. Rev. Genet. *42*, 587–617.

Becker, M., Müller, S., Nellen, W., Jurkowski, T.P., Jeltsch, A., and Ehrenhofer-Murray, A.E. (2012). Pmt1, a Dnmt2 homolog in Schizosaccharomyces pombe, mediates tRNA methylation in response to nutrient signaling. Nucleic Acids Research *40*, 11648–11658.

Begley, U., Dyavaiah, M., Patil, A., Rooney, J.P., DiRenzo, D., Young, C.M., Conklin, D.S., Zitomer, R.S., and Begley, T.J. (2007). Trm9-catalyzed tRNA modifications link translation to the DNA damage response. Mol Cell *28*, 860–870.

Bokar, J.A., Shambaugh, M.E., Polayes, D., Matera, A.G., and Rottman, F.M. (1997). Purification and cDNA cloning of the AdoMet-binding subunit of the human mRNA (N6-adenosine)-methyltransferase. Rna *3*, 1233–1247.

Borsani, O., Zhu, J., Verslues, P.E., Sunkar, R., and Zhu, J.-K. (2005). Endogenous siRNAs derived from a pair of natural cis-antisense transcripts regulate salt tolerance in Arabidopsis. Cell *123*, 1279–1291.

Böhne, A., Brunet, F., Galiana-Arnoux, D., Schultheis, C., and Volff, J.-N. (2008). Transposable elements as drivers of genomic and biological diversity in vertebrates. Chromosome Res. *16*, 203–215.

Bradford, M.M. (1976). A Rapid and Sensitive Methode for the Quantitation of Microgram Quantities of Proteins Utilizing the Principle of Protein-Dye Binding. 1–7.

Brzezicha, B., Schmidt, M., Makalowska, I., Jarmolowski, A., Pienkowska, J., and Szweykowska-Kulinska, Z. (2006). Identification of human tRNA:m5C methyltransferase catalysing intron-dependent m5C formation in the first position of the anticodon of the pre-tRNA Leu (CAA). Nucleic Acids Research *34*, 6034–6043.

Bujnicki, J.M., Feder, M., Radlinska, M., and Blumenthal, R.M. (2002). Structure prediction and phylogenetic analysis of a functionally diverse family of proteins homologous to the MT-A70 subunit of the human mRNA:m(6)A methyltransferase. J. Mol. Evol. *55*, 431–444.

Burroughs, A.M., Ando, Y., de Hoon, M.J.L., Tomaru, Y., Suzuki, H., Hayashizaki, Y., and Daub, C.O. (2011). Deep-sequencing of human Argonaute-associated small RNAs provides insight into miRNA sorting and reveals Argonaute association with RNA fragments of diverse origin. Rnabiology *8*, 158–177.

Butler, A.R., Porter, M., and Stark, M.J. (1991). Intracellular expression of Kluyveromyces lactis toxin gamma subunit mimics treatment with exogenous toxin and distinguishes two classes of toxin-resistant mutant. Yeast *7*, 617–625.

Carthew, R.W., and Sontheimer, E.J. (2009). Origins and Mechanisms of miRNAs and siRNAs. Cell *136*, 642–655.

Cernilogar, F.M., Onorati, M.C., Kothe, G.O., Burroughs, A.M., Parsi, K.M., Breiling, A., Sardo, Lo, F., Saxena, A., Miyoshi, K., Siomi, H., et al. (2011). Chromatin-associated RNA interference components contribute to transcriptional regulation in Drosophila. Nature *480*, 391–395.

Chan, C.T.Y., Chionh, Y.H., Ho, C.-H., Lim, K.S., Babu, I.R., Ang, E., Wenwei, L., Alonso, S., and Dedon, P.C. (2011). Identification of N6,N6-dimethyladenosine in transfer RNA from Mycobacterium bovis Bacille Calmette-Guérin. Molecules *16*, 5168–5181.

Chan, C.T.Y., Dyavaiah, M., DeMott, M.S., Taghizadeh, K., Dedon, P.C., and Begley, T.J. (2010). A quantitative systems approach reveals dynamic control of tRNA modifications during cellular stress. PLoS Genet. *6*, e1001247.

Chan, C.T.Y., Pang, Y.L.J., Deng, W., Babu, I.R., Dyavaiah, M., Begley, T.J., and Dedon, P.C. (2012). Reprogramming of tRNA modifications controls the oxidative stress response by codon-biased translation of proteins. Nat Commun *3*, 937.

Chen, P.Y., Manninga, H., Slanchev, K., Chien, M., Russo, J.J., Ju, J., Sheridan, R., John, B., Marks, D.S., Gaidatzis, D., et al. (2005). The developmental miRNA profiles of zebrafish as determined by small RNA cloning. Genes & Development *19*, 1288–1293.

Cherry, S., and Perrimon, N. (2004). Entry is a rate-limiting step for viral infection in a Drosophila melanogaster model of pathogenesis. Nat Immunol *5*, 81–87.

Cherry, S., Kunte, A., Wang, H., Coyne, C., Rawson, R.B., and Perrimon, N. (2006). COPI activity coupled with fatty acid biosynthesis is required for viral replication. PLoS Pathog. *2*, e102.

Chung, W.-J., Okamura, K., Martin, R., and Lai, E.C. (2008). Endogenous RNA interference provides a somatic defense against Drosophila transposons. Curr. Biol. *18*, 795–802.

Clavarino, G., Cláudio, N., Couderc, T., Dalet, A., Judith, D., Camosseto, V., Schmidt, E.K., Wenger, T., Lecuit, M., Gatti, E., et al. (2012). Induction of GADD34 is necessary for dsRNA-dependent interferon-β production and participates in the control of Chikungunya virus infection. PLoS Pathog. *8*, e1002708.

Cole, C., Sobala, A., Lu, C., Thatcher, S.R., Bowman, A., Brown, J.W.S., Green, P.J., Barton, G.J., and Hutvagner, G. (2009). Filtering of deep sequencing data reveals the existence of abundant Dicer-dependent small RNAs derived from tRNAs. Rna *15*, 2147–2160.

Couvillion, M.T., Sachidanandam, R., and Collins, K. (2010). A growth-essential Tetrahymena Piwi protein carries tRNA fragment cargo. Genes & Development *24*, 2742–2747.

Czech, B., Malone, C.D., Zhou, R., Stark, A., Schlingeheyde, C., Dus, M., Perrimon, N., Kellis, M., Wohlschlegel, J.A., Sachidanandam, R., et al. (2008). An endogenous small interfering RNA pathway in Drosophila. Nature *453*, 798–802.

Davanloo, P., Sprinzl, M., Watanabe, K., Albani, M., and Kersten, H. (1979). Role of ribothymidine in the thermal stability of transfer RNA as monitored by proton magnetic resonance. Nucleic Acids Research *6*, 1571–1581.

Deddouche, S., Matt, N., Budd, A., Mueller, S., Kemp, C., Galiana-Arnoux, D., Dostert, C., Antoniewski, C., Hoffmann, J.A., and Imler, J.-L. (2008). The DExD/H-box helicase Dicer-2 mediates the induction of antiviral activity in drosophila. Nat Immunol *9*, 1425–1432.

Detzer, A., Engel, C., Wünsche, W., and Sczakiel, G. (2011). Cell stress is related to re-localization of Argonaute 2 and to decreased RNA interference in human cells. Nucleic Acids Research *39*, 2727–2741.

Dominissini, D., Moshitch-Moshkovitz, S., Schwartz, S., Salmon-Divon, M., Ungar, L., Osenberg, S., Cesarkas, K., Jacob-Hirsch, J., Amariglio, N., Kupiec, M., et al. (2012). Topology of the human and mouse m6A RNA methylomes revealed by m6A-seq. Nature *485*, 201–206.

Dong, A., Yoder, J.A., Zhang, X., Zhou, L., Bestor, T.H., and Cheng, X. (2001). Structure of human DNMT2, an enigmatic DNA methyltransferase homolog that displays denaturant-resistant binding to DNA. Nucleic Acids Research *29*, 439–448.

Dostert, C., Jouanguy, E., Irving, P., Troxler, L., Galiana-Arnoux, D., Hetru, C., Hoffmann, J.A., and Imler, J.-L. (2005). The Jak-STAT signaling pathway is required but not sufficient for the antiviral response of drosophila. Nat Immunol *6*, 946–953.

Durdevic, Z., and Schaefer, M. (2013). tRNA modifications: Necessary for correct tRNA-derived fragments during the recovery from stress? Bioessays *35*, 323–327.

Durdevic, Z., Hanna, K., Gold, B., Pollex, T., Cherry, S., Lyko, F., and Schaefer, M. (2013). Efficient RNA virus control in Drosophila requires the RNA methyltransferase Dnmt2. EMBO Rep. *14*, 269–275.

Emara, M.M., Ivanov, P., Hickman, T., Dawra, N., Tisdale, S., Kedersha, N., Hu, G.-F., and Anderson, P. (2010). Angiogenin-induced tRNA-derived stress-induced RNAs promote stress-induced stress granule assembly. J. Biol. Chem. *285*, 10959–10968.

Falckenhayn, C., Radatz, G., Lyko, F. (2012). BiSQuID: Bisulfite sequencing quantification and identification. German Conference on Bioinformatics, Jena.

Feng, G., Leem, Y.-E., and Levin, H.L. (2013). Transposon integration enhances expression of stress response genes. Nucleic Acids Research *41*, 775–789.

Fire, A., Xu, S., Montgomery, M.K., Kostas, S.A., Driver, S.E., and Mello, C.C. (1998). Potent and specific genetic interference by double-stranded RNA in Caenorhabditis elegans. Nature *391*, 806–811.

Fisher, O., Siman-Tov, R., and Ankri, S. (2004). Characterization of cytosine methylated regions and 5-cytosine DNA methyltransferase (Ehmeth) in the protozoan parasite Entamoeba histolytica. Nucleic Acids Research *32*, 287–297.

Flajnik, M.F., and Pasquier, Du, L. (2004). Evolution of innate and adaptive immunity: can we draw a line? Trends Immunol. *25*, 640–644.

Fu, H., Feng, J., Liu, Q., Sun, F., Tie, Y., Zhu, J., Xing, R., Sun, Z., and Zheng, X. (2009). Stress induces tRNA cleavage by angiogenin in mammalian cells. FEBS Letters *583*, 437–442.

Gangaraju, V.K., Yin, H., Weiner, M.M., Wang, J., Huang, X.A., and Lin, H. (2011). Drosophila Piwi functions in Hsp90-mediated suppression of phenotypic variation. Nat. Genet. *43*, 153–158.

Ghildiyal, M., and Zamore, P.D. (2009). Small silencing RNAs: an expanding universe. Nat. Rev. Genet. *10*, 94–108.

Ghildiyal, M., Seitz, H., Horwich, M.D., Li, C., Du, T., Lee, S., Xu, J., Kittler, E.L.W., Zapp, M.L., Weng, Z., et al. (2008). Endogenous siRNAs derived from transposons and mRNAs in Drosophila somatic cells. Science *320*, 1077–1081.

Goll, M.G., Kirpekar, F., Maggert, K.A., Yoder, J.A., Hsieh, C.-L., Zhang, X., Golic, K.G., Jacobsen, S.E., and Bestor, T.H. (2006). Methylation of tRNAAsp by the DNA methyltransferase homolog Dnmt2. Science *311*, 395–398.

Gottar, M., Gobert, V., Michel, T., Belvin, M., Duyk, G., Hoffmann, J.A., Ferrandon, D., and Royet, J. (2002). The Drosophila immune response against Gram-negative bacteria is mediated by a peptidoglycan recognition protein. Nature *416*, 640–644.

Haiser, H.J., Karginov, F.V., Hannon, G.J., and Elliot, M.A. (2008). Developmentally regulated cleavage of tRNAs in the bacterium Streptomyces coelicolor. Nucleic Acids Research *36*, 732–741.

Haussecker, D., Huang, Y., Lau, A., Parameswaran, P., Fire, A.Z., and Kay, M.A. (2010). Human tRNA-derived small RNAs in the global regulation of RNA silencing. Rna *16*, 673–695.

He, Y., Vogelstein, B., Velculescu, V.E., Papadopoulos, N., and Kinzler, K.W. (2008). The antisense transcriptomes of human cells. Science *322*, 1855–1857.

Helm, M., Giegé, R., and Florentz, C. (1999). A Watson-Crick base-pair-disrupting methyl group (m1A9) is sufficient for cloverleaf folding of human mitochondrial tRNALys. Biochemistry *38*, 13338–13346.

Hermann, A., Schmitt, S., and Jeltsch, A. (2003). The human Dnmt2 has residual DNA-(cytosine-C5) methyltransferase activity. J. Biol. Chem. *278*, 31717–31721.

Heyer, R., Dörr, M., Jellen-Ritter, A., Späth, B., Babski, J., Jaschinski, K., Soppa, J., and Marchfelder, A. (2012). High throughput sequencing reveals a plethora of small RNAs including tRNA derived fragments in Haloferax volcanii. Rnabiology *9*, 1011–1018.

Hoffmann, A., and Merilä, J. (1999). Heritable variation and evolution under favourable and unfavourable conditions. Trends Ecol. Evol. (Amst.) *14*, 96–101.

Hodgson, C.P., Elder, P.K., Ono, T., Foster, D.N., and Getz, M.J. (1983). Structure and expression of mouse VL30 genes. Mol. Cell. Biol. *3*, 2221–2231.

Holcik, M., and Sonenberg, N. (2005). Translational control in stress and apoptosis. Nat. Rev. Mol. Cell Biol. *6*, 318–327.

Hsieh, L.-C., Lin, S.-I., Shih, A.C.-C., Chen, J.-W., Lin, W.-Y., Tseng, C.-Y., Li, W.-H., and Chiou, T.-J. (2009). Uncovering small RNA-mediated responses to phosphate deficiency in Arabidopsis by deep sequencing. Plant Physiology *151*, 2120–2132.

Iida, T., Nakayama, J.-I., and Moazed, D. (2008). siRNA-mediated heterochromatin establishment requires HP1 and is associated with antisense transcription. Molecular Cell *31*, 178–189.

Ishizu, H., Siomi, H., and Siomi, M.C. (2012). Biology of PIWI-interacting RNAs: new insights into biogenesis and function inside and outside of germlines. Genes & Development *26*, 2361–2373.

Ito, H., Gaubert, H., Bucher, E., Mirouze, M., Vaillant, I., and Paszkowski, J. (2011). An siRNA pathway prevents transgenerational retrotransposition in plants subjected to stress. Nature *472*, 115–119.

Ivanov, P., Emara, M.M., Villen, J., Gygi, S.P., and Anderson, P. (2011). Angiogenin-induced tRNA fragments inhibit translation initiation. Molecular Cell *43*, 613–623.

Jia, G., Fu, Y., and He, C. (2013). Reversible RNA adenosine methylation in biological regulation. Trends in Genetics *29*, 108–115.

Jia, G., Fu, Y., Zhao, X., Dai, Q., Zheng, G., Yang, Y., Yi, C., Lindahl, T., Pan, T., Yang, Y.-G., et al. (2011). N6-methyladenosine in nuclear RNA is a major substrate of the obesity-associated FTO. Nat. Chem. Biol. *7*, 885–887.

Jiang, Y., Meidler, R., Amitsur, M., and Kaufmann, G. (2001). Specific interaction between anticodon nuclease and the tRNA(Lys) wobble base. Journal of Molecular Biology *305*, 377–388.

Johansson, M.J.O., Esberg, A., Huang, B., Björk, G.R., and Byström, A.S. (2008). Eukaryotic wobble uridine modifications promote a functionally redundant decoding system. Mol. Cell. Biol. *28*, 3301–3312.

Jurkowski, T.P., and Jeltsch, A. (2011). On the evolutionary origin of eukaryotic DNA methyltransferases and Dnmt2. PLoS ONE *6*, e28104.

Jurkowski, T.P., Meusburger, M., Phalke, S., Helm, M., Nellen, W., Reuter, G., and Jeltsch, A. (2008). Human DNMT2 methylates tRNA(Asp) molecules using a DNA methyltransferase-like catalytic mechanism. Rna *14*, 1663–1670.

Katiyar-Agarwal, S., Morgan, R., Dahlbeck, D., Borsani, O., Villegas, A., Zhu, J.-K., Staskawicz, B.J., and Jin, H. (2006). A pathogen-inducible endogenous siRNA in plant immunity. Proc. Natl. Acad. Sci. U.S.a. *103*, 18002–18007.

Kawai, G., Yamamoto, Y., Kamimura, T., Masegi, T., Sekine, M., Hata, T., Iimori, T., Watanabe, T., Miyazawa, T., and Yokoyama, S. (1992). Conformational rigidity of specific pyrimidine residues in tRNA arises from posttranscriptional modifications that enhance steric interaction between the base and the 2'-hydroxyl group. Biochemistry *31*, 1040–1046.

Kawamura, Y., Saito, K., Kin, T., Ono, Y., Asai, K., Sunohara, T., Okada, T.N., Siomi, M.C., and Siomi, H. (2008). Drosophila endogenous small RNAs bind to Argonaute 2 in somatic cells. Nature *453*, 793–797.

Khoddami, V., and Cairns, B.R. (2013). Identification of direct targets and modified bases of RNA cytosine methyltransferases. Nat. Biotechnol.

Kim, V.N. (2005). MicroRNA biogenesis: coordinated cropping and dicing. Nat. Rev. Mol. Cell Biol. *6*, 376–385.

Klassen, R., Paluszynski, J.P., Wemhoff, S., Pfeiffer, A., Fricke, J., and Meinhardt, F. (2008). The primary target of the killer toxin from Pichia acaciae is tRNA(Gln). Molecular Microbiology *69*, 681–697.

Kojima, E., Takeuchi, A., Haneda, M., Yagi, A., Hasegawa, T., Yamaki, K.-I., Takeda, K., Akira, S., Shimokata, K., and Isobe, K.-I. (2003). The function of GADD34 is a recovery from a shutoff of protein synthesis induced by ER stress: elucidation by GADD34-deficient mice. Faseb J. *17*, 1573–1575.

Kuhlmann, M., Borisova, B.E., Kaller, M., Larsson, P., Stach, D., Na, J., Eichinger, L., Lyko, F., Ambros, V., Söderbom, F., et al. (2005). Silencing of retrotransposons in Dictyostelium by DNA methylation and RNAi. Nucleic Acids Research *33*, 6405–6417.

Kunert, N., Marhold, J., Stanke, J., Stach, D., and Lyko, F. (2003). A Dnmt2-like protein mediates DNA methylation in Drosophila. Development *130*, 5083–5090.

Laemmli, U.K. (1970). Cleavage of structural proteins during the assembly of the head of bacteriophage T4. Nature *227*, 680–685.

Lee, A.-H., Iwakoshi, N.N., and Glimcher, L.H. (2003). XBP-1 regulates a subset of endoplasmic reticulum resident chaperone genes in the unfolded protein response. Mol. Cell. Biol. *23*, 7448–7459.

Lee, R.C., Feinbaum, R.L., and Ambros, V. (1993). The C. elegans heterochronic gene lin-4 encodes small RNAs with antisense complementarity to lin-14. Cell *75*, 843–854.

Lee, S.R., and Collins, K. (2005). Starvation-induced cleavage of the tRNA anticodon loop in Tetrahymena thermophila. J. Biol. Chem. *280*, 42744–42749.

Lee, Y.S., Shibata, Y., Malhotra, A., and Dutta, A. (2009a). A novel class of small RNAs: tRNA-derived RNA fragments (tRFs). Genes & Development *23*, 2639–2649.

Lee, Y.S., Pressman, S., Andress, A.P., Kim, K., White, J.L., Cassidy, J.J., Li, X., Lubell, K., Lim, D.H., Cho, I.S., et al. (2009b). Silencing by small RNAs is linked to endosomal trafficking. Nat. Cell Biol. *11*, 1150–1156.

Lemaitre, B., and Hoffmann, J. (2007). The host defense of Drosophila melanogaster. Annu. Rev. Immunol. *25*, 697–743.

Leung, A.K.L., and Sharp, P.A. (2010). MicroRNA functions in stress responses. Molecular Cell *40*, 205–215.

Leung, A.K.L., Calabrese, J.M., and Sharp, P.A. (2006). Quantitative analysis of Argonaute protein reveals microRNA-dependent localization to stress granules. Proc. Natl. Acad. Sci. U.S.a. *103*, 18125–18130.

Li, H., Li, W.-X., and Ding, S.-W. (2002). Induction and suppression of RNA silencing by an animal virus. Science *296*, 1319–1321.

Li, Y., Luo, J., Zhou, H., Liao, J.-Y., Ma, L.-M., Chen, Y.-Q., and Qu, L.-H. (2008). Stress-induced tRNA-derived RNAs: a novel class of small RNAs in the primitive eukaryote Giardia lamblia. Nucleic Acids Research *36*, 6048–6055.

Li, Z., Ender, C., Meister, G., Moore, P.S., Chang, Y., and John, B. (2012). Extensive terminal and asymmetric processing of small RNAs from rRNAs, snoRNAs, snRNAs, and tRNAs. Nucleic Acids Research *40*, 6787–6799.

Liu, Y., and Santi, D.V. (2000). m5C RNA and m5C DNA methyl transferases use different cysteine residues as catalysts. Proc. Natl. Acad. Sci. U.S.a. *97*, 8263–8265.

Lloyd, R.E. (2013). Regulation of stress granules and P-bodies during RNA virus infection. WIREs RNA.

Lu, J., Esberg, A., Huang, B., and Byström, A.S. (2008). Kluyveromyces lactis gamma-toxin, a ribonuclease that recognizes the anticodon stem loop of tRNA. Nucleic Acids Research *36*, 1072–1080.

Lu, R., Maduro, M., Li, F., Li, H.W., Broitman-Maduro, G., Li, W.X., and Ding, S.W. (2005). Animal virus replication and RNAi-mediated antiviral silencing in Caenorhabditis elegans. Nature *436*, 1040–1043.

Lucchetta, E.M., Carthew, R.W., and Ismagilov, R.F. (2009). The endo-siRNA pathway is essential for robust development of the Drosophila embryo. PLoS ONE *4*, e7576.

Malone, C.D., and Hannon, G.J. (2009). Small RNAs as guardians of the genome. Cell *136*, 656–668.

Marciniak, S.J., Yun, C.Y., Oyadomari, S., Novoa, I., Zhang, Y., Jungreis, R., Nagata, K., Harding, H.P., and Ron, D. (2004). CHOP induces death by promoting protein synthesis and oxidation in the stressed endoplasmic reticulum. Genes & Development *18*, 3066–3077.

Marquet, R., Isel, C., Ehresmann, C., and Ehresmann, B. (1995). tRNAs as primer of reverse transcriptases. Biochimie *77*, 113–124.

Mas, G., de Nadal, E., Dechant, R., Rodríguez de la Concepción, M.L., Logie, C., Jimeno-González, S., Chávez, S., Ammerer, G., and Posas, F. (2009). Recruitment of a chromatin remodelling complex by the Hog1 MAP kinase to stress genes. Embo J. *28*, 326–336.

Miller, C., Schwalb, B., Maier, K., Schulz, D., Dümcke, S., Zacher, B., Mayer, A., Sydow, J., Marcinowski, L., Dölken, L., et al. (2011). Dynamic transcriptome analysis measures rates of mRNA synthesis and decay in yeast. Mol. Syst. Biol. *7*, 458.

Miyagawa, R., Mizuno, R., Watanabe, K., and Ijiri, K. (2012). Formation of tRNA granules in the nucleus of heat-induced human cells. Biochemical and Biophysical Research Communications *418*, 149–155.

Motorin, Y., and Grosjean, H. (1999). Multisite-specific tRNA:m5C-methyltransferase (Trm4) in yeast Saccharomyces cerevisiae: identification of the gene and substrate specificity of the enzyme. Rna *5*, 1105–1118.

Motorin, Y., and Helm, M. (2010). tRNA stabilization by modified nucleotides. Biochemistry *49*, 4934–4944.

Myles, K.M., Wiley, M.R., Morazzani, E.M., and Adelman, Z.N. (2008). Alphavirus-derived small RNAs modulate pathogenesis in disease vector mosquitoes. Proc. Natl. Acad. Sci. U.S.a. *105*, 19938–19943.

Nameki, N., Asahara, H., Shimizu, M., Okada, N., and Himeno, H. (1995). Identity elements of Saccharomyces cerevisiae tRNA(His). Nucleic Acids Research *23*, 389–394.

Niu, Y., Zhao, X., Wu, Y.-S., Li, M.-M., Wang, X.-J., and Yang, Y.-G. (2013). N6-methyl-adenosine (m6A) in RNA: an old modification with a novel epigenetic function. Genomics Proteomics Bioinformatics *11*, 8–17.

Novoa, E.M., and Ribas de Pouplana, L. (2012). Speeding with control: codon usage, tRNAs, and ribosomes. Trends in Genetics *28*, 574–581.

Ogawa, T., Tomita, K., Ueda, T., Watanabe, K., Uozumi, T., and Masaki, H. (1999). A cytotoxic ribonuclease targeting specific transfer RNA anticodons. Science *283*, 2097–2100.

Okamura, K., Balla, S., Martin, R., Liu, N., and Lai, E.C. (2008a). Two distinct mechanisms generate endogenous siRNAs from bidirectional transcription in Drosophila melanogaster. Nature Publishing Group *15*, 581–590.

Okamura, K., Chung, W.-J., Ruby, J.G., Guo, H., Bartel, D.P., and Lai, E.C. (2008b). The Drosophila hairpin RNA pathway generates endogenous short interfering RNAs. Nature *453*, 803–806.

Okano, M., Xie, S., and Li, E. (1998). Cloning and characterization of a family of novel mammalian DNA (cytosine-5) methyltransferases. Nat. Genet. *19*, 219–220.

Oliver, K.R., and Greene, W.K. (2012). Transposable elements and viruses as factors in adaptation and evolution: an expansion and strengthening of the TE-Thrust hypothesis. Ecol Evol *2*, 2912–2933.

Pare, J.M., Tahbaz, N., López-Orozco, J., LaPointe, P., Lasko, P., and Hobman, T.C. (2009). Hsp90 regulates the function of argonaute 2 and its recruitment to stress granules and P-bodies. Molecular Biology of the Cell *20*, 3273–3284.

Perry, R.P., Kelley, D.E., Friderici, K., and Rottman, F. (1975). The methylated constituents of L cell messenger RNA: evidence for an unusual cluster at the 5' terminus. Cell *4*, 387–394.

Petesch, S.J., and Lis, J.T. (2008). Rapid, transcription-independent loss of nucleosomes over a large chromatin domain at Hsp70 loci. Cell *134*, 74–84.

Phalke, S., Nickel, O., Walluscheck, D., Hortig, F., Onorati, M.C., and Reuter, G. (2009). Retrotransposon silencing and telomere integrity in somatic cells of Drosophila depends on the cytosine-5 methyltransferase DNMT2. Nat. Genet. *41*, 696–702.

Phizicky, E.M., and Hopper K.A. (2010). tRNA biology charges to the front. Genes & Development *24*, 1832-1860.

Polex, T. (2010). Investigation of the role of Dnmt2 during stress response and in the regulation of gene expression. Master Thesis, Heidelberg University.

Qu, F., Ye, X., Hou, G., Sato, S., Clemente, T.E., and Morris, T.J. (2005). RDR6 has a broad-spectrum but temperature-dependent antiviral defense role in Nicotiana benthamiana. J. Virol. *79*, 15209–15217.

Raddatz, G., Guzzardo, P.M., Olova, N., Fantappié, M.R., Rampp, M., Schaefer, M., Reik, W., Hannon, G.H. and Lyko, F. (2013) Dnmt2-dependent methylomes lack defined DNA methylation patterns. PNAS (in print).

Rehwinkel, J., Natalin, P., Stark, A., Brennecke, J., Cohen, S.M., and Izaurralde, E. (2006). Genome-wide analysis of mRNAs regulated by Drosha and Argonaute proteins in Drosophila melanogaster. Mol. Cell. Biol. *26*, 2965–2975.

Rodriguez, A., Zhou, Z., Tang, M.L., Meller, S., Chen, J., Bellen, H., and Kimbrell, D.A. (1996). Identification of immune system and response genes, and novel mutations causing melanotic tumor formation in Drosophila melanogaster. Genetics *143*, 929–940.

Ron, M., Alandete Saez, M., Eshed Williams, L., Fletcher, J.C., and McCormick, S. (2010). Proper regulation of a sperm-specific cis-nat-siRNA is essential for double fertilization in Arabidopsis. Genes & Development *24*, 1010–1021.

Rottman, F., Shatkin, A.J., and Perry, R.P. (1974). Sequences containing methylated nucleotides at the 5' termini of messenger RNAs: possible implications for processing. Cell *3*, 197–199.

Rouget, C., Papin, C., Boureux, A., Meunier, A.-C., Franco, B., Robine, N., Lai, E.C., Pelisson, A., and Simonelig, M. (2010). Maternal mRNA deadenylation and decay by the piRNA pathway in the early Drosophila embryo. Nature *467*, 1128–1132.

Saikia, M., Krokowski, D., Guan, B.-J., Ivanov, P., Parisien, M., Hu, G.-F., Anderson, P., Pan, T., and Hatzoglou, M. (2012). Genome-wide identification and quantitative analysis of cleaved tRNA fragments induced by cellular stress. J. Biol. Chem. *287*, 42708–42725.

Saleh, M.-C., Tassetto, M., van Rij, R.P., Goic, B., Gausson, V., Berry, B., Jacquier, C., Antoniewski, C., and Andino, R. (2009). Antiviral immunity in Drosophila requires systemic RNA interference spread. Nature *458*, 346–350.

Saleh, M.-C., van Rij, R.P., Hekele, A., Gillis, A., Foley, E., O'Farrell, P.H., and Andino, R. (2006). The endocytic pathway mediates cell entry of dsRNA to induce RNAi silencing. Nat. Cell Biol. *8*, 793–802.

Saxena, S.K., Sirdeshmukh, R., Ardelt, W., Mikulski, S.M., Shogen, K., and Youle, R.J. (2002). Entry into cells and selective degradation of tRNAs by a cytotoxic member of the RNase A family. J. Biol. Chem. *277*, 15142–15146.

Schaefer, M., Pollex, T., Hanna, K., and Lyko, F. (2009). RNA cytosine methylation analysis by bisulfite sequencing. Nucleic Acids Research *37*, e12–e12.

Schaefer, M., and Lyko, F. (2010). Lack of evidence for DNA methylation of Invader4 retroelements in Drosophila and implications for Dnmt2-mediated epigenetic regulation. Nat. Genet. *42*, 920–1–authorreply921.

Schaefer, M., Pollex, T., Hanna, K., Tuorto, F., Meusburger, M., Helm, M., and Lyko, F. (2010). RNA methylation by Dnmt2 protects transfer RNAs against stress-induced cleavage. Genes & Development *24*, 1590–1595.

Schaefer, M., Steringer, J.P., and Lyko, F. (2008). The Drosophila cytosine-5 methyltransferase Dnmt2 is associated with the nuclear matrix and can access DNA during mitosis. PLoS ONE *3*, e1414.

Siomi, H., and Siomi, M.C. (2009). RISC hitches onto endosome trafficking. Nat. Cell Biol. *11*, 1049–1051.

Smalheiser, N.R., Lugli, G., Thimmapuram, J., Cook, E.H., and Larson, J. (2011). Endogenous siRNAs and noncoding RNA-derived small RNAs are expressed in adult mouse hippocampus and are up-regulated in olfactory discrimination training. Rna *17*, 166–181.

Southern, E.M. (1975). Detection of specific sequences among DNA fragments separated by gel electrophoresis. Journal of Molecular Biology *98*, 503–517.

Schönborn, J.J., Oberstrass, J.J., Breyel, E.E., Tittgen, J.J., Schumacher, J.J., and Lukacs, N.N. (1991). Monoclonal antibodies to double-stranded RNA as probes of RNA structure in crude nucleic acid extracts. Nucleic Acids Res *19*, 2993–3000.

Specchia, V., Piacentini, L., Tritto, P., Fanti, L., D'Alessandro, R., Palumbo, G., Pimpinelli, S., and Bozzetti, M.P. (2010). Hsp90 prevents phenotypic variation by suppressing the mutagenic activity of transposons. Nature *463*, 662–665.

Spriggs, K.A., Bushell, M., and Willis, A.E. (2010). Translational regulation of gene expression during conditions of cell stress. Molecular Cell *40*, 228–237.

Spriggs, K.A., Stoneley, M., Bushell, M., and Willis, A.E. (2008). Re-programming of translation following cell stress allows IRES-mediated translation to predominate. Biol. Cell *100*, 27–38.

Squires, J.E., Patel, H.R., Nousch, M., Sibbritt, T., Humphreys, D.T., Parker, B.J., Suter, C.M., and Preiss, T. (2012). Widespread occurrence of 5-methylcytosine in human coding and non-coding RNA. Nucleic Acids Research *40*, 5023–5033.

Talbert, P.B., and Henikoff, S. (2006). Spreading of silent chromatin: inaction at a distance. Nat. Rev. Genet. *7*, 793–803.

Tam, O.H., Aravin, A.A., Stein, P., Girard, A., Murchison, E.P., Cheloufi, S., Hodges, E., Anger, M., Sachidanandam, R., Schultz, R.M., et al. (2008). Pseudogene-derived small interfering RNAs regulate gene expression in mouse oocytes. Nature *453*, 534–538.

Thiagarajan, D., Dev, R.R., and Khosla, S. (2011). The DNA methyltranferase Dnmt2 participates in RNA processing during cellular stress. Epigenetics *6*, 103–113.

Thomas, P.S. (1980). Hybridization of denatured RNA and small DNA fragments transferred to nitrocellulose. Proc. Natl. Acad. Sci. U.S.a. *77*, 5201–5205.

Thompson, D.M., and Parker, R. (2009). The RNase Rny1p cleaves tRNAs and promotes cell death during oxidative stress in Saccharomyces cerevisiae. The Journal of Cell Biology *185*, 43–50.

Thompson, D.M., Lu, C., Green, P.J., and Parker, R. (2008). tRNA cleavage is a conserved response to oxidative stress in eukaryotes. Rna *14*, 2095–2103.

Thompson, S.R. (2012). Tricks an IRES uses to enslave ribosomes. Trends Microbiol. *20*, 558–566.

Tittel-Elmer, M., Bucher, E., Broger, L., Mathieu, O., Paszkowski, J., and Vaillant, I. (2010). Stress-induced activation of heterochromatic transcription. PLoS Genet. *6*, e1001175.

Tomita, K., Ogawa, T., Uozumi, T., Watanabe, K., and Masaki, H. (2000). A cytotoxic ribonuclease which specifically cleaves four isoaccepting arginine tRNAs at their anticodon loops. Proc. Natl. Acad. Sci. U.S.a. *97*, 8278–8283.

Towbin, H., Staehelin, T., and Gordon, J. (1979). Electrophoretic transfer of proteins from polyacrylamide gels to nitrocellulose sheets: procedure and some applications. Proc. Natl. Acad. Sci. U.S.a. *76*, 4350–4354.

Tuorto, F., Liebers, R., Musch, T., Schaefer, M., Hofmann, S., Kellner, S., Frye, M., Helm, M., Stoecklin, G., and Lyko, F. (2012). RNA cytosine methylation by Dnmt2 and NSun2 promotes tRNA stability and protein synthesis. Nature Publishing Group *19*, 900–905.

van Rij, R.P., Saleh, M.-C., Berry, B., Foo, C., Houk, A., Antoniewski, C., and Andino, R. (2006). The RNA silencing endonuclease Argonaute 2 mediates specific antiviral immunity in Drosophila melanogaster. Genes & Development *20*, 2985–2995.

Vasilyeva, L.A., Bubenshchikova, E.V., and Ratner, V.A. (1999). Heavy heat shock induced retrotransposon transposition in Drosophila. Genet. Res. *74*, 111–119.

Vazquez, F., Vaucheret, H., Rajagopalan, R., Lepers, C., Gasciolli, V., Mallory, A.C., Hilbert, J.-L., Bartel, D.P., and Crété, P. (2004). Endogenous trans-acting siRNAs regulate the accumulation of Arabidopsis mRNAs. Mol Cell *16*, 69–79.

Vilcek, J. (2006). Fifty years of interferon research: aiming at a moving target. Immunity *25*, 343–348.

Voinnet, O. (2008). Use, tolerance and avoidance of amplified RNA silencing by plants. Trends Plant Sci. *13*, 317–328.

Waddington, C.M. (1942). Canalization of Development and the Inheritance of Acquired Characters. 1–3.

Wang, X.-H., Aliyari, R., Li, W.-X., Li, H.-W., Kim, K., Carthew, R., Atkinson, P., and Ding, S.-W. (2006). RNA interference directs innate immunity against viruses in adult Drosophila. Science *312*, 452–454.

Watanabe, T., Totoki, Y., Toyoda, A., Kaneda, M., Kuramochi-Miyagawa, S., Obata, Y., Chiba, H., Kohara, Y., Kono, T., Nakano, T., et al. (2008). Endogenous siRNAs from naturally formed dsRNAs regulate transcripts in mouse oocytes. Nature *453*, 539–543.

Watson, K.L., Johnson, T.K., and Denell, R.E. (1991). Lethal(1) aberrant immune response mutations leading to melanotic tumor formation in Drosophila melanogaster. Dev. Genet. *12*, 173–187.

Wei, C.M., Gershowitz, A., and Moss, B. (1976). 5'-Terminal and internal methylated nucleotide sequences in HeLa cell mRNA. Biochemistry *15*, 397–401.

Werren, J.H. (2011). Selfish genetic elements, genetic conflict, and evolutionary innovation. Proc. Natl. Acad. Sci. U.S.a. *108 Suppl 2*, 10863–10870.

Wilkins, C., Dishongh, R., Moore, S.C., Whitt, M.A., Chow, M., and Machaca, K. (2005). RNA interference is an antiviral defence mechanism in Caenorhabditis elegans. Nature *436*, 1044–1047.

Wilkinson, C.R., Bartlett, R., Nurse, P., and Bird, A.P. (1995). The fission yeast gene pmt1+ encodes a DNA methyltransferase homologue. Nucleic Acids Research *23*, 203–210.

Wong, C.N.A., Ng, P., and Douglas, A.E. (2011). Low-diversity bacterial community in the gut of the fruitfly Drosophila melanogaster. Environ. Microbiol. *13*, 1889–1900.

Woolcock, K.J., Stunnenberg, R., Gaidatzis, D., Hotz, H.-R., Emmerth, S., Barraud, P., and Bühler, M. (2012). RNAi keeps Atf1-bound stress response genes in check at nuclear pores. Genes & Development *26*, 683–692.

Wright, B.E. (2004). Stress-directed adaptive mutations and evolution. Molecular Microbiology *52*, 643–650.

Yamasaki, S., Ivanov, P., Hu, G.-F., and Anderson, P. (2009). Angiogenin cleaves tRNA and promotes stress-induced translational repression. The Journal of Cell Biology *185*, 35–42.

Yoder, J.A., and Bestor, T.H. (1998). A candidate mammalian DNA methyltransferase related to pmt1p of fission yeast. Hum. Mol. Genet. *7*, 279–284.

Yoshida, H., Matsui, T., Yamamoto, A., Okada, T., and Mori, K. (2001). XBP1 mRNA is induced by ATF6 and spliced by IRE1 in response to ER stress to produce a highly active transcription factor. Cell *107*, 881–891.

Zanton, S.J., and Pugh, B.F. (2006). Full and partial genome-wide assembly and disassembly of the yeast transcription machinery in response to heat shock. Genes & Development *20*, 2250–2265.

Zhang, K., and Kaufman, R.J. (2008). From endoplasmic-reticulum stress to the inflammatory response. Nature *454*, 455–462.

Zhang, S., Sun, L., and Kragler, F. (2009). The phloem-delivered RNA pool contains small noncoding RNAs and interferes with translation. Plant Physiology *150*, 378–387.

Zheng, G., Dahl, J.A., Niu, Y., Fedorcsak, P., Huang, C.-M., Li, C.J., Vågbø, C.B., Shi, Y., Wang, W.-L., Song, S.-H., et al. (2013a). ALKBH5 is a mammalian RNA demethylase that impacts RNA metabolism and mouse fertility. Molecular Cell *49*, 18–29.

Zheng, G., Dahl, J.A., Niu, Y., Fu, Y., Klungland, A., Yang, Y.-G., and He, C. (2013b). Sprouts of RNA epigenetics: The discovery of mammalian RNA demethylases. Rnabiology *10*.

Zilberman, D., Cao, X., and Jacobsen, S.E. (2003). ARGONAUTE4 control of locus-specific siRNA accumulation and DNA and histone methylation. Science *299*, 716–719.

Zinszner, H., Kuroda, M., Wang, X., Batchvarova, N., Lightfoot, R.T., Remotti, H., Stevens, J.L., and Ron, D. (1998). CHOP is implicated in programmed cell death in response to impaired function of the endoplasmic reticulum. Genes & Development *12*, 982–995.

Acknowledgments

First and foremost, I would like to thank Matthias for outstanding and extraordinary supervision and for his guidance through many technical and theoretical problems. His enthusiasm and endless ideas were always inspiring and our many exciting discussions deeply broadened my knowledge. Above all, I am sincerely grateful for his friendship.

I would like to express my gratitude to Frank for his supervision, support and for giving me the opportunity to conduct my PhD in his lab.

I am particularly thankful to Katharina not only for great scientific and technical support but most of all for her kindness and friendship.

Furthermore, I want to thank all the former and current members of the Lyko lab for friendly and inspiring atmosphere, scientific support and discussions. Special thanks goes to “coffee breakers” for cheerful times in the “Casino” and truly unscientific conversations.

I want to thank Cassandra, Sebastian and Günter for bioinformatics support, Nevcin for establishing RIP protocol and Prof. Dr. Günter Reuter for the HA-1925 fly stocks.

I want also to thank Georg Stöcklin for being my second referee and to all members of my thesis advisory committee for their time and helpful suggestions.

I thank the Hartmut Hoffmann-Berling International Graduate School of Molecular and Cellular Biology (HBIGS) for offering excellent training opportunities.

Above all, I am most grateful to my parents, my dearest sister and my grandmothers for their love and support.

Finally, I dedicate this work to my beloved wife Sanja for her love, support, understanding and always believing in me.